The Early Flooding Signal

# Ethylene Acclimates Plants To Survive Low-Oxygen Stress

Sjon Hartman

**Thesis Committee**
Prof. dr. J. Bailey-Serres
Prof. dr. M.J. Holdsworth
Prof. dr. A. Mustroph
Prof. dr. J.C.M. Smeekens
Dr. I. Rieu

Plant Ecophysiology | Utrecht University | 2020
Author: Sjon Hartman
ISBN: 978-90-393-7231-9
Thesis design: Rutger van Aken | persoonlijkproefschrift.nl
Photography: Iris Hartman | irishartmanfotografie.nl
Printing: Ridderprint BV | ridderprint.nl

The early flooding signal

# Ethylene Acclimates Plants To Survive Low-Oxygen Stress

**Het vroege overstromingssignaal ethyleen bereidt planten voor om zuurstofgebrek te overleven**

(met een samenvatting in het Nederlands)

**Proefschrift**

ter verkrijging van de graad van doctor aan de
Universiteit Utrecht
op gezag van de
rector magnificus, prof.dr. H.R.B.M. Kummeling,
ingevolge het besluit van het college voor promoties
in het openbaar te verdedigen op

woensdag 22 januari 2020 des middags te 12.45 uur

door

**Johannes Gerardus Wilhelmus Hartman**

geboren op 28 december 1987
te Woerden

**Promotor:**
Prof. dr. L.A.C.J. Voesenek

**Copromotor:**
Dr. R. Sasidharan

Dit proefschrift werd (mede) mogelijk gemaakt met financiële steun van de Nederlandse organisatie voor Wetenschappelijk Onderzoek (EPS talentenprogramma nr. 831.15.001).

## CONTENTS

| | | |
|---|---|---|
| **Chapter 1** | General introduction | 7 |
| **Chapter 2** | Ethylene is a rapid submergence signal that acclimates plants to hypoxia stress | 17 |
| **Chapter 3** | Ethylene augments the hypoxia response through group VII Ethylene Response Factors | 37 |
| **Chapter 4** | NO problem: ethylene-induced nitric oxide depletion limits ERFVII proteolysis through PHYTOGLOBIN1 | 61 |
| **Chapter 5** | Ethylene regulates proteins involved in hypoxia acclimation, mitochondrial respiration and ROS homeostasis | 77 |
| **Chapter 6** | Exploring ethylene-mediated hypoxia tolerance in wild and cultivated *Solanum* species | 105 |
| **Chapter 7** | General Discussion | 123 |
| **References** | | 129 |
| **Appendix** | | 140 |
| **Samenvatting** | | 144 |
| **Résumé** | | 147 |
| **Acknowledgements** | | 148 |
| **About the author** | | 152 |
| **Publications** | | 153 |

# CHAPTER 1

## GENERAL INTRODUCTION

**MODIFIED EXCERPTS OF THIS CHAPTER ARE PUBLISHED IN:**
- Hartman, S., *et al.* (2019). The role of ethylene in metabolic acclimations to low oxygen. New Phytologist, Accepted.

## PLANT GROWTH IN AN UNDERWATER WORLD

Anthropogenic climate change has contributed to a significant increase in the frequency and severity of flooding events worldwide (Hirabayashi *et al.*, 2013). Floods have a devastating impact on plant biodiversity and agricultural crop productivity, challenging global food security (Voesenek & Bailey-Serres, 2015a). In order to enhance flooding tolerance in crops, it is crucial to understand the processes that cause stunted plant growth under water and how plants control flood-adaptive mechanisms (Bailey-Serres *et al.*, 2012). Compared to an aerated environment, underwater gas diffusion is decreased $10^4$-fold due to Fick's Law (Fick, 1855), which restricts oxygen ($O_2$) and carbon dioxide ($CO_2$) exchange in submerged plant tissues (Voesenek *et al.*, 2016; Sasidharan *et al.*, 2018). Moreover, reduced light penetration through typically turbid floodwaters can further limit photosynthesis and subsequent carbohydrate and $O_2$ production (Pedersen *et al.*, 2018). Consequently, submerged terrestrial plants ultimately suffer from severe $O_2$ deprivation (hypoxia), terminating mitochondrial respiration. The resulting carbohydrate and energy crisis seriously reduces plant performance and survival (van Dongen *et al.*, 2014; Voesenek & Bailey-Serres, 2015a). Paradoxically, de-submergence further impairs plant survival as returning to ambient light and $O_2$ (normoxia) levels coincides with excessive formation of reactive oxygen species (ROS) (Sasidharan *et al.*, 2018; Yeung *et al.*, 2019).

Plants have evolved several strategies to either avoid or acclimate to flooding-induced hypoxia. Several terrestrial and semi aquatic plant species induce the so-called 'escape' strategy, to restore gas exchange with the atmosphere when fully submerged (Ku *et al.*, 1970; Hattori *et al.*, 2009; van Veen *et al.*, 2013; Voesenek & Bailey-Serres, 2015a). The escape strategy consists of upward leaf movement (hyponasty) and enhanced petiole/internode elongation. The leaf blades that emerge above water function as a snorkel to allow $O_2$ and $CO_2$ diffusion through constitutive or inducible interconnected air-filled tissues (aerenchyma) in the plant (Pierik *et al.*, 2009; Akman *et al.*, 2012). Additional morphological and anatomical flood-adaptive traits include the induction of barriers to radial $O_2$ loss (ROL) in roots, adventitious root (AR) formation and gas film formation at the leaf surface (Colmer, 2003; Pedersen *et al.*, 2009; Voesenek & Bailey-Serres, 2015a). The induction of one or more of these traits assists plants to survive shallow and long-term submergence. Conversely, plants can induce a 'quiescence' strategy, where metabolism and growth are reduced to survive severe hypoxia or even the absence of $O_2$ (anoxia) (Xu *et al.*, 2006; van Veen *et al.*, 2013; Voesenek & Bailey-Serres, 2015a). In order to maintain cellular homeostasis under hypoxia, glycolysis, the

bifurcated tricarboxylic acid (TCA) cycle and fermentation pathways are engaged to fuel anaerobic metabolism and ATP production (Voesenek & Bailey-Serres, 2015a). In addition, several ROS detoxification mechanisms are induced (Fukao *et al.*, 2011; Yeung *et al.*, 2018). These quiescence pathways prolong survival of hypoxic plant tissues affected by long term flooding conditions, such as un-escapable deep floods or waterlogging (root submergence). Moreover, metabolic hypoxia acclimation can enhance flooding survival of terrestrial plant species that have not evolved escape strategies, including the vast majority of crop species (Mustroph, 2018). A complex and not yet fully understood web of signal dynamics and interactions during plant submergence controls these flood-adaptive responses and includes changes in levels of the gases $O_2$, $CO_2$, nitric oxide (NO), ROS and the volatile plant hormone ethylene (Sasidharan *et al.*, 2018).

### Ethylene controls flooding-adaptive responses

Ethylene is produced in all plant cells and its production pathways are conserved across the majority of terrestrial plants, with the exception of some aquatic plant species with a fully submerged life style (Ju *et al.*, 2015; Voesenek *et al.*, 2015). Ethylene is synthesized through conversion of its pre-cursor 1-aminocyclopropane-1-carboxylic acid (ACC) by ACC oxidase (ACO). ACC itself is produced by conversion of *S*-adenosyl-methionine (SAM) and is facilitated by ACC synthases (ACS), which is thought to be the rate-limiting step in ethylene biosynthesis (Pierik *et al.*, 2006). In *Arabidopsis thaliana* (hereafter Arabidopsis), ethylene perception and signaling is initiated by physical binding of ethylene to a family of five ethylene-binding receptors including ETHYLENE RESPONSIVE 1 and ETR2 (Guo & Ecker, 2004; Pierik *et al.*, 2006). These ethylene receptors repress the negative ethylene response regulator CONSTITUTIVE REPONSE 1 (CTR1), and upon ethylene perception activate ethylene signaling through removing CTR1-dependent repression of ETHYLENE INSENSITIVE 2 (EIN2) (Guo & Ecker, 2004; An *et al.*, 2010). Following CTR1 repression, C-terminal EIN2 fragments translocate from the endoplasmic reticulum to the nucleus where they stabilize EIN3 and EIN3 LIKE1 (EIL1) transcription factors via enhanced proteolysis of EIN3 BINDING F BOX proteins EBF1 and EBF2 (An *et al.*, 2010; Wen *et al.*, 2012). Through this signaling cascade, ethylene co-regulates a plethora of plant developmental and stress responses in an EIN3-dependent manner, including flooding responses (Voesenek & Sasidharan, 2013; Chang *et al.*, 2013; Sasidharan *et al.*, 2018).

Under non-stressed conditions, ethylene generally diffuses out of the plant through membranes and the stomata. However, submerged plant tissues rapidly accumulate





high ethylene levels due to the restricted gas diffusion under water (Sasidharan *et al.*, 2018). Indeed, ethylene was shown to reach physiologically saturating levels (>1µll$^{-1}$) in *Rumex* species (Banga *et al.*, 1996) and led to EIN3 stability in Arabidopsis within 1 hour of plant submergence (Xie *et al.*, 2015). Accordingly, ethylene is a well-known early flooding signal that regulates the adaptive morphological and anatomical modifications during submergence to avoid severe hypoxia (Voesenek & Bailey-Serres, 2015a). In addition, ethylene initiates both the 'escape' and 'quiescence' strategies in several plant species (van Veen *et al.*, 2013; Voesenek & Bailey-Serres, 2015a). For example, ethylene activates the group VII ethylene response factor (ERFVII) transcription factors SNORKEL1(SK1) and SK2 in deepwater rice, which in turn enhance internode elongation to successfully restore above water gas exchange (Hattori *et al.*, 2009; Voesenek & Bailey-Serres, 2015a). Conversely, ethylene also represses shoot elongation in lowland rice varieties, through induction of the ERFVII SUBMERGENCE 1A (SUB1A) (Xu *et al.*, 2006). SUB1A rice varieties confer flooding tolerance through conservation of energy until flood waters recede and have made a massive impact for rice farmers across Asia and Africa (Bailey-Serres *et al.*, 2010; Lin *et al.*, 2019). Interestingly, while ethylene is key for flood-adaptive growth responses that avoid or delay hypoxia, it has hardly been linked to metabolic processes that allow plants to deal with the consequences of severe hypoxia (Peng, 2001; Yamauchi *et al.*, 2014; Voesenek & Bailey-Serres, 2015a; Sasidharan *et al.*, 2018).

### Hypoxia acclimation through oxygen sensing

The spatial and temporal $O_2$ dynamics in flooded plants are highly dependent on the type of plant tissue and the environmental conditions (Colmer & Pedersen, 2008; Vashisht *et al.*, 2011; Sasidharan *et al.*, 2018). As long as light is available, submerged photosynthetic tissues (e.g shoots) generally do not reach hypoxic $O_2$ levels (<21%), and can even become hyperoxic (>21%) as $O_2$ derived from photosynthesis is trapped inside these tissues (Colmer & Pedersen, 2008; Vashisht *et al.*, 2011; Pedersen *et al.*, 2018). However, upon darkness shoot tissues decline in $O_2$ content to reach an equilibrium resulting from the leaf respiration rate and the $O_2$ gradient to the water layer (<1-10% $O_2$). Similarly, the underground root tissues of submerged plants are generally hypoxic and the hypoxia severity highly depends on root respiration, tissue porosity, the presence of ROL barriers, the microbial activity in surrounding soils and shoot derived $O_2$ (Voesenek & Sasidharan, 2013). This is illustrated by $O_2$ measurements in root tissues of submerged Arabidopsis and rice (*Oryza sativa*) plants where $O_2$ levels quickly diminished from 3-6% $O_2$ in the light to 0% $O_2$ in the dark (Colmer & Pedersen, 2008; Lee *et al.*, 2011; Vashisht *et*

*al.*, 2011). Interestingly, recent reports indicate that even under non-stressed conditions, shoot apical meristems, roots and lateral root primordia may be constitutively hypoxic (~5-10%) (Lee *et al.*, 2011; Shukla *et al.*, 2019; Weits *et al.*, 2019).

Both hypoxia and submergence induce a highly similar transcriptional response that is thought to facilitate hypoxia acclimation in plants (Mustroph *et al.*, 2010; Lee *et al.*, 2011). In Arabidopsis, hypoxia acclimation includes the expression of a core hypoxia gene set that is conserved across cell types of both shoots and roots (Mustroph *et al.*, 2009). These hypoxia adaptive genes are largely regulated by Arabidopsis ERFVII transcription factors in an $O_2$-dependent manner. In Arabidopsis, the ERFVIIs include the three constitutively synthesized ERVIIs RELATED TO APETALA2.12 (RAP2.12), RAP2.2 and RAP2.3 and the hypoxia-induced ERFVIIs HYPOXIA RESPONSIVE ERF 1 (HRE1) and HRE2 (Licausi *et al.*, 2010a; Bui *et al.*, 2015). The highly expressed RAP2.12 and RAP2.2 redundantly activate hypoxia-responsive genes by direct recognition of a conserved cis-regulatory motif called the Hypoxia Responsive Promoter Element (HRPE) (Hinz *et al.*, 2010; Gasch *et al.*, 2016). While RAP2.3 is thought to contribute to this redundancy, the hypoxia-inducible ERFVIIs *HRE1* and *HRE2* are considered to mediate prolonged hypoxia gene regulation (Licausi *et al.*, 2010a; Bui *et al.*, 2015; Gasch *et al.*, 2016).

Interestingly, ectopic expression of the ERFVIIs only caused enhanced hypoxia-responsive gene expression upon hypoxia, suggesting an $O_2$-dependent regulatory mechanism (Gibbs *et al.*, 2011; Licausi *et al.*, 2011). Indeed, the ERFVIIs are components of a mechanism that senses both $O_2$ and NO through the PROTEOLYSIS 6 (PRT6) N-degron pathway (Gibbs *et al.*, 2011, 2014; Licausi *et al.*, 2011; Varshavsky, 2019). ERFVIIs contain a conserved N-terminal (Nt) sequence of Methionine-Cysteine (MC), which operates as an N-degron through the arginylation(Arg) branch of the N-degron pathway (Gibbs *et al.*, 2011, 2014; Licausi *et al.*, 2011). After cleavage of the $Met_1$ by methionine aminopeptidases (MetAPs), the exposed $Cys_2$ is oxidized in the presence of $O_2$ by plant cysteine oxidases (PCOs) to Cys-sulphinate or Cys-sulphonate (Weits *et al.*, 2014; White *et al.*, 2017). Following subsequent arginylation through arginyl tRNA transferases (ATEs), the protein is flagged by the E3 ligase PRT6 for ubiquitination and proteosomal degradation (Garzón *et al.*, 2007; Graciet *et al.*, 2010; Varshavsky, 2019). How NO exactly contributes to ERFVII proteolysis is still unclear. Oxidation of ERFVII Nt $Cys_2$ by PCOs *in vitro* and in yeast only requires $O_2$ and not NO (White *et al.*, 2017; Puerta *et al.*, 2019). Still, ERFVIIs and other Nt MC-proteins accumulated under NO depleted conditions (Gibbs *et al.*, 2014, 2018; Vicente *et al.*, 2019). Consequently,



when either $O_2$ or NO levels decline, the ERFVIIs stabilize and cause transcriptional upregulation of hypoxia-responsive genes that in turn facilitate hypoxia acclimation (Gibbs *et al.*, 2011, 2014; Licausi *et al.*, 2011).

## A tale of three gases

Although ethylene is a well-established regulator of flood-adaptive anatomical and growth responses that avoid or delay hypoxia, it is hardly known to mediate metabolic hypoxia acclimation in plants (Voesenek & Bailey-Serres, 2015a; Sasidharan *et al.*, 2018). However, several findings suggest that ethylene could play a key role as an early flooding signal that pre-adapts plants to survive longer under (impending) hypoxic conditions. Firstly, ethylene was shown to rapidly and invariably accumulate to high levels in submerged plants, while $O_2$ levels *in planta* only strongly declined in dense tissues with high respiration rates and when light was a limiting factor (Colmer & Pedersen, 2008; Voesenek & Sasidharan, 2013). Moreover, shoot survival under hypoxia was strongly enhanced after an ethylene pre-treatment in *Rumex palustris* (van Veen *et al.*, 2013), illustrating that ethylene can prepare plants to later occurring hypoxia. This enhanced hypoxia tolerance after ethylene pre-treatment correlated with ethylene-enhanced induction of orthologues of hypoxia-adaptive genes when $O_2$ levels declined. Among these genes, were transcripts encoding for enzymes that control fermentation pathways such as *ALCOHOL DEHYDROGENASE1* (*ADH1*) (Zabalza *et al.*, 2008; van Veen *et al.*, 2013). Also in Arabidopsis, wheat (*Triticum aestivum* L.) and grapevine (*Vitis vinifera* L.) ethylene is essential for adequate induction of *ADH1* and hypoxia-induced fermentation (Peng, 2001; Tesniere *et al.*, 2004; Yamauchi *et al.*, 2014). Interestingly, ethylene was also shown to enhance transcript abundance of several ERFVIIs in multiple plant species, including in Arabidopsis, rice and *R. palustris* (Hattori *et al.*, 2009; Hinz *et al.*, 2010; Bailey-Serres *et al.*, 2012; Chang *et al.*, 2013; van Veen *et al.*, 2013).

Several clues suggest that ethylene could also contribute to enhanced ERFVII stability through impairment of NO-dependent proteolysis. For example, in the aerial tissues of waterlogged Arabidopsis and cotton (*Gossypium hirsutum* L.) plants, increasing ethylene levels correlated with reduced NO emission (Magalhaes *et al.*, 2000; Zhang *et al.*, 2017). Moreover, excess iron stress in Arabidopsis root tips reduced NO levels in an ethylene-dependent manner (Zhang *et al.*, 2018b). Finally, a short ethylene treatment was shown to enhance the transcript levels of the NO-scavenger *PHYTOGLOBIN1* (*PGB1*) in *R. palustris* but not in the related *R. acetosa* (van Veen *et al.*, 2013). Interestingly, the ability of ethylene to increase

*PGB1* in *R. palustris* correlated with enhanced hypoxia-responsive genes and hypoxia survival. Likewise, the inability to enhance *PGB1* transcripts in *R. acetosa* corresponded to unaltered hypoxia-responsive genes and survival (van Veen *et al.*, 2013). From these observations, we can draw a hypothesis that the interaction of the three gaseous signals; ethylene, NO and $O_2$ mediate early flooding responses to prepare plants for upcoming hypoxic conditions. We propose as a general hypothesis for this thesis that entrapped ethylene in submerged plant tissues leads to NO removal, enhanced ERFVII stability, enhanced hypoxia-responsive gene induction and subsequently pre-adapts plants for impending hypoxia (Voesenek & Sasidharan, 2013).

## Thesis outline

The aim of the research presented in this thesis is to unravel the molecular mechanism of how ethylene prepares plants for future hypoxia. In **Chapter 2**, we first investigated the dynamics of ethylene signaling upon plant submergence, using the Arabidopsis root tip as a study model. In addition, we assessed whether Arabidopsis is a useful plant species to unravel the mechanism of ethylene-mediated hypoxia tolerance. We show that ethylene is a rapidly perceived flooding signal in Arabidopsis root tips that enhances shoot and root meristem survival under subsequent hypoxic conditions. Moreover, we conclude that the Arabidopsis root tip is a practical and reliable model to further resolve the mechanism of ethylene-mediated hypoxia tolerance.

In **Chapter 3** we assessed how ethylene pre-treatment enhances subsequent hypoxia tolerance. We uncover that ethylene strongly augments the transcriptional hypoxia response and that this is mediated by the ERFVIIs RAP2.2 and RAP2.12. In addition, we discovered that ethylene can stabilize the ERFVIIs RAP2.3 and RAP2.12 under normoxic conditions. Finally, we show that enhanced ERFVII stability is dependent on ethylene-mediated NO removal.

To uncover how ethylene regulates NO levels in Arabidopsis, we tested the effects of ethylene on processes known to control NO homeostasis in plants. The results in **Chapter 4** demonstrate that ethylene strongly enhances protein levels of NO-scavenger PGB1. In addition, we show that ethylene-enhanced ERFVII stability, hypoxia-responsive gene regulation and hypoxia survival are dependent on PGB1-mediated NO removal.



Knowing that ethylene is an early flooding signal that mediates hypoxia acclimation in plants, we aimed to discover other unknown proteins that are controlled by ethylene using quantitative proteomics. **Chapter 5** uncovers that ethylene regulates several proteins involved in hypoxia responses, ROS amelioration and mitochondrial respiration. In addition, we demonstrate that ethylene mediates oxidative stress damage during hypoxia and subsequent re-oxygenation through up-regulation of antioxidant proteins in root tips.

After the identification of key players that mediate enhanced hypoxia tolerance in Arabidopsis, we assessed how cultivated and wild *Solanum* species integrate the early flooding signal ethylene to control subsequent hypoxia acclimation. The results in **Chapter 6** suggest that the Arabidopsis mechanism of ethylene-mediated hypoxia tolerance is conserved in the wild species bittersweet and a waterlogging-tolerant potato cultivar. Conversely, in a waterlogging-intolerant potato cultivar and tomato plants, ethylene signaling did not uniformly enhance subsequent hypoxia-responsive genes. We propose that testing marker genes indicative of ethylene-mediated hypoxia survival is a useful approach to uncover signaling cascades that confer flooding tolerance in crops.

In **Chapter 7** we integrate and discuss the components that contribute to a functional mechanism in which rapid ethylene signaling prepares submerged plant tissues to later occurring hypoxia. The impact and the limitations of these findings are also discussed.

# CHAPTER 2

## ETHYLENE IS A RAPID SUBMERGENCE SIGNAL THAT ACCLIMATES PLANTS TO HYPOXIA STRESS


Sjon Hartman
Zeguang Liu
Shanice Martopawiro
Nienke van Dongen
Johanna Kociemba
Joris te Riele
Hans van Veen
Rashmi Sasidharan*
Laurentius A.C.J. Voesenek*



**MODIFIED EXCERPTS OF THIS CHAPTER ARE PUBLISHED IN:**

- Hartman, S., *et al.* (2019). Ethylene-mediated nitric oxide depletion pre-adapts plants to hypoxia stress, Nature Communications, 10 (1), 4020.



Plant Ecophysiology, Institute of Environmental Biology, Utrecht University, Utrecht, The Netherlands

*Shared senior authors

## ABSTRACT

Due to restricted gas diffusion underwater, flooded plants ultimately experience cellular oxygen (O2) deprivation (hypoxia). Flooding survival therefore strongly depends on molecular responses that enhance hypoxia tolerance. Ethylene rapidly accumulates in submerged plant tissues and is known to regulate morphological and anatomical flooding-adaptive responses. In addition, an ethylene pre-treatment could substantially enhance hypoxia survival in the wetland species Rumex palustris. Therefore, we proposed that ethylene could function as an early submergence signal to prepare plants for impending hypoxic conditions. Our results show that entrapped ethylene is rapidly perceived in Arabidopsis root tips upon submergence and that this signal is critical for subsequent hypoxia acclimation. In addition, we show that ethylene-induced hypoxia tolerance is highly robust during a variety of conditions and is conserved in root and shoot meristematic tissues of multiple Arabidopsis accessions. The discovery of ethylene-enhanced hypoxia tolerance has significant potential to unravel how plants acclimate during early submergence and subsequently confer flooding tolerance. Furthermore, we propose that studying hypoxia tolerance of the Arabidopsis root tip is a reliable tool for unraveling the mechanism of ethylene-mediated hypoxia tolerance.




## INTRODUCTION

Global flood risk has increased significantly in the last several decades (Hirabayashi *et al.*, 2013). These flooding events have disastrous effects on plant biodiversity and crop production, and threaten global food security (Hirabayashi *et al.*, 2013; Voesenek & Bailey-Serres, 2015a). In order to ameliorate crop losses it is paramount to uncover what processes impair plant growth underwater, what natural mechanisms plants have evolved to survive floods and what signals initiate and regulate these flood-adaptive mechanisms (Voesenek & Bailey-Serres, 2015a).



Performance of terrestrial plants under water is severely hampered due to Fick's Law, which restricts gas diffusion ~10.000-fold compared to aerated conditions. This reduced gas diffusion limits oxygen ($O_2$) and carbon dioxide ($CO_2$) availability in submerged plant tissues and can eventually lead to cellular $O_2$ deprivation (hypoxia) (Voesenek *et al.*, 2016; Sasidharan *et al.*, 2018). Furthermore, the often reduced light availability in turbid floodwaters limits photosynthesis and subsequent molecular $O_2$ and carbohydrate synthesis. The declining carbohydrate pool and $O_2$ levels ultimately terminate mitochondrial respiration and will subsequently seriously hinder plant growth and survival (Voesenek & Sasidharan, 2013; van Dongen & Licausi, 2015). Plant survival therefore strongly depends on the ability to quickly sense submergence and in turn avoid or acclimate to (impending) hypoxia to minimize cellular damage.

Plants can use a variety of signals to sense and integrate submergence (Sasidharan *et al.*, 2018). Both $O_2$ and $CO_2$ dynamics during submergence are highly variable in time and depend strongly on the plant organ, plant morphology, metabolic activity and the available light levels (Colmer & Pedersen, 2008). While the readout of these gases is important for a tailored response to the stress, they are unlikely to be specific and reliable enough for initial flood detection (Sasidharan *et al.*, 2018). However, the gaseous phytohormone ethylene could play that important role in early submergence recognition. In 1970, researchers proposed for the first time that entrapped ethylene inside submerged rice (*Oryza sativa*) seedlings could drive coleoptile elongation to restore contact with the atmosphere and above water gas exchange (Ku *et al.*, 1970). Five decades later, ethylene is a well-established regulator of flood-adaptive responses that include petiole/stem elongation, aerenchyma formation and adventitious root growth (Voesenek & Bailey-Serres, 2015a; Sasidharan *et al.*, 2018). As a result of Fick's law (Fick, 1855), continuously synthesized ethylene accumulates inside intercellular spaces and cells to physiologically saturating levels within 1 hour of submergence in multiple plant species (summa-

rized in Voesenek and Sasidharan, 2013). This ethylene entrapment did not show diurnal fluctuations and persisted for days, making it a potentially fast and reliable signal (Métraux & Kende, 1983; Banga *et al.*, 1996). However, while ethylene was shown to rapidly accumulate in submerged plants, it is currently unknown how quickly this leads to ethylene-dependent signaling upon submergence. In the model species *Arabidopsis thaliana*, ethylene-dependent signaling is mediated through the stability of the nuclear transcription factors ETHYLENE INSENSITIVE 3 (EIN3) and EIN3 LIKE 1 (EIL1), that mediate the downstream ethylene transcriptional response (Alonso *et al.*, 2003; Guo & Ecker, 2004; Chang *et al.*, 2013). It is unclear whether this ethylene-mediated signaling under submergence is tissue specific and is under the control of additional flooding-induced signals, such as hypoxia.

Moreover, while ethylene is crucial for adaptive morphological and anatomical modifications during submergence that avoid hypoxia, it has hardly been linked to metabolic responses that reduce hypoxia damage (Peng, 2001; Voesenek & Bailey-Serres, 2015a; Sasidharan *et al.*, 2018). Recent reports indicate that plants can use ethylene as a reliable early signal to anticipate and acclimate to later occurring hypoxic conditions (van Veen *et al.*, 2013). In this work it was shown that a short pre-treatment with ethylene was sufficient to strongly enhance subsequent hypoxia survival in the shoot tissues of wetland species *Rumex palustris,* but not in the closely related terrestrial species *Rumex acetosa*. Interestingly, the presence or absence of ability to enhance hypoxia tolerance after ethylene pre-treatment correlated with enhanced induction of hypoxia adaptive gene orthologue transcripts in these species (Mustroph *et al.*, 2010; van Veen *et al.*, 2013). These results suggest that ethylene can be an important early signal in plants to enhance the transcriptional hypoxic response and confer subsequent hypoxia tolerance. Unfortunately, the lack of genetic resources in *Rumex* hindered investigation into the molecular mechanism of how an early ethylene signal improves the subsequent hypoxia response.

The model species Arabidopsis is widely used in plant science for its short life cycle and powerful toolset in genetics and molecular biology (Somerville & Koornneef, 2002; Koornneef & Meinke, 2010) and it harbors significant natural variation for flooding tolerance among its accessions (Vashisht *et al.*, 2011). We therefore aimed to unravel how quickly ethylene entrapment led to actual ethylene-dependent signaling in submerged Arabidopsis plants. Here we followed the nuclear EIN3-GFP signal in root tips, which are due to their downward location naturally the first plant organs to detect the consequences of flooding (Xie *et al.*, 2015). Moreover, we studied whether this rapid ethylene accumulation prepares Arabidopsis root



and shoot tissues for subsequent hypoxia. Finally, we aimed to reveal whether Arabidopsis accessions show variation for ethylene-mediated hypoxia tolerance. Our results reveal that submergence quickly leads to EIN3-dependent signaling in Arabidopsis root tips and that this signal is crucial to prepare plants for impending hypoxia. Ethylene-mediated hypoxia tolerance was highly robust under a multitude of conditions but did not show extensive variation between Arabidopsis accessions. We conclude that early ethylene signaling can acclimate Arabidopsis roots and shoots for impending hypoxia and that the root tip could prove to be a valuable tool in unraveling the mechanism of ethylene-mediated hypoxia tolerance.



## RESULTS

### Ethylene entrapment is rapidly perceived in submerged root tip cells.

In order to reveal spatial and temporal dynamics of ethylene signaling upon plant submergence, we followed the nuclear signal of the ethylene transcriptional master regulator EIN3 (Guo & Ecker, 2004; Xie *et al.*, 2015). Both ethylene and submergence treatments showed nuclear localization of EIN3-GFP in Arabidopsis seedling root tips within 1 hour of treatment (Fig. 2.1A). This difference in EIN3 signal could be quantified within 2 hours and further increased up to 4 hours of treatment with ethylene or submergence (Fig. 2.1B). Interestingly, the EIN3 signal was predominantly observed in the stele and meristem cells in the earlier time-points and later spread throughout the whole root tip (Fig. 2.1A). This ethylene- and submergence-induced EIN3 signal could not be detected when the seedlings were pre-treated with the ethylene inhibitor 1-methylcyclopropene (1-MCP) (Fig. 2.1C). Interestingly, EIN3 signaling was abolished after 48h of continuous ethylene treatment (Fig. S2.1A). Moreover, a 1-MCP pre-treatment of 1 hour no longer blocked ethylene signaling after 24h of its application (Fig. S2.1B).

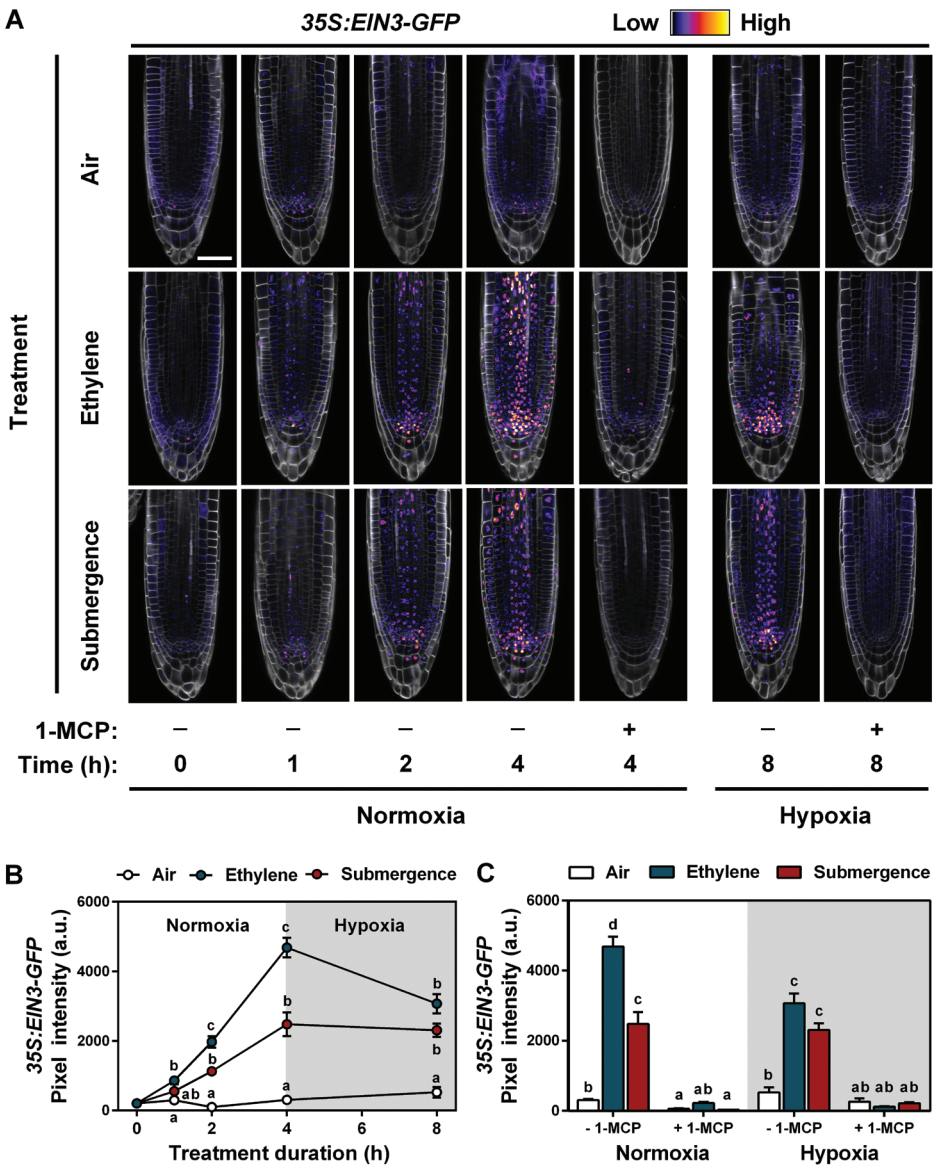


**Figure 2.1. Ethylene signaling during early submergence and subsequent hypoxia.**
**(A)** Representative confocal images of protein stability and localization of the ethylene master regulator EIN3, using the *35S:EIN3-GFP* (*ein3eil1* background) signal in Arabidopsis root tips. Seedlings were treated for up to 4 hours with air, ~5µll$^{-1}$ ethylene or submergence followed by 4h hypoxia, either in combination with or without a pre-treatment of ethylene action inhibitor 1-MCP at the 4 and 8 hour time-points. Cell walls were visualized using Calcofluor White stain (scale bar= 50µm). **(B)** Quantification of *35S:EIN3-GFP* in root tips during 4 hours of treatment with air (white), ~5µll$^{-1}$ ethylene (blue) or submergence (red), followed by 4h of hypoxia. Different letters indicate significant differences per time-point (Error bars are SEM, p<0.05, 2-way ANOVA, Tukey's HSD, n=5-12 roots). **(C)** Quantification of *35S:EIN3-GFP* in root tips after 4 hours of treatment with air (white), ~5µll$^{-1}$ ethylene (blue) or submergence (red) and 4h of hypoxia, either in combination with or without a pre-treatment of 1-MCP. Samples without 1-MCP are the same as in Fig. 2.1B at time-points 4h and 8h. Statistically similar groups are indicated using the same letter (Error bars are SEM, p<0.05, 2-way ANOVA, Tukey's HSD, n=5-11 roots). Mean GFP pixel intensity inside the root tips was quantified using ICY imaging software.



When an ethylene or submergence treatment was followed by hypoxia, the EIN3 signal was clearly maintained (Fig. 2.1A, B). However, a hypoxia treatment alone did not induce EIN3 signaling in root tips (Fig. 2.1A, B). Similar responses were observed for ethylene-regulated transcriptional responses (Fig. 2.2). Indeed, the EIN3 targets (Chang *et al.*, 2013) and ethylene-regulated mRNA transcripts of *ETHYLENE RESPONSE 2* (*ETR2*), *ACC OXIDASE 2* (*ACO2*) and *EIN3-BINDING F BOX PROTEIN 2* (*EBF2*) were quickly induced upon ethylene in Arabidopsis rosettes and were saturated within 1 to 2 hours of ethylene treatment (Fig. 2.2). Similar to EIN3 localization, these target genes were maintained, but not induced further by subsequent hypoxia. These results illustrate that passively entrapped ethylene is rapidly perceived upon submergence but that hypoxia alone does not induce the conventional ethylene-signaling pathway within this timeframe.

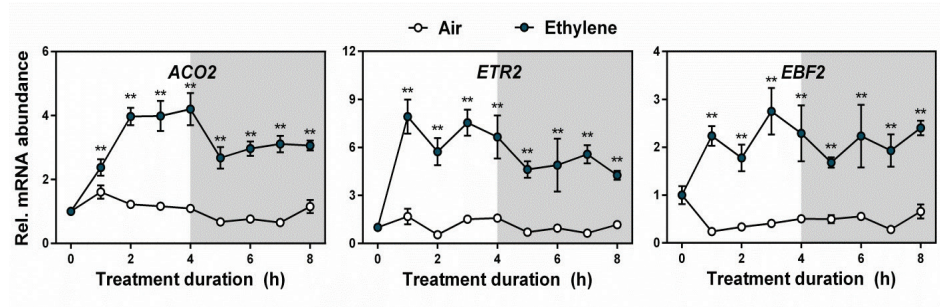


**Figure 2.2. Ethylene-induced dynamics of EIN3 regulated genes.**
Relative mRNA transcript abundance of the EIN3 regulated genes *ACO2*, *ETR2* and *EBF2* in rosettes of Col-0 plants during 4 hours of treatment with air (white) or ~5µll$^{-1}$ ethylene (blue), followed 4 hours of hypoxia (gray shaded). Asterisks indicate significant differences between air and ethylene (Error bars are SEM, **p<0,01, ANOVA with planned comparisons, Tukey's HSD, n=5 biological replicates consisting of 2 adult rosettes).

## Early ethylene signaling enhances subsequent hypoxia acclimation

To investigate whether flooding-induced ethylene entrapment has functional consequences for subsequent hypoxia acclimation, Arabidopsis seedlings were treated with severe hypoxia (<0.00% $O_2$) after different pre-treatments. An ethylene or submergence pre-treatment of only 4 hours was sufficient to strongly increase root meristem survival during subsequent hypoxia (Fig. 2.3A). These responses were abolished after a pre-treatment with 1-MCP and ethylene did not enhance survival in ethylene signaling mutants (Fig. 2.3A, B). In addition, an ethylene pre-treatment did not only extend hypoxia survival in seedling root tips, but also

in seedling lateral roots, seedling shoot meristems and adult rosettes (Fig. 2.4A-C). Interestingly, basal hypoxia tolerance differed between these organs. Primary root tips were most sensitive to hypoxia, followed by lateral root tips, seedling shoot meristems and adult shoot rosettes (Fig. 2.4A-C). Similar to seedling root tips, the ethylene-induced effect was abolished in adult rosettes of the ethylene signaling mutant *ein3eil1* (Fig. S2.2). Furthermore, the beneficial effect of ethylene was already saturated at a concentration of 1µll$^{-1}$ and after a pre-treatment duration of 3 hours (Fig. S2.3A, B).

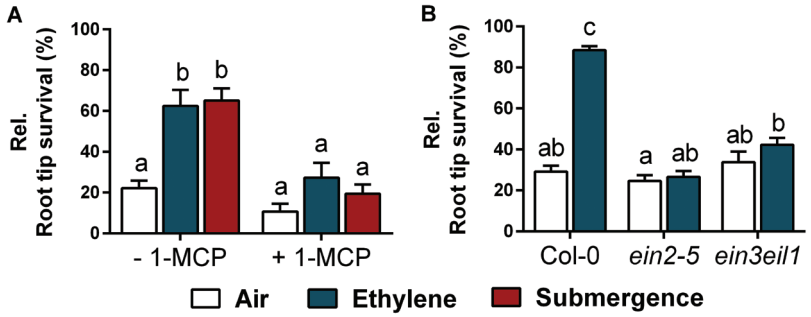


**Figure 2.3. Ethylene acclimates Arabidopsis root tips to survive hypoxia stress.**
**(A)** Seedling root tip survival of Col-0 after 4 hours of pre-treatment with air (white), ~5µll$^{-1}$ ethylene (blue) or submergence (red), either in combination with or without a pre-treatment of ethylene action inhibitor 1-MCP, followed by 4 hours of hypoxia and 3 days of recovery. Values are relative to control (normoxia) plants. Statistically similar groups are indicated using the same letter (Error bars are SEM, p<0.05, 2-way ANOVA, Tukey's HSD, n=8 rows of ~23 seedlings). **(B)** Seedling root tip survival of Col-0 and two ethylene signaling pathway loss-of-function mutants after 4 hours of pre-treatment with air (white) or ~5µll$^{-1}$ ethylene (blue) followed by 4 hours of hypoxia and 3 days of recovery. Values are relative to control (normoxia) plants. Statistically similar groups are indicated using the same letter (Error bars are SEM, p<0.05, 2-way ANOVA, Tukey's HSD, n=8 rows of ~23 seedlings).

## Ethylene-induced hypoxia tolerance is stable under a multitude of conditions

To unravel the robustness of ethylene-mediated hypoxia tolerance in Arabidopsis, we performed root tip survival assays under a variety of developmental and external conditions. We tested whether differences in seedling age, light intensity, temperature, hypoxia severity affected ethylene-induced hypoxia tolerance. Interestingly, basal hypoxia tolerance was dependent on developmental stage and the light intensity during experimental conditions, but seedlings still benefitted from an ethylene pre-treatment (Fig. 2.5A, B). The root tips of older seedlings and seedlings exposed to higher light levels during the pre-treatment had decreased hypoxia survival rates (Fig. 2.5A, B). We observed that temperatures in the desiccators exposed to higher light intensities were higher (from 20°C to 27°C) and wondered if the decrease in hypoxia tolerance was caused by an increase in



temperature. However, temperature differences (20°C or 27°C), during the air or ethylene pre-treatment did not affect subsequent hypoxia root tip survival (Fig. 2.5C). Finally, early ethylene signaling also benefited tolerance to "mild" hypoxia (~0.2% $O_2$), although the hypoxia duration had to be strongly increased to impair root tip survival (Fig. 2.5D).

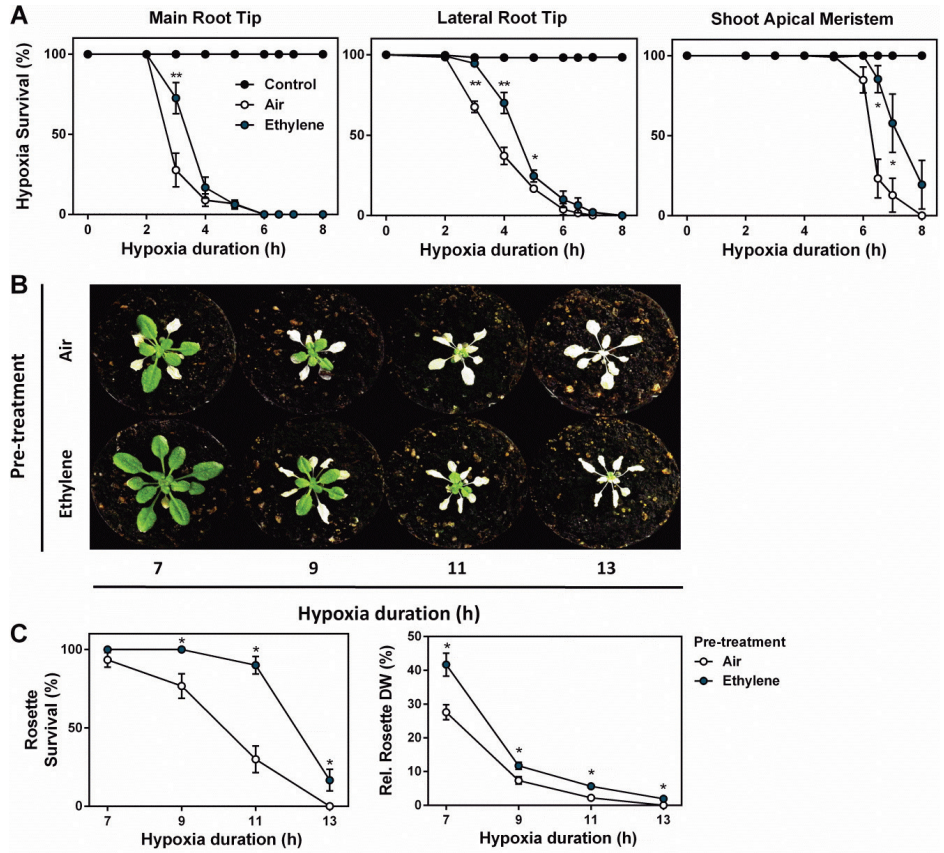


**Figure 2.4. Ethylene-induced hypoxia tolerance is conserved in multiple Arabidopsis organs.**
**(A)** Main root tip, lateral root tip and shoot apical meristem survival of 10-day old seedlings after 4 hours of pre-treatment with air (white) or ~5µll$^{-1}$ ethylene (blue) followed by 0-8h of hypoxia and recovery (3 days for roots, 7 days for shoots). Control plants (black) received no hypoxic treatment. Asterisks indicate significant differences between air and ethylene at given time point (Error bars are SEM, **p<0.01, *p<0.05, ANOVA with planned comparisons, Tukey's HSD, n=2-8 replicate experiments that each contained at least 4 biological replicate plates). **(B)** Arabidopsis (Col-0) rosette phenotypes after 4 hours of pre-treatment (air/ ~5µll$^{-1}$ ethylene) followed by hypoxia and 7 days recovery. **(C)** Arabidopsis adult rosette survival and dry weight (DW) of survived plants after 4 hours of air (white) or ~5µll$^{-1}$ ethylene (blue) followed by hypoxia and 7 days of recovery. Values are relative to control (normoxia) plants. Asterisks indicate significant differences between air and ethylene (Error bars are SEM, *p<0.05, Generalized linear model, negative binomial error structure, n=30 plants).

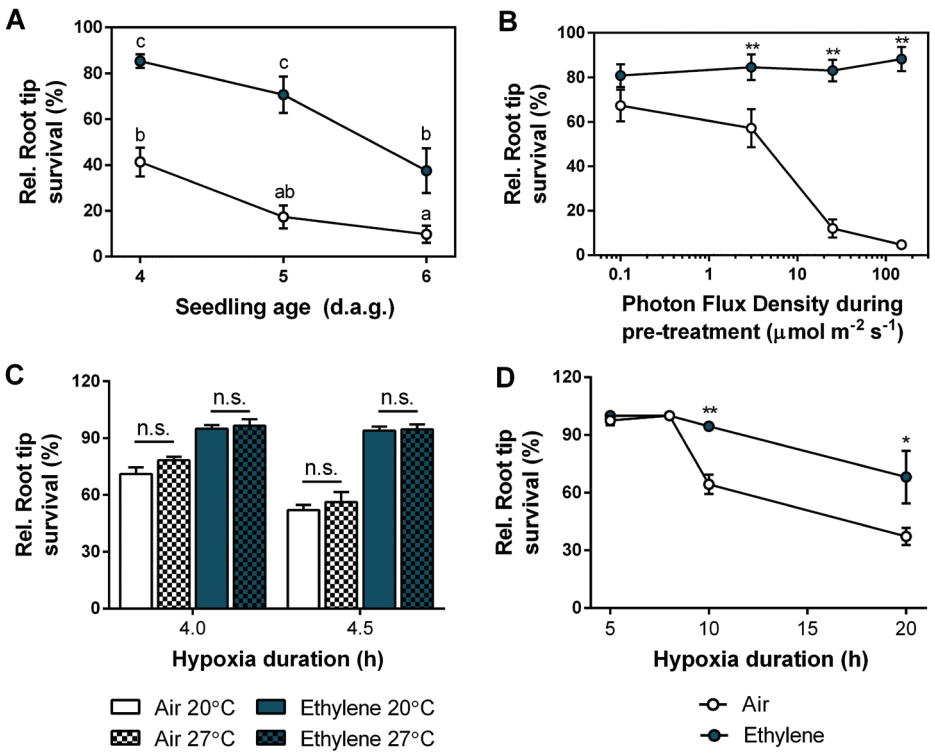


**Figure 2.5. Ethylene-induced hypoxia tolerance is robust under a multitude of conditions.**
**(A)** Root tip survival of 4 to 6-day old Arabidopsis seedlings after 4 hours of pre-treatment with air (white) or ~5µll$^{-1}$ ethylene (blue) followed by 4 hours of hypoxia and 3 days of recovery. Values are relative to control (normoxia) plants. Statistically similar groups are indicated using the same letter (Error bars are SEM, p<0.05, 2-way ANOVA, Tukey's HSD, n=8 plates containing ~46 seedlings). **(B)** Root tip survival of Arabidopsis seedlings after 4 hours of pre-treatment with air (white) or ~5µll$^{-1}$ ethylene (blue) under 4 different light intensities, followed by 4 hours of hypoxia and 3 days of recovery. Values are relative to control (normoxia) plants. Asterisks indicate significant differences between air and ethylene (Error bars are SEM, **p<0.01, ANOVA with planned comparisons, Tukey's HSD, n=8 plates containing ~46 seedlings). **(C)** Root tip survival of Arabidopsis seedlings after 4 hours of pre-treatment with air (white) or ~5µll$^{-1}$ ethylene (blue) in the dark, under either 20°C or 27°C, followed by 4 and 4.5 hours of hypoxia and 3 days of recovery. Values are relative to control (normoxia) plants. No significant differences were found between the different temperature treatments (Error bars are SEM, p<0.01, ANOVA with planned comparisons, Tukey's HSD, n=4 plates containing ~46 seedlings). **(D)** Root tip survival of Arabidopsis seedlings after 4 hours of pre-treatment with air (white) or ~5µll$^{-1}$ ethylene (blue) followed by mild hypoxia (~0.2% $O_2$) and 3 days of recovery. Values are relative to control (normoxia) plants. Asterisks indicate significant differences between air and ethylene (Error bars are SEM, **p<0.01, ANOVA with planned comparisons, Tukey's HSD, n=8 rows of ~23 seedlings).



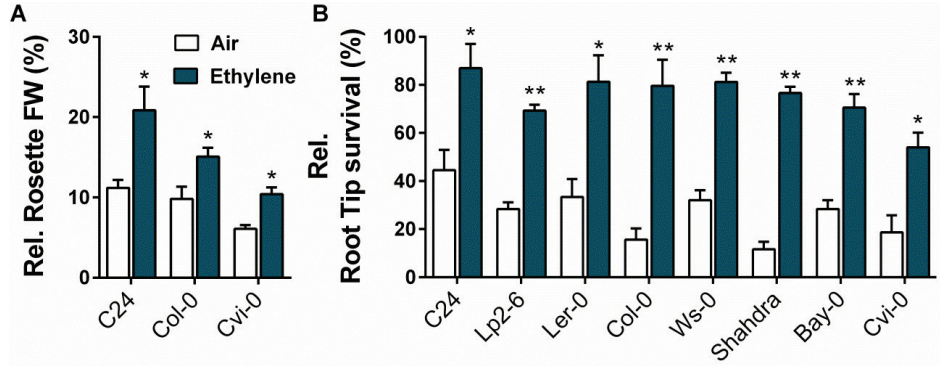


**Figure 2.6. Ethylene-induced hypoxia tolerance is conserved in Arabidopsis accessions.**
**(A)** Relative rosette fresh weight (FW) of adult Arabidopsis accessions C24, Col-0 and Cvi-0 plants after 4 hours of pre-treatment with air (white) or ~5µll$^{-1}$ ethylene (blue) followed by 9 hours of hypoxia and 7 days of recovery. FW was measured only from surviving plants (Error bars are SEM, *p<0.05, Student's t test, n=10 plants). **(B)** Root tip survival of 8 different Arabidopsis accessions after 4 hours of pre-treatment with air (white) or ~5µll$^{-1}$ ethylene (blue) followed by 4 hours of hypoxia and 3 days of recovery. Values are relative to control (normoxia) plants. Asterisks indicate significant differences between air and ethylene (Error bars are SEM, **p<0.01, Student's t test, n=8 rows of ~23 seedlings).

### Ethylene-induced hypoxia tolerance is conserved among Arabidopsis accessions.

Arabidopsis natural accessions display considerable variation in submergence tolerance (Vashisht *et al.*, 2011). To unravel whether similar variation exists for ethylene-induced hypoxia tolerance, we assessed the hypoxia survival performance of multiple Arabidopsis accessions. In addition to Col-0, the accessions C24 and Cvi-0 also benefited from an early ethylene signal to acclimate to hypoxia at the adult rosette level (Fig. 2.6A). Similarly, we found that root tip survival could be enhanced by an ethylene pre-treatment in at least 8 different Arabidopsis accessions (Fig. 2.6B). These results indicate that variation for ethylene-induced hypoxia tolerance among Arabidopsis accessions is limited but the mechanism itself is likely conserved.

## DISCUSSION

Ethylene is known to rapidly accumulate in submerged plant tissues and regulates morphological and anatomical flooding-adaptive responses (Voesenek & Bailey-Serres, 2015a; Sasidharan *et al.*, 2018). In addition, an ethylene pre-treatment could substantially extend hypoxia survival in the wetland species *R. palustris,* but not in the terrestrial species *R. acetosa* (van Veen *et al.*, 2013). In this chapter, we therefore hypothesized that ethylene could function as an early submergence signal to pre-adapt plants for impending hypoxic conditions. With the ultimate aim to unravel the mechanism of how ethylene mediates hypoxia tolerance, we

assessed early ethylene signaling dynamics in submerged Arabidopsis seedlings. In addition, we unraveled to what extent this rapid ethylene accumulation primes Arabidopsis roots and shoots for later-occurring hypoxia. Our results show that entrapped ethylene is rapidly perceived in Arabidopsis root tips upon submergence and that this signal is crucial for subsequent hypoxia acclimation.

EIN3 is the master regulator of the ethylene transcriptional response and its stability is assumed to be a reliable marker for ethylene-induced transcriptional responses (Alonso *et al.*, 2003; An *et al.*, 2010; Chang *et al.*, 2013; Xie *et al.*, 2015). We observed that submergence and ethylene lead to ethylene- and EIN3-dependent signaling within 2 hours in Arabidopsis root tips (Fig. 2.1A, B). Consistently, the mRNA abundance of EIN3-target genes was saturated within 2 hours of ethylene treatment in adult rosette tissues (Fig. 2.2). These results suggest, that even though the EIN3-GFP signal was still increasing after 2 hours of ethylene and submergence treatment, its absolute levels do not represent its downstream effects, as these were already saturated within 2 hours.

nterestingly, while ethylene-dependent EIN3 signaling was switched on rapidly upon ethylene treatments (Fig. 2.1A, B; Fig. S2.1), it was also strongly reduced again after 48 hours of continuous ethylene exposure (Fig. S2.1). This experiment was conducted under continuous ethylene exposure, which means that EIN3-signaling was down-regulated and not caused by the ethylene production itself. EIN3 proteolysis is mediated by EBF1 and EBF2 (Gagne *et al.*, 2004), and we observed enhanced *EBF2* transcripts upon ethylene exposure (Fig. 2.2). A plausible explanation is therefore that a gradual build-up of EBF2 during continuous ethylene mediates the EIN3 degradation we observed after 24 and 48 hours (Fig. S2.1). Down-regulation of long-term ethylene signaling could be an adaptive response under certain conditions as it interferes with growth responses and will ultimately stunt growth (Voesenek *et al.*, 2015). Furthermore, hypoxia did not clearly induce ethylene responses in our experiments, but did maintain EIN3 stability and downstream signaling (Fig. 2.1A, B & 2.2). Hypoxia impairs ethylene biosynthesis as the catalytic conversion of the ethylene pre-cursor 1-aminocyclopropane-1-carboxylate (ACC) to ethylene by ACC oxidase requires molecular $O_2$ (Guo & Ecker, 2004; Rocklin *et al.*, 2004). If ethylene signaling is important for hypoxia acclimation, it would be beneficial for the plant to maintain downstream EIN3 signaling independently of ethylene biosynthesis.



We investigated whether early ethylene signaling during submergence is indeed important for subsequent hypoxia acclimation. A pre-treatment with submergence or ethylene strongly increased root tip meristem survival during subsequent hypoxia (Fig. 2.3A). Ethylene signaling during submergence was fully responsible for the subsequent enhanced hypoxia acclimation, as the beneficial effect of a submergence pre-treatment was fully abolished in combination with the ethylene action inhibitor 1-MCP (Fig. 2.3A). Moreover, these results illustrate that the benefit of submergence-induced ethylene signaling for hypoxia acclimation can be fully mimicked by a short ethylene treatment (Fig. 2.3A). We therefore assessed whether a pre-treatment with ethylene could increase the survival of other Arabidopsis meristematic tissues. Similar to *R. palustris* (van Veen *et al.*, 2013), ethylene-mediated hypoxia survival is conserved in adult rosettes, in addition to seedling shoot, lateral and main root meristems of Arabidopsis (Fig. 2.4). In addition, ethylene-enhanced hypoxia survival is mediated through the established EIN3-dependent ethylene signaling pathway in both root tips and shoots as the benefits of ethylene were abolished in these ethylene signaling mutants (Fig. 2.3B & Fig. S2.2)(Guo & Ecker, 2004). Taken together, our results suggest that the Arabidopsis main root tip could be a representative organ to study the mechanism of ethylene-mediated hypoxia tolerance.

This is corroborated by the robustness of ethylene-mediated hypoxia tolerance in root tips. Differences in the developmental stage of the seedlings, light intensity, temperature and the severity of the hypoxia treatment did not drastically alter the beneficial effect of ethylene on subsequent hypoxia acclimation (Fig. 2.5). Surprisingly, variation between Arabidopsis accessions to benefit from ethylene as an early warning signal for hypoxia acclimation was limited (Fig. 2.6). These results imply that while Arabidopsis could be useful to unravel the mechanism of ethylene-mediated hypoxia tolerance, it does not explain the observed natural variation for submergence tolerance in whole plants across Arabidopsis accessions (Vashisht et al., 2011).

Still, ethylene is clearly important as an early signal to maximize hypoxia survival in most Arabidopsis meristematic tissues. This chain of events could be of crucial importance in natural situations where ethylene precedes severe hypoxia. For instance, when flooding and rapid passive ethylene entrapment occurs during the day and is followed by sudden anoxia at the onset of night due to lack of $O_2$ production (Colmer & Pedersen, 2008; Sasidharan *et al.*, 2018). The discovery of ethylene-mediated hypoxia tolerance could therefore have significant potential for

understanding how plants acclimate during early submergence and confer flooding tolerance. Finally, the observation that ethylene-mediated hypoxia tolerance in the Arabidopsis root tip is highly robust and representative for other plant organs, makes it a powerful and high-throughput experimental tool to unravel the molecular mechanism(s) of how ethylene prepares plants for hypoxia.

## ACKNOWLEDGEMENTS

We thank Emilie Reinen, Ankie Ammerlaan and Rob Welschen for technical assistance. We also kindly acknowledge the people named in the methods section for providing seeds of the genotypes used in this chapter.

## MATERIALS AND METHODS

### Plant material and growth conditions

Plant material: *Arabidopsis thaliana* seeds of ecotypes Col-0, Cvi-0, C24, Lp2-6, Ws-0, Shahdra, Bay-0 and mutants *ein2-5* and *ein3eil1-1* (Col-0 Background) (Alonso *et al.*, 1999, 2003) were obtained from the Nottingham Arabidopsis Stock Centre. Other germlines used in this study were kindly provided by the following individuals: Ler-0, from Prof. Angelika Mustroph (Gasch *et al.*, 2016) and *35S:EIN3-GFP* (*ein3eil1* mutant background) from Prof. Shi Xiao (Xie *et al.*, 2015). All mutant and transgenic lines were confirmed by either conventional genotyping PCRs and/or antibiotic resistance selection (Primer and additional info in Appendix I).

Growth conditions adult rosettes: Arabidopsis seeds of all reported genotypes were placed on potting soil (Primasta) in medium sized pots and stratified at 4°C in the dark for at least 3 days. Pots were then transferred to a growth chamber for germination under short day conditions (8:00 – 17:00, Temperature (T) = 20°C, Photosynthetic Photon Flux Density (PPFD) = ~150 µmol $m^{-2}s^{-1}$, Relative Humidity (RH) = 70%). After 7 days, seedlings were transplanted individually into single pots (70ml) that were filled with the similar potting soil (Primasta). Plants continued growing under identical short day conditions and were automatically watered daily to field capacity. Per genotype, homogeneous groups of 10-leaf-stage plants were selected and randomized over treatment groups for phenotypic and molecular analysis under various treatments. Plants used for these experiments were transferred back to the same growth room conditions after treatments to recover for 7 days.

Growth conditions seedlings: Seeds were vapor sterilized by incubation with a beaker containing a mixture of 50 ml bleach and 3 ml of 37% fuming HCl in a gas



tight desiccator jar for 3 to 4 hours. Seeds were then individually transplanted in (2 or 3) rows of 23 seeds on sterile square petri dishes containing 25 ml autoclaved and solidified ¼ MS, 1% plant agar without additional sucrose. Petri dishes were sealed with gas-permeable tape (Leukopor, Duchefa) and stratified at 4°C in the dark for 3 to 4 days. Seedlings were grown vertically on the agar plates under short day conditions (9:00 – 17:00, T= 20°C, PPFD = ~120 µmol $m^{-2}s^{-1}$, RH= 70%) for generally 5 days, except when stated otherwise in the figure legends.

### Experimental setup and (pre)treatments

Ethylene treatments: Pre-treatments were optimized for temperature, light conditions, ethylene concentration and duration (results are shown in Fig. 2.5 and Fig. S2.3). Lids of the agar plates of the vertically grown seedlings were removed during all (pre-) treatments and plates were placed vertically into glass desiccators (22.5 L volume). Air (control) and ~5µl$l^{-1}$ ethylene (pre-) treatments (by injection with a syringe) were applied at the start of the light period (9:00 for seedlings, 8:00 for adult rosettes) and were performed by keeping the seedlings/plants in air-tight closed glass desiccators under low light conditions (T= 20°C, PPFD = ~3-5 µmol $m^{-2}s^{-1}$) for 4 hours. Ethylene concentrations in all desiccators were verified by gas chromatography (Syntech Spectras GC955) at the beginning and end of the pre-treatment.

Hypoxia treatments: After 4 hours of any pre-treatment plants/seedlings were flushed with $O_2$-depleted air (humidified 100% $N_2$ gas) at a rate of 2.00 l/min under dark conditions to prevent oxygen production by photosynthesis. Oxygen levels generally reached 0.00% oxygen within 40 minutes of the hypoxia treatment as measured with a Neofox oxygen probe (Ocean optics, Florida, USA) (Appendix III). Control plants and seedlings were flushed with humidified air for the duration of the hypoxia treatment in the dark. Hypoxia treatment durations varied depending on the developmental stage and plant species and are specified in the appropriate figure legends.

1-MCP: Seedlings were placed in closed glass desiccators (22.5l volume) and exposed to 5µ$l^{-1}$ 1-MCP for 1 hour prior to other (pre-) treatments.

Submergence: For submergence (pre-) treatments, the plates of vertically grown seedlings were placed horizontally and were carefully filled with autoclaved tap water until the seedlings were fully submerged.

### Hypoxia tolerance assays

Adult rosette plants: 10-leaf stage plants received ethylene and air pre-treatments followed by several durations of hypoxia and were subsequently placed back under short day growth chamber conditions to recover. After 7 days of recovery survival rates (visual presence of green tissue in shoot meristem) and biomass (fresh and dry weight of green tissue of surviving plants) were determined.

Survival performance of seedlings: 5-day old seedlings grown vertically on agar plates received pre-treatments (described above) followed by several durations of hypoxia (generally 4 hours for mutant analysis). After the hypoxia treatment, agar plates were closed and sealed again with Leukopor tape and the location of root tips was marked at the back of the agar plate using a marker pen (0.8mm fine tip). Plates were then placed back (during the dark night period) vertically under short day growth conditions for recovery. After 3-4 days of recovery, seedling root tips were scored as either alive or dead based on clear root tip re-growth beyond the line on the back of the agar plate. Primary root tip survival was calculated as the percentage of seedlings that showed root tip re-growth out of a row of (maximally) 23 seedlings. Root tip survival was expressed as relative survival compared to control plates that received similar pre-treatments but no hypoxia. Seedlings of 10 days old were used to assess hypoxia survival of seedling primary roots, lateral roots and shoot meristems in Fig. 2.4A. Lateral roots were scored as described for primary root tip survival, whereas seedlings shoots were quantified as alive by visual presence of green tissue and the presence of new leaf formation in the shoot apical meristem.

### RNA extraction, RNA quantification, cDNA synthesis and RT-qPCR

Adult rosette (2 whole rosettes per sample) samples were harvested by snap freezing in liquid nitrogen. Total sample RNA was extracted from frozen pulverized tissue using the RNeasy Plant Mini Kit protocol (Qiagen, Dusseldorf, Germany) with on-column DNAse treatment Kit (Qiagen, Dusseldorf, Germany) and quantified using a NanoDrop ND-1000 UV-Vis spectrophotometer (Nanodrop Technology). Single-stranded cDNA was synthesized from 500 ng RNA using random hexamer primers (Invitrogen, Waltham, USA). RT-qPCR was performed using the Applied Biosystems ViiA 7 Real-Time PCR System (Thermo Fisher Scientific) with a 5µl reaction mixture containing 2.5µl 2× SYBR Green MasterMix (Bio-Rad, Hercules, USA), 0.25µL of both 10µM forward and reverse primers and 2µl cDNA (5ng/µl). Average sample CT values were derived from 2 technical replicates. Relative transcript abundance was calculated using the comparative CT method (Livak & Schmittgen, 2001), fold change was generally expressed as fold change relative to air treated samples of Col-0. *ADENINE PHOSPHORIBOSYL TRANSFERASE 1* (*APT1*) was amplified, stable in all treatments and used as a reference gene. Primers used for RT-qPCR can be found in Appendix II.





### Confocal Microscopy

Transgenic Arabidopsis seedlings of *35S:EIN3-GFP* were fixed in 4% paraformaldehyde (PFA) (pH 6.9) right after treatments, kept under gentle agitation for 1h, were subsequently washed twice for 1 min in 1 x phosphate-buffered saline (PBS) buffer and stored in ClearSee clearing solution (xylitol 10% (w/v), sodium deoxycholate 15% (w/v) and urea 25% (w/v) (Ursache *et al.*, 2018). Seedlings were transferred to 0.01% Calcofluor White (in ClearSee solution) 24 hours before imaging. Fluorescence was visualized using a Zeiss Observer Z1 LSM700 confocal microscope (oil immersion, 40x objective Plan-Neofluar N.A. 1.30) with excitation at 488nm and emission at 490-555nm for GFP and excitation at 405 nm and emission at 400-490 nm for Calcofluor White. Within experiments, laser power, pinhole, digital gain and detector offset were identical for all samples. Mean GFP fluorescence pixel intensity in root tips was determined in similar areas of ~17000 $\mu m^2$ between epidermis layers using ICY software (http://icy.bioimageanalysis.org/).

### Statistical analyses

Data was plotted using Graphpad Prism software. The statistical tests were performed using either Graphpad Prism or R software and the "LSmeans and "multmultcompView" packages. Survival data was analyzed with either a generalized linear modeling (GLM) approach or an Analyses of Variances (ANOVA) on arcsin transformation of the surviving fraction. A negative binomial error structure was used for the GLM. Arcsin transformation ensured a homogeneity and normal distribution of the variances, especially for data that did not have treatments with all living or all death responses. The remaining data were analyzed with either Students t-test, 1-way or 2-way ANOVAs. Here data were log transformed if necessary to adhere to ANOVA prerequisites. Multiple comparisons were corrected for with Tukey's honestly significant difference (HSD).

## SUPPLEMENTAL FIGURES

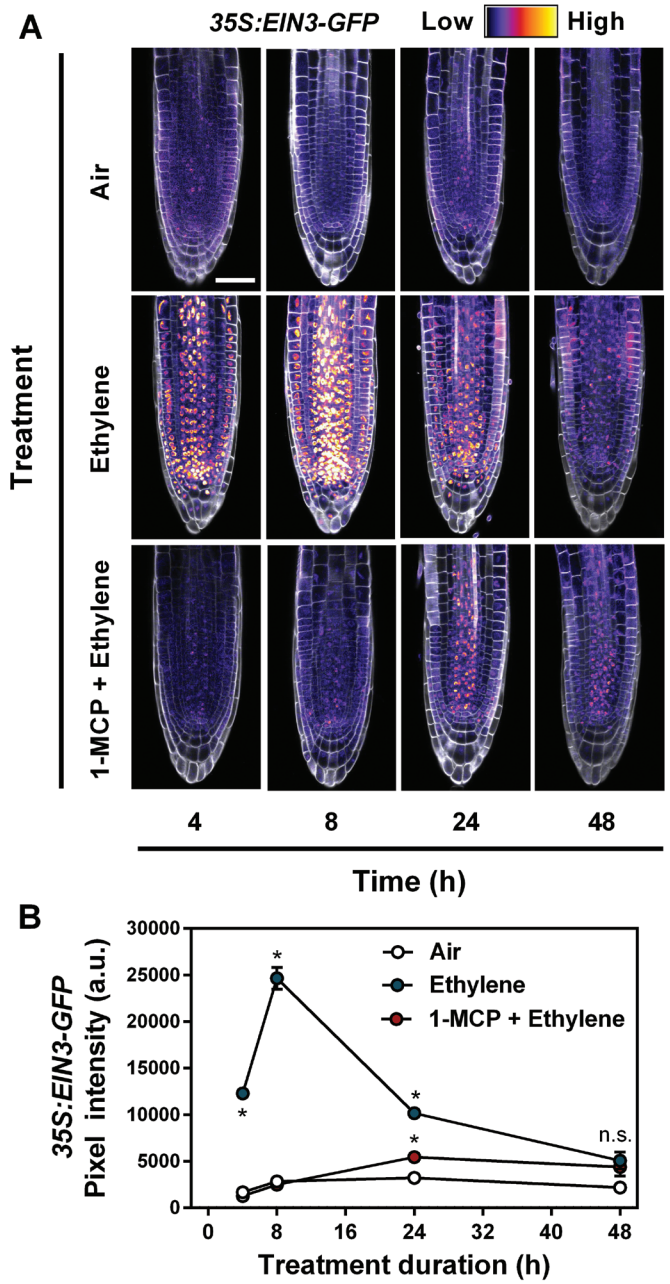


**Figure S2.1. Effects of ethylene and the ethylene antagonist 1-MCP on temporal EIN3 signaling dynamics.**

**(A, B)** Representative confocal images **(A)** and quantification **(B)** of protein stability and localization of the ethylene master regulator EIN3, using the *35S:EIN3-GFP* (*ein3eil1* background) signal in Arabidopsis root tips. Seedlings were treated for up to 48 hours with air, ~5µll$^{-1}$ ethylene or ethylene action inhibitor 1-MCP followed by 5µll$^{-1}$ ethylene. Cell walls were visualized using Calcofluor White stain (**(A)** scale bar= 50µm). **(B)** Mean GFP pixel intensity inside the root tips was quantified using ICY imaging software. Asterisks indicate a significant difference of treatments compared to air treatment, per time-point (Error bars are SEM, p<0.05, 1-way ANOVA, Tukey's HSD, n=2-4 roots).



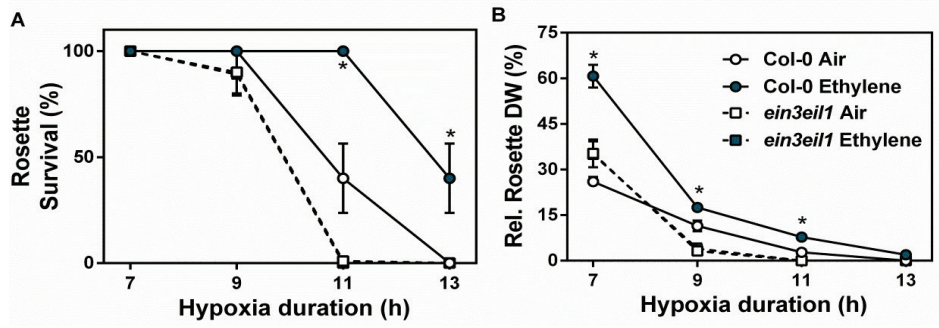


**Figure S2.2. Ethylene-induced hypoxia tolerance is mediated by EIN3 and EIL1**

**(A, B)** Arabidopsis adult rosette survival and dry weight (DW) of survived Col-0 and ethylene signaling impaired mutant *ein3eil1* plants after 4 hours of air (white) or ~5µll$^{-1}$ ethylene (blue) followed by hypoxia and 7 days of recovery. Values are relative to control (normoxia) plants. Asterisks indicate significant differences between air and ethylene in Col-0. Data points of *ein3eil1* are close to identical and therefore difficult to discriminate. No significant differences were found in *ein3eil1* (Error bars are SEM, p<0.05, Generalized linear model, negative binomial error structure, n=10 plants).

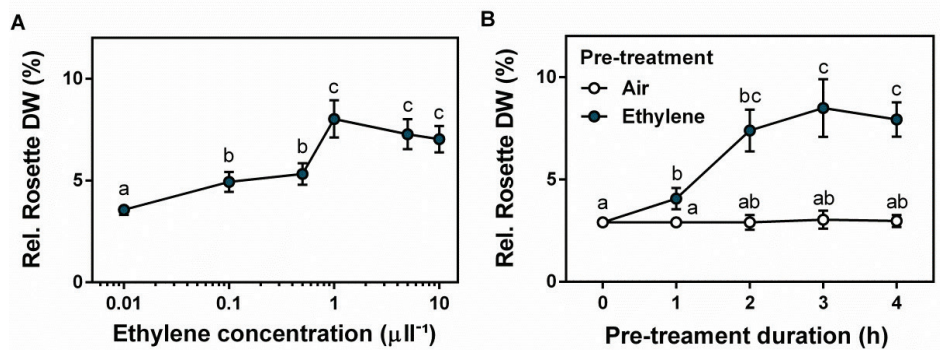


**Figure S2.3. Optimal ethylene concentration and duration for enhanced hypoxia tolerance.**

**(A)** Arabidopsis adult rosette dry weight (DW) of survived Col-0 plants after 4 hours of varying ethylene concentrations followed by 9 hours of hypoxia and 7 days of recovery. Values are relative to control (normoxia) plants. Statistically similar groups are indicated using the same letter (Error bars are SEM, p<0.05, 1-way ANOVA, Tukey's HSD, n=10 plants). **(B)** Arabidopsis adult rosette dry weight (DW) of survived Col-0 plants after varying durations of air (white) or ~5µll$^{-1}$ ethylene (blue) pre-treatments followed by 9 hours of hypoxia and 7 days of recovery. Values are relative to control (normoxia) plants. Statistically similar groups are indicated using the same letter (Error bars are SEM, p<0.05, 2-way ANOVA, Tukey's HSD, n=10 plants).

# CHAPTER 3

## ETHYLENE AUGMENTS THE HYPOXIA RESPONSE THROUGH GROUP VII ETHYLENE RESPONSE FACTORS


Sjon Hartman[1]
Zeguang Liu[1]
Nienke van Dongen[1]
Shanice Martopawiro[1]
Hans van Veen[1]
Emilie Reinen[1]
Eric J.W. Visser[2]
Michael J. Holdsworth[3]*
Rashmi Sasidharan[1]*
Laurentius A.C.J. Voesenek[1]*


**MODIFIED EXCERPTS OF THIS CHAPTER ARE PUBLISHED IN:**

- Hartman, S., *et al.* (2019). Ethylene-mediated nitric oxide depletion pre-adapts plants to hypoxia stress, Nature Communications, 10 (1), 4020.


[1] Plant Ecophysiology, Institute of Environmental Biology, Utrecht University, Utrecht, The Netherlands
[2] Department of Experimental Plant Ecology, Institute for Water and Wetland Research, Radboud University Nijmegen, Nijmegen, the Netherlands
[3] School of Biosciences, University of Nottingham, Loughborough, United Kingdom

*Shared senior authors

## ABSTRACT

Submerged plants ultimately experience oxygen (O2) deprivation (hypoxia) as a consequence of the impaired gas diffusion under water. Timely perception of submergence is therefore critical to activate molecular responses that enhance hypoxia survival. In Arabidopsis thaliana, changes in O2 and nitric oxide (NO) levels control the stability of group VII Ethylene Response Factor (ERFVII) transcription factors. ERFVII proteolysis is regulated by the N-degron pathway and controls the adaptive transcriptional hypoxia response. Interestingly, passively entrapped ethylene in submerged plant tissues was shown to lead to rapid ethylene signaling that subsequently acclimates plants to impending hypoxia stress. With the aim to uncover the molecular mechanism of how ethylene prepares plants for hypoxia stress, we followed the effects of ethylene on ERFVIIs and the associated transcriptional hypoxia response. Our results show that ethylene pre-treatment augments the hypoxia response when O2 levels decline. Furthermore, we reveal that ethylene-mediated hypoxia tolerance is controlled by the ERFVIIs RELATED TO APETALA2.2 (RAP2.2) and RAP2.12. Finally, we demonstrate that ethylene can stabilize ERFVIIs prior to hypoxia through impairment of NO-dependent ERFVII proteolysis. We conclude that ethylene-mediated NO depletion and consequent ERFVII accumulation primes the transcriptional hypoxia response and pre-adapts plants to survive subsequent hypoxia.




## INTRODUCTION

The increasing frequency of floods due to climate change has devastating effects on agricultural productivity worldwide (Hirabayashi *et al.*, 2013; Voesenek & Bailey-Serres, 2015a). Due to the restricted gas diffusion underwater, flooded terrestrial plants ultimately experience cellular oxygen ($O_2$) deprivation (hypoxia) and survival strongly depends on molecular responses that enhance hypoxia tolerance (Shiono *et al.*, 2008; Voesenek & Bailey-Serres, 2015a). In submerged plant tissues, limited gas diffusion also causes passive ethylene accumulation. This rapid ethylene build-up can occur prior to the onset of severe hypoxia, making it a timely and reliable signal for submergence (Chapter 2, Voesenek and Sasidharan, 2013; Sasidharan *et al.*, 2018). Ethylene is known to regulate many adaptive responses to flooding that involve morphological and anatomical modifications that prevent hypoxia (Voesenek & Sasidharan, 2013). However, recent findings in the wetland species *Rumex palustris* and model species *Arabidopsis thaliana* suggest that ethylene can also enhance metabolic adaptation to hypoxia (Veen *et al.*, 2013; Chapter 2). In *R. palustris* this ethylene-mediated hypoxia tolerance correlated with the enhanced induction of core hypoxia gene orthologues (van Veen *et al.*, 2013). Also in Arabidopsis, ethylene is thought to be required for adequate induction of hypoxia-induced fermentation pathways (Peng, 2001; Tesniere *et al.*, 2004).

In order to unravel how ethylene confers hypoxia tolerance, it is key to understand how ethylene mediates the transcriptional hypoxia response in plants. In Arabidopsis, hypoxia acclimation includes the up-regulation of 49 genes; the so-called core hypoxia genes (Mustroph *et al.*, 2009). This core hypoxia-adaptive gene set includes genes that control fermentation, carbohydrate metabolism, energy maintenance, ethylene biosynthesis, hypoxia signalling and oxidative stress homeostasis (Mustroph *et al.*, 2009, 2010). In completely submerged Arabidopsis plants of the ecotype Col-0, 34 of these genes show a similar induction response, suggesting a strong overlapping transcriptional pattern for hypoxia and submergence acclimation (Lee *et al.*, 2011). Hypoxia adaptive genes are largely regulated by group VII Ethylene Response Factor transcription factors (ERFVIIs), which are components of a mechanism that senses $O_2$ and nitric oxide (NO) via the cysteine-branch of the PROTEOLYSIS 6 (PRT6) N-degron pathway (Gibbs *et al.*, 2011, 2014; Licausi *et al.*, 2011). The constitutively synthesized ERVIIs RELATED TO APETALA2.12 (RAP2.12) and RAP2.2 redundantly act as the principal activators of many hypoxia adaptive genes by binding to an evolutionarily conserved 12-basepair cis-regulatory motif called the Hypoxia Responsive Promoter Element (HRPE) (Hinz *et al.*, 2010; Gasch *et al.*, 2016). RAP2.3 is suggested to contribute to this redundancy, while

two other ERFVIIs, *HYPOXIA RESPONSIVE ERF1* (*HRE*1) and *HRE2,* are thought to play a minor role in hypoxia gene regulation (Licausi *et al.*, 2010a; Bui *et al.*, 2015; Gasch *et al.*, 2016).

The ERFVIIs contain a conserved N-terminal (Nt) sequence of Methionine-Cysteine (MC), which functions as an N-degron through the arginylation(Arg)/N-degron pathway of proteolysis in the presence of both $O_2$ and NO (Gibbs *et al.*, 2011, 2014; Licausi *et al.*, 2011). Following constitutive cleavage of the $Met_1$ by methionine aminopeptidases (MetAPs), the exposed $Cys_2$ is oxidized in the presence of $O_2$ by plant cysteine oxidases (PCOs) to Cys-sulphinate or Cys-sulphonate (White *et al.*, 2017; Varshavsky, 2019). After subsequent arginylation through arginyl tRNA transferases (ATEs), the Nt is recognised by the E3 ligase PRT6 that flags the protein for ubiquitination and subsequent degradation (Varshavsky, 2019). Accordingly, a decline in either $O_2$ or NO stabilizes ERFVIIs, leading to transcriptional up-regulation of hypoxia adaptive genes (Gibbs *et al.*, 2011, 2014; Licausi *et al.*, 2011).

Several additional processes have been reported to mediate ERFVII stability and action. Under normal oxygen conditions (21%; normoxia), the ERFVII RAP2.12 can be protected from the PRT6 N-degron pathway through sequestration at the plasma membrane via direct binding with ACYL-COA BINDING PROTEINs (ACBPs) (Licausi *et al.*, 2011; Schmidt & van Dongen, 2019). Upon hypoxia, a drop in ATP levels and LONG-CHAIN ACYL-COA SYNTHETASEs (LACS) activity causes RAP2.12 to dissociate from the membrane-bound ACBPs and allows subsequent hypoxia-specific target gene expression (Schmidt *et al.*, 2018). Furthermore, SEVEN IN ABSENTIA (SINAT1) and SINAT2 were shown to impair RAP2.2 and RAP2.12 stability independently of the PRT6 N-degron pathway (Wu, 2002; Papdi *et al.*, 2015). Moreover, OCTADECANOID-RESPONSIVE ARABIDOPSIS 59 (ORA59) was recently discovered to regulate ethylene-dependent nuclear localisation of RAP2.3 (Kim *et al.*, 2018). Finally, multiple studies suggest that transcription of several ERFVIIs is ethylene-mediated. Indeed, transcript abundance of *HRE1* increased upon ethylene exposure and RAP2.3 was shown to be a target of ethylene master regulator ETHYLENE INSENSITIVE3 (EIN3) (Hess *et al.*, 2011; Chang *et al.*, 2013). In *R. palustris*, the orthologue of RAP2.12 was enhanced upon ethylene treatment (van Veen *et al.*, 2013). Taken together, these data suggest that ethylene controls several ERFVIIs at the transcriptional level and could accordingly facilitate hypoxia-induced fermentation pathways.



In chapter 2 we show that ethylene is an early flooding signal that acclimates Arabidopsis plants to hypoxia. To unravel how ethylene mediates hypoxia tolerance, we studied the core hypoxia transcriptional response in Arabidopsis after ethylene pre-treatment. In addition, we assessed whether ethylene-enhanced hypoxia tolerance is ERFVII dependent and to what extent ethylene modulates ERFVII transcript and protein levels. Our results reveal that ethylene has little effect on the hypoxia response alone, but strongly enhances the hypoxia response after a subsequent decline in $O_2$ levels. Furthermore, we show that ethylene-mediated hypoxia tolerance is largely dependent on RAP2.2 and RAP2.12. Finally, we discovered that ethylene can enhance ERFVII stability prior to hypoxia by limiting NO-dependent proteolysis. We conclude that ethylene pre-adapts Arabidopsis plants to hypoxia stress through an augmented hypoxia response that is ERFVII dependent.



## RESULTS

### Ethylene enhances the transcriptional hypoxia response when O2 levels decline

In order to reveal how ethylene confers hypoxia tolerance in Arabidopsis, we monitored the transcript abundance of several hypoxia adaptive genes during treatments with air, ethylene, ethylene followed by hypoxia, and hypoxia alone. Ethylene treatment rapidly increased *ETHYLENE RESPONSE 2* (*ETR2*), *ACC OXIDASE 1* (*ACO1*) and *PHYTOGLOBIN* (*PGB1*) transcripts in Arabidopsis rosette and seedling root tip tissues, but had little to no effect on the majority of other hypoxia genes tested (Fig. 2.2, 3.1 & 3.2). However, ethylene pre-treatment strongly enhanced the transcript abundance of hypoxia adaptive genes when $O_2$ levels declined (Fig. 3.1 & 3.2). Surprisingly, hypoxia alone had only a limited effect on hypoxia-regulated genes in adult rosette tissues, but the hypoxia response was strongly augmented following an ethylene pre-treatment (Fig. 3.1). Additionally, hypoxia strongly increased transcript levels in seedling root tips, and also here ethylene stimulated this response (Fig. 3.2). Together, these results suggest that ethylene primes the hypoxia-induced transcriptional response of hypoxia adaptive genes.

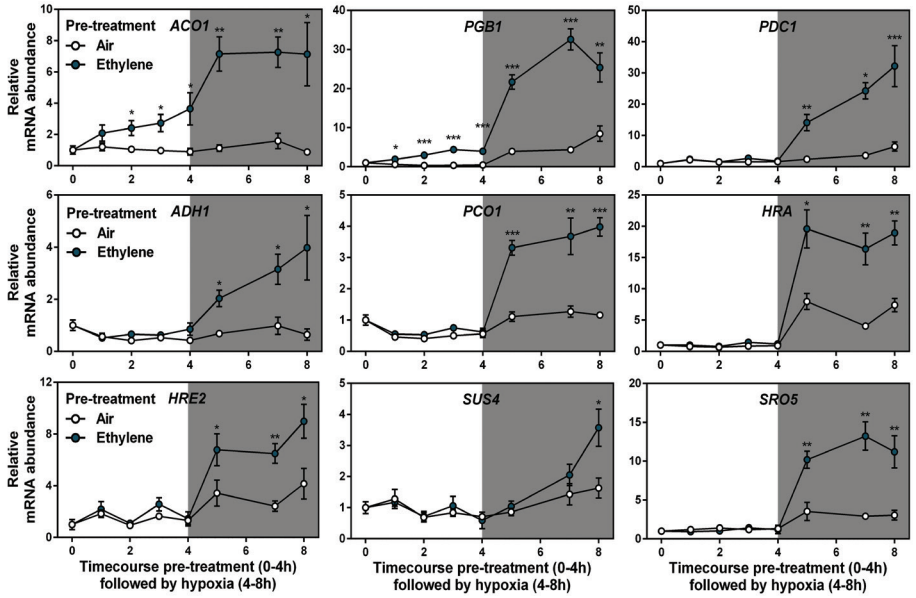


**Figure 3.1. Ethylene pre-treatment augments hypoxia adaptive gene transcripts upon hypoxia in adult rosette tissues.**

Relative mRNA transcript abundance of 9 hypoxia adaptive genes in adult rosettes of Col-0 during 4 hours of pre-treatment with air (white) or ~5µll$^{-1}$ ethylene (blue), followed by 4 hours of hypoxia. Values are relative to air treated samples at t=0. Asterisks indicate significant differences between air and ethylene (Error bars are SEM, *p<0.05, **p<0.01, ***p<0.001, 1- Way ANOVA with planned comparisons, Tukey's HSD correction for multiple comparisons, n=5 replicates of 2 rosettes).

## Ethylene-mediated hypoxia tolerance redundantly involves RAP2.2 and RAP2.12

The majority of the core hypoxia genes are controlled by constitutively expressed ERFVII transcription factors (Bui *et al.*, 2015; Gasch *et al.*, 2016). Therefore, we explored whether ethylene-mediated hypoxia tolerance of Arabidopsis seedling root tips is ERFVII dependent. Single loss-of-function mutants of *RAP2.12*, *RAP2.3*, and the *hre1 hre2* double mutant, responded to ethylene pre-treatment similarly as their Col-0 wildtype (WT) backgrounds (Fig. 3.3A). Interestingly, a knock-out mutant of *RAP2.2* showed reduced hypoxia tolerance compared to its Ler-0 WT background, but still benefited from an ethylene pre-treatment. However, two independent *rap2.2rap2.12* loss-of-function double mutants showed no improved hypoxia tolerance after ethylene pre-treatment (Fig. 3.3B, C), while their WT background crosses did (Fig. 3.3B). Finally, overexpression of a stable N-terminal variant of RAP2.12 and inhibition of the PRT6 N-degron pathway in the *prt6-1* mutant both enhanced hypoxia tolerance without an ethylene pre-treatment (Fig. 3.3C). These data suggest that ethylene-induced hypoxia tolerance occurs through the PRT6 N-degron pathway and redundantly involves at least RAP2.2 and RAP2.12.



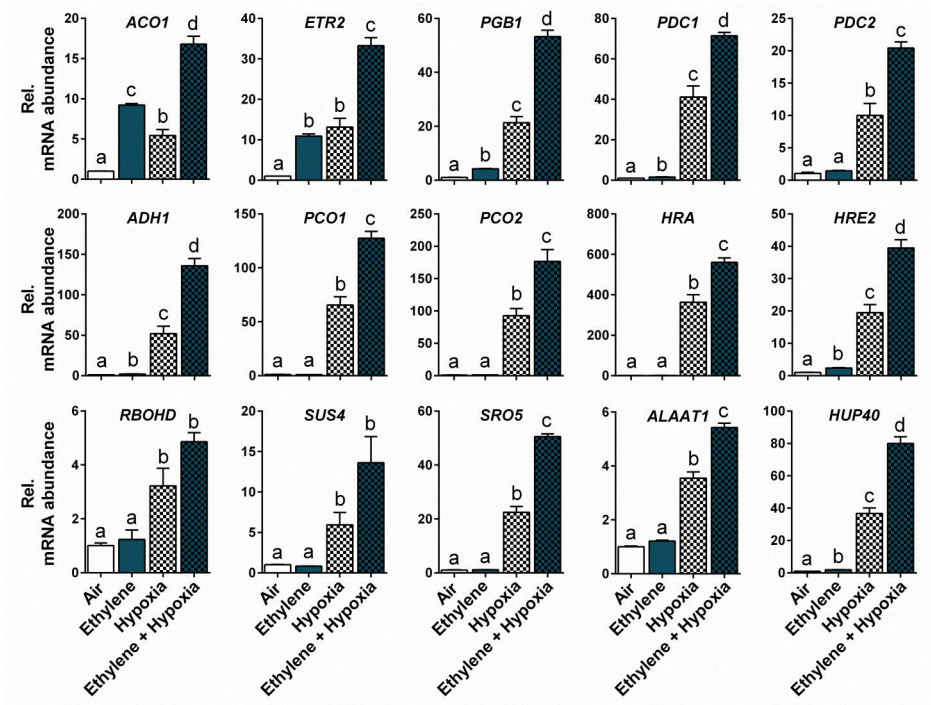


**Figure 3.2. Ethylene pre-treatment augments hypoxia adaptive gene transcripts upon hypoxia in seedling root tips.**

Relative mRNA transcript abundance of 15 hypoxia adaptive genes in seedling root tips of Col-0 after 4 hours of pre-treatment with air (white) or ~5µll$^{-1}$ ethylene (blue), followed by (4h) hypoxia (blocks). Values are relative to air treated samples. Different letters indicate significant differences (Error bars are SEM, p<0.05, 1-way ANOVA, Tukey's HSD, n=3-4 replicates containing ~400 root tips).

## Ethylene enhances ERFVII transcript and protein abundance

Next we explored whether ethylene regulates ERFVII mRNA and protein abundance. Ethylene increased *RAP2.12*, *RAP2.2* and *RAP2.3* mRNAs in adult rosette tissues and *RAP2.2*, *RAP2.3*, *HRE1* and *HRE2* transcripts in seedling root tips (Fig. 3.4A, B). Since ERFVII levels are strongly regulated through post-translational modification (Gibbs *et al.*, 2011; Licausi *et al.*, 2011), we used multiple techniques to also assess ERFVII protein stability in response to ethylene. Visualization and quantification of RAP2.12 abundance using transgenic *promRAP2.12:RAP2.12-GUS* and *35S:RAP2.12-GFP* protein-fusion lines revealed that ethylene strongly enhanced RAP2.12 protein abundance under normoxia in meristematic zones of seedling shoots, main root tips and lateral root tips (Fig. 3.4C, D, Fig. 3.5). In addition, Western Blot analysis of *35S:RAP2.3-HA* showed that ethylene increased RAP2.3 levels in whole Arabidopsis seedlings (Fig. 3.4E). Subsequent hypoxia treatments further increased RAP2.3 and RAP2.12 protein levels (Fig. 3.4E, Fig. 3.5). Interestingly,

ethylene-mediated RAP2.12 stabilization in root tips appeared within nuclei across most cell types and was independent of ethylene-enhanced RAP2.12 transcript abundance (Fig. 3.4B, C). Moreover, since *35S:RAP2.12-GFP* and *35S:RAP2.3-HA* are uncoupled from ethylene-triggered transcription, our data suggests that ethylene-enhanced ERFVII accumulation is regulated by post-translational processes.

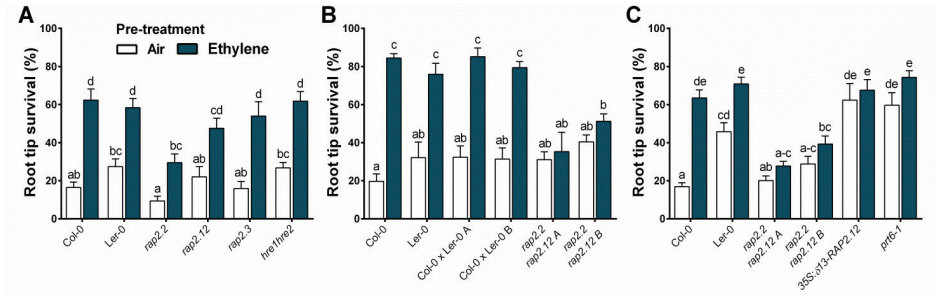


**Figure 3.3. Ethylene-induced hypoxia tolerance is regulated by RAP2.2 and RAP2.12.**
**(A-C)** Seedling root tip survival of Col-0, Ler-0, ERFVII mutants *rap2.2* (Ler-0 background), *rap2.12*, *rap2.3* and *hre1hre2* (all Col-0 background) in **(A)**, Col-0, Ler-0, 2 Col-0 x Ler-0 WT crosses and ERFVII double mutants *rap2.2rap2.12* (2 independent lines in Col-0 x Ler-0 background) in **(B)** and Col-0, Ler-0, *rap2.2rap2.12*, a constitutively expressed stable version of RAP2.12 and N-degron pathway mutant *prt6-1* in **(C)**, after 4 hours air or ~5µll$^{-1}$ ethylene followed by 4 hours of hypoxia and 3 days recovery. Values are relative to control (normoxia) plants (mean ± sem). Statistically similar groups are indicated using the same letter (p<0.05, 2-way ANOVA, Tukey's HSD, n=4-21 rows in A, n=8 rows in B, n=20-28 rows in C, with every row containing ~23 seedlings).

## Ethylene limits ERFVII proteolysis through NO depletion

In order to investigate how ethylene enhances ERFVII stability under ambient $O_2$, we studied the effect of ethylene on mRNA transcripts of genes known to encode PRT6 N-degron pathway enzymes. In addition, we assessed whether genes encoding proteins known to shield RAP2.12 from proteolysis, the ACBPs, are differentially regulated by ethylene. In response to ethylene, none of these genes showed changes in transcript abundance (Fig. 3.6A, B). Accordingly, a loss-of-function mutant of ACBP1 showed similar responses for ethylene-mediated hypoxia root tip survival compared to its WT background (Fig. 3.6C). Interestingly, a loss-of-function mutant of ORA59, which is impaired in ethylene-mediated nuclear localisation of RAP2.3 (Kim *et al.*, 2018), showed a mild but significant reduction in ethylene-mediated hypoxia tolerance compared to Col-0 (Fig. 3.6C). However, over-expression of ORA59 did not alter the hypoxia tolerance compared to its WT background (Fig. 3.6C). While these data suggest that ORA59 might be involved in ethylene-mediated hypoxia tolerance, it does not explain the observed enhanced ERFVII stability under ambient $O_2$.



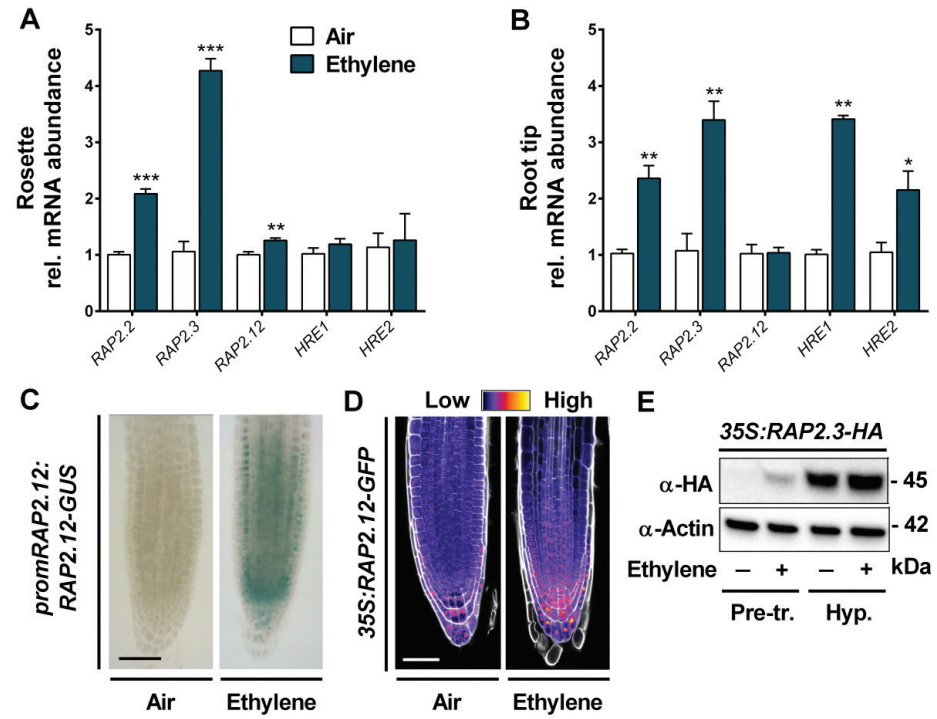


**Figure 3.4. Ethylene mediates ERFVII transcript and protein levels.**
**(A, B)** Relative mRNA transcript abundance of all 5 ERFVIIs in adult rosette shoots **(A)** and root tips of Col-0 seedlings **(B)** after 4 hours of treatment with air (white) or ~5µll$^{-1}$ ethylene (blue). Asterisks indicate significant differences between air and ethylene (Error bars are SEM,*p<0.05, **p<0.01, ***p<0.001, Student's t-Test, n=5 replicates of 2 rosettes for A, n=3-4 replicates containing 200 root tips for B). **(C, D)** Representative root tip images showing representative *promRAP2.12:RAP2.12-GUS* staining **(C)** and confocal images of *35S:RAP2.12-GFP* intensity **(D)** in seedling root tips after 4 hours of air or ~5µll$^{-1}$ ethylene. Cell walls were visualized using Calcofluor White stain (D). Scale bar is 50µm. **(E)** RAP2.3 protein levels in 10-day old *35S:RAP2.3-HA* seedlings (Col-0) after 4 hours of air and ethylene treatments followed by 4 hours of hypoxia.

As both $O_2$ and NO promote ERFVII proteolysis (Gibbs *et al.*, 2015), and since ethylene was administered at normoxia and did not lead to hypoxia in desiccators (Appendix III), it is unlikely that hypoxia causes the observed ERFVII stabilization. Since NO was previously shown to control proteolysis of ERFVIIs (Gibbs *et al.*, 2014), we hypothesized that ethylene could reduce NO levels. Roots treated with the NO probe 4-amino-5-methylamino-2′,7′-difluorofluorescein (DAF-FM) diacetate (Planchet & Kaiser, 2006) revealed an ethylene-induced reduction in fluorescence, indicating that ethylene can impair NO levels (Fig. 3.7A, B). Next, we investigated whether this decline in NO is indeed required for ethylene-mediated hypoxia tolerance and ERFVII stabilization. In order to do so, we first assessed if and which concentrations of NO gas impairs ethylene-mediated hypoxia tolerance

in Arabidopsis root tips. Applying concentrations of 25 µll$^{-1}$ NO gas and higher into the treatment desiccators appeared to be toxic, as they strongly impaired seedling survival (Fig. S3.1A). Simultaneous injection of 1 or 10 µll$^{-1}$ NO at the start of the ethylene pre-treatment did not affect hypoxia root tip survival. However, injecting a 10 µll$^{-1}$ NO pulse 3 hours into the ethylene pre-treatment (1 hour prior to hypoxia) consistently reduced ethylene-mediated hypoxia survival, but had no effect on basal hypoxia tolerance (Fig. S3.1A). Conversely, we tested whether ethylene-independent NO removal prior to hypoxia could enhance subsequent hypoxia tolerance. Applying 5 µl droplets of the NO-scavenging compound 2-(4-carboxyphenyl)-4,4,5,5-tetramethylimidazoline-1-oxyl-3-oxide (cPTIO) directly on single Arabidopsis root tips 4 hours prior to hypoxia enhanced subsequent hypoxia survival compared to mock pre-treatments (Fig. S3.1B). Either single or double application of two different concentrations of cPTIO (250 µM or 500 µM) led to similar enhanced hypoxia tolerance (Fig. S3.1B). With this in mind, we used either application of a 10 µll$^{-1}$ NO pulse during, or application of 250 µM cPTIO prior to the air and ethylene pre-treatments to unravel the effects of ethylene-mediated NO depletion on ERFVII stabilization and ERFVII-dependent ethylene-mediated hypoxia tolerance.

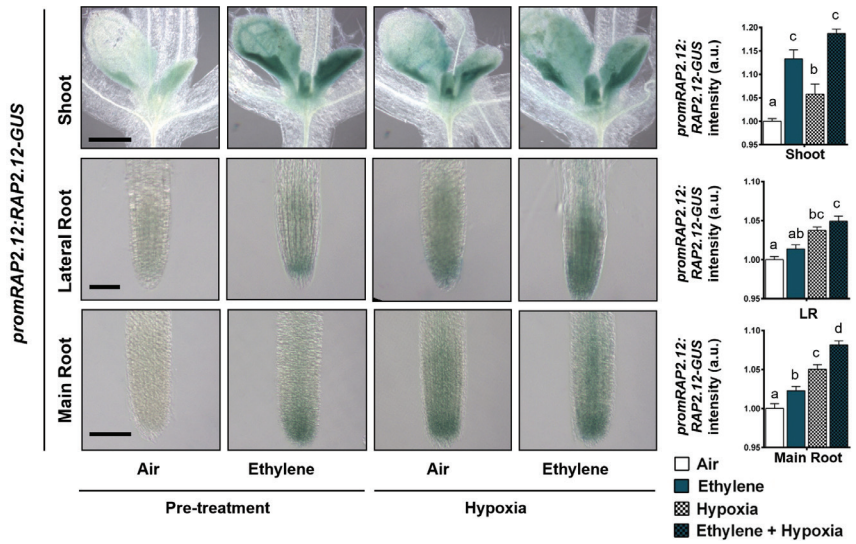


**Figure 3.5. Ethylene enhances RAP2.12 protein levels in meristematic tissues.**
Representative DIC microscopy images and quantification of *promRAP2.12:RAP2.12-GUS* in 10-day old seedling shoots, lateral roots and main root tips after 4 hours of treatment with air (white) or ~5µll$^{-1}$ ethylene (blue) or subsequent (4h) hypoxia (block pattern). Scale bars; shoot = 180µm, lateral root = 60µm, main root = 100µm. Values are relative to air treated samples. Statistically similar groups are indicated using the same letter per tissue (Error bars are SEM, p<0.05, 1-way ANOVA, Tukey's HSD, n=5-20 replicates).



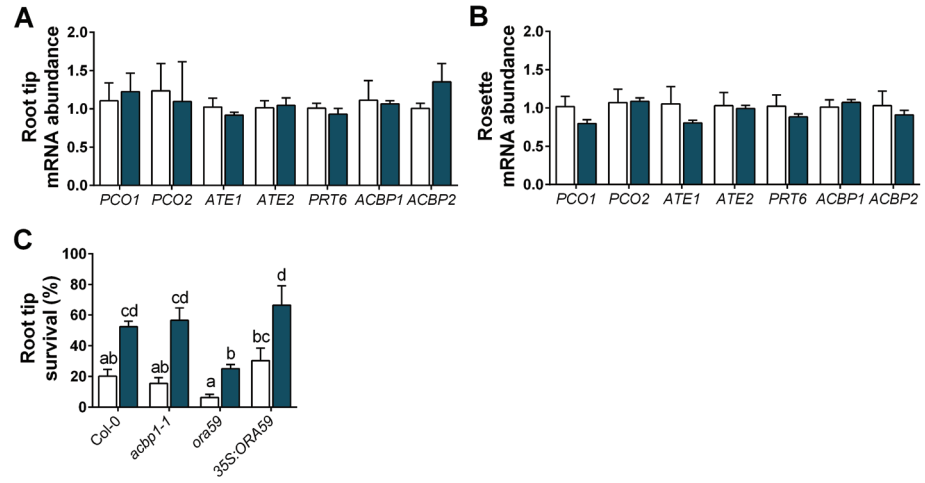


**Figure 3.6. The effects of ethylene on processes known to control ERFVII stability and function.**
**(A, B)** Relative mRNA transcript abundance of genes encoding enzymes involved in the PRT6 N-degron pathway or RAP2.12-sequestering proteins ACBP1 and ACBP2 in root tips of Col-0 seedlings **(A)** and adult rosettes **(B)** after 4 hours of treatment with air (white) or ~5µll$^{-1}$ ethylene (blue). Values are relative to Col-0 air treated samples. No significant differences were found between air and ethylene (Error bars are SEM, Student's t test, n=3-4 replicates containing ~200 root tips for A, n=5 replicates of 2 rosettes for B). **(C)** Seedling root tip survival of Col-0, *acbp1-1*, *ora59* and *35S:ORA59* after 4 hours air or ~5µll$^{-1}$ ethylene followed by 4 hours of hypoxia and 3 days recovery. Values are relative to control (normoxia) plants (mean ± sem). Statistically similar groups are indicated using the same letter (p<0.05, 2-way ANOVA, Tukey's HSD, n=8-12 rows containing ~23 seedlings).

Both ethylene and cPTIO increased RAP2.12 and RAP2.3 stability in Arabidopsis root tips under normoxia (Fig. 3.7C-E). However, the ethylene-mediated increase in RAP2.12 and RAP2.3 stability was abolished when an NO pulse was applied concomitantly suggesting a role for NO depletion in ethylene-triggered ERFVII stabilization of both these RAPs during normoxia. Application of hypoxia after pre-treatments resulted in stabilization of RAP2.12, demonstrating that the plants were viable and the PRT6 N-degron pathway could still be impaired (Fig. 3.7C-E). These data together illustrate that enhanced stability of both RAP2.12 and RAP2.3 depends on ethylene-mediated NO-depletion. In addition, we assessed the functional consequences of ethylene-induced NO-dependent RAP2.12 stabilization for hypoxia acclimation using the root meristem survival assay. Ethylene pre-treatment enhanced hypoxia survival, which was largely abolished by an NO pulse (Fig. 3.7F). Furthermore, pre-treatment with cPTIO to scavenge intracellular NO before hypoxia resulted in increased survival in the absence of ethylene.

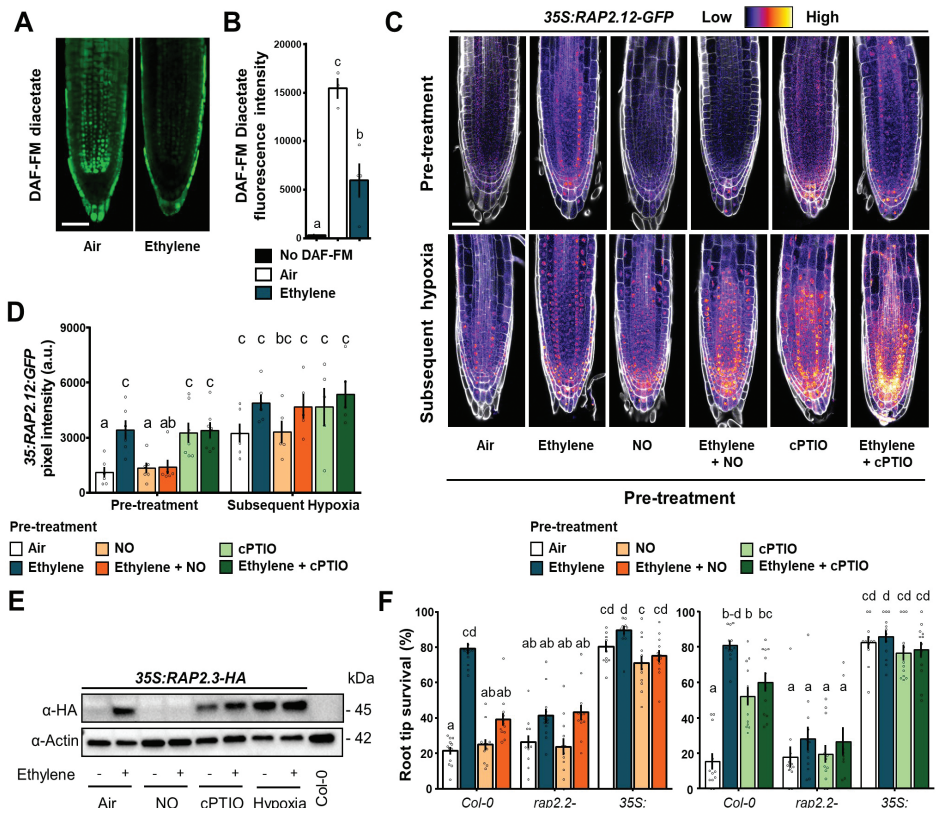


**Figure 3.7. Ethylene-mediated NO depletion leads to ERFVII stability and enhanced hypoxia survival. (A, B)**
Representative confocal images visualizing **(A)** and quantifying **(B)** NO, using fluorescent probe DAF-FM diacetate in Col-0 seedling root tips after 4 hours of air or ~5µll$^{-1}$ ethylene (scale bar = 50µm). (Letters indicate significant differences (1-way ANOVA, Tukey's HSD, n=3-5). **(C, D)** Representative confocal images visualizing **(C)** and quantifying **(D)** *35S::RAP2.12-GFP* intensity in seedling root tips after indicated pre-treatments and subsequent hypoxia (4h). Cell walls were visualized using Calcofluor White stain (scale bar = 50µm). (Letters indicate significant differences ($p<0.05$, 2-way ANOVA, Tukey's HSD, n=5-7). **(E)** RAP2.3 protein levels in 35S::MC-RAP2.3-HA seedlings (Col-0) after indicated treatments. **(F)** Seedling root tip survival of Col-0, *rap2.2rap2.12*-A and an over-expressed stable version of RAP2.12 after indicated pre-treatments followed by hypoxia (4h) and 3 days recovery. Values are relative to control (normoxia) plants. Letters indicate significant differences ($p<0.05$, 2-way ANOVA, Tukey's HSD, n=12 rows of ~23 seedlings). All data shown are mean ± sem.

However, in genotypes lacking both RAP2.12 and RAP2.2, in a line overexpressing a stable N-terminal variant of RAP2.12 and in PRT6 N-degron pathway mutant *prt6-1*, neither ethylene nor NO manipulation had any effect on subsequent hypoxia survival (Fig. 3.7F, S3.2). These results demonstrate that local NO removal, through cPTIO application or as a result of elevated ethylene, is both essential and sufficient to enhance RAP2.12 and RAP2.3 stability during normoxia, and that increased



hypoxia tolerance conferred by ethylene strongly depends on NO-mediated stabilization of RAP2.12 and RAP2.2 prior to hypoxia. Finally, to assess whether ethylene-mediated NO depletion is also required for ERFVII stability and hypoxia acclimation in Arabidopsis shoots, we performed NO manipulation experiments on adult rosettes and 10-day old seedlings. In both adult rosettes and seedling shoots, NO application during the ethylene pre-treatment reduced subsequent hypoxia tolerance (Fig. S3.3A, B). In seedlings shoot meristems, this impaired survival correlated with reduced RAP2.12 stability (Fig. S3.3C). Together our results suggest that ethylene can impair NO-dependent ERFVII proteolysis under normoxia which in turn primes the transcriptional hypoxia response and enhanced hypoxia survival in Arabidopsis.

## DISCUSSION

Ethylene is a fast and reliable signal upon submergence that pre-adapts plants to subsequent hypoxia stress (Chapter 2; Veen *et al.*, 2013; Sasidharan *et al.*, 2018). To uncover how ethylene mediates hypoxia tolerance, we studied the effects of ethylene on the hypoxia transcriptional response and its transcriptional regulators. Our results reveal that ethylene augments the hypoxia response through enhanced ERFVII stability prior to hypoxia.

Indeed, both adult shoot tissues and seedling root tips benefitted from an early ethylene signal to enhance the subsequent transcriptional hypoxia response when $O_2$ levels declined (Fig. 3.1 & 3.2). The induction of hypoxia adaptive genes was both faster and stronger after ethylene pre-treatment in Arabidopsis rosette tissues (Fig. 3.1). Surprisingly, hypoxia alone did not strongly enhance hypoxia-responsive transcripts in adult rosette tissues compared to the seedling root tips (Fig. 3.1 & 3.2). Interestingly, optimal induction of hypoxia-responsive fermentation pathways was previously shown to be sugar- and starch dependent (Loreti *et al.*, 2018). Since our experiments are performed at the start of the light-period and plants generally deplete their carbohydrate reserves during the night (Geiger & Servaites, 2003; Loreti *et al.*, 2018), it is likely that the rosettes used in this study are still sugar- and starch depleted at the onset of hypoxia, explaining the limited induction of hypoxia genes. Conversely, carbohydrate levels in young seedlings are still supplied by the seed's endosperm reserves (Roberts, 1986) and could therefore be sufficient to induce hypoxia response genes. Still, ethylene pre-treatment strongly enhanced the subsequent hypoxic response of genes known to control fermentation, carbohydrate metabolism, ethylene biosynthesis, hypoxia signalling and oxidative stress homeostasis (Mustroph *et al.*, 2009, 2010). It is currently unknown how each

individual core hypoxia gene contributes to hypoxia tolerance. However, several studies show that ethylene controls adequate induction of fermentation (Peng, 2001; Tesniere *et al.*, 2004) and ROS homeostasis under hypoxia, submergence and re-oxygenation (Tsai *et al.*, 2014; Yeung *et al.*, 2018). It is therefore highly likely that the collective enhancement by ethylene of this hypoxia adaptive gene set contributes to ethylene-mediated hypoxia tolerance.

The majority of the core hypoxia genes are regulated by the PRT6 N-degron pathway targets RAP2.2 and RAP2.12 (Gibbs *et al.*, 2011; Licausi *et al.*, 2011; Gasch *et al.*, 2016). We show that ethylene-mediated hypoxia tolerance of Arabidopsis root tips is also dependent on this proteolytic pathway and redundantly involves both RAP2.2 and RAP2.12 (Fig. 3.3). Since we did not assess tolerance of any other combination of RAP-mutants, it is still possible that RAP2.3 contributes to this redundancy. While a single mutant of RAP2.2 in the Ler-0 background could still benefit from an ethylene pre-treatment, it did show reduced hypoxia tolerance compared to its WT, suggesting that RAP2.2 is the dominant ERFVII for conferring hypoxia tolerance in Arabidopsis root tips (Fig. 3.3A). While a plethora of reports has identified the ERFVIIs as collective regulators of many developmental, biotic and abiotic stress responses, single specific ERFVII regulatory roles remain largely unattributed (Abbas *et al.*, 2015; Vicente *et al.*, 2017; Liu *et al.*, 2018; Kim *et al.*, 2018). Future research is therefore required to reveal the common and unique ERFVII regulatory targets that confer (ethylene-mediated) hypoxia tolerance.

We show that the majority of ERFVII transcripts are enhanced by ethylene, with the exception of *HRE1* and *HRE2* in shoots, and *RAP2.12* in roots (Fig. 3.4A, B). While transcriptional regulation of several ERFVIIs has been described previously (Hess *et al.*, 2011; van Veen *et al.*, 2013), we show that ethylene also leads to increased protein levels of RAP2.12 and RAP2.3 (Fig. 3.4C-E, 3.5). This enhanced stability of ERFVIIs was not caused by changes in the transcriptional regulation of genes encoding PRT6 N-degron pathway enzymes (Fig. 3.6A, B). Increased RAP2.12 protein abundance under normoxia could potentially also be achieved by increased sequestration to ACBPs at the plasma membrane, where the protein is shielded from proteolysis (Licausi *et al.*, 2011; Schmidt *et al.*, 2018; Schmidt & van Dongen, 2019). However, we did not find evidence for enhanced sequestration through ethylene, as *ACBP1* and *ACBP2* transcript abundance were unaltered and the *acbp1* mutant showed similar hypoxia root tip survival as its WT background (Fig. 3.6). Moreover, we did not observe any clear RAP2.12 localization at the plasma membrane in Arabidopsis root tips under any of the tested conditions



(Fig. 3.4C& D, 3.7C). Previous research on ACBP-RAP2.12 interactions was solely studied in leaf epidermal cells and our results suggest that this interaction may not occur in seedling root tips (Licausi *et al.*, 2011; Schmidt *et al.*, 2018). In fact, our results suggest that RAP2.12 in root tips is mainly cytosolic and nuclear localized, with ethylene and hypoxia both enhancing RAP2.12 abundance and nuclear localization (Fig. 3.4D, 3.7C). Whether nuclear RAP2.12 localization is directly ethylene-mediated or an indirect consequence of enhanced stability remains to be uncovered. However, ethylene-mediated nuclear localization of RAP2.3 was previously shown to be dependent on direct binding of RAP2.3 to ORA59 in order to enhance disease resistance (He *et al.*, 2017; Kim *et al.*, 2018). Interestingly, our results show that the loss-of-function mutant *ora59* has reduced ethylene-mediated hypoxia tolerance in root tips (Fig. 3.6C), while a single knock-out line of its binding partner RAP2.3 showed no such reduction in hypoxia tolerance (Fig. 3.3A). These results imply that ORA59 could either play a role in nuclear localization of other RAPs or contributes to ethylene-mediated hypoxia tolerance independently of RAP2.2 and RAP2.12.

Moreover, while ethylene signalling prior to hypoxia leads to nuclear stabilization of RAP2.12 in root meristems (Fig. 3.4D, 3.7C), it does not trigger accumulation of most hypoxia adaptive gene transcripts until hypoxia sets in (Fig. 3.2). Apparently, stabilization of ERFVIIs alone is insufficient to trigger full activation of hypoxia-regulated gene transcription and additional hypoxia-specific signals such as altered ATP and/or $Ca^{2+}$ levels are required (Wang *et al.*, 2017; Igamberdiev & Hill, 2018; Schmidt *et al.*, 2018). In addition, the possible existence of undiscovered plant $O_2$ sensors was recently discussed and could potentially contribute to this hypoxia-specific response (Holdsworth, 2017; Wang *et al.*, 2017).

Finally, we uncovered that ethylene-mediated ERFVII stability and hypoxia tolerance is dependent on NO reduction (Fig. 3.7, S3.3). How exactly NO contributes to N-degron proteolysis of ERFVIIs is still a debated topic. N-terminal ERFVII $Cys_2$-oxidation by PCOs requires $O_2$ but does not require NO *in vitro* and in yeast (White *et al.*, 2017; Puerta *et al.*, 2019). However, ERFVIIs and other Nt MC-proteins stabilized when NO levels were reduced either genetically or pharmaceutically (Gibbs *et al.*, 2014, 2018; Vicente *et al.*, 2017). Recent reports indicate that PRT6 contains a modified heme $NO/O_2$ interacting motif, suggesting that PRT6 activity could be NO dependent (Zarban *et al.*, 2019). An alternative hypothesis could be that NO does not directly control the PRT6 N-degron pathway, but indirectly controls cellular $O_2$ levels and therefore ERFVII proteostasis through direct inhibition

of cytochrome C oxidase (COX) (Millar *et al.*, 1997). Previous research has shown that NO application reversibly inhibits mitochondrial respiration by binding to COX, impairing $O_2$ consumption and raising local $O_2$ levels in plants cells (Yamasaki *et al.*, 2001; Borisjuk & Rolletschek, 2008). Under these $O_2$ replete conditions, $Cys_2$-oxidation would lead to ERFVII proteolysis. Conversely, lack of NO was shown to increase COX-dependent respiration and $O_2$ consumption (Bloom *et al.*, 1992; Yamasaki *et al.*, 2001; Zottini *et al.*, 2002), which could increase local hypoxia in densely compact tissues, and therefore impair $O_2$-dependent ERFVII proteolysis. Consistently, in the fruits of strawberry and tomato, ethylene strongly enhanced respiration rates in a dose-responsive manner (Boe & Salunkhe, 1967; Tian, 1998). Additional experiments are required to test whether altered NO homeostasis really controls local $O_2$ levels to such an extent that it would impair ERFVII proteolysis.

Still, our results clearly indicate that ethylene reduces NO levels and that this NO depletion is required for ethylene-enhanced ERFVII stability and hypoxia tolerance. The question remains how ethylene leads to an NO reduction in Arabidopsis seedling root tips. NO homeostasis is mainly controlled through NO biosynthesis via NITRATE REDUCTASE (NR)-dependent nitrite reduction on the one hand, and NO-scavenging by non-symbiotic phytoglobins PGBs on the other (Gupta *et al.*, 2011; Hebelstrup *et al.*, 2012; Chamizo-Ampudia *et al.*, 2017). Interestingly, we observed that *PGB1* transcript levels quickly increased in response to ethylene in both shoot and root tissues (Fig. 3.1, 3.2). *PGB1* was also induced in *R. palustris* upon ethylene exposure (van Veen *et al.*, 2013). We therefore hypothesize that ethylene reduces NO levels through induction of the NO-scavenger *PGB1*, limiting NO-dependent ERFVII proteolysis and enhancing ERFVII stability under normoxia. This hypothesis is tested in chapter 4 of this thesis. In conclusion, we show that ethylene-mediated NO depletion and consequent ERFVII accumulation primes the transcriptional hypoxia response and pre-adapts plants to survive subsequent hypoxia stress.

## ACKNOWLEDGEMENTS

We thank George Bassel and Sophie Berckhan for the construction of the *promRAP2.12:MC-RAP2.12-GUS* transgenic line. We also thank Jorge Vicente, Femke Bosman, Ankie Ammerlaan and Rob Welschen for technical assistance. Finally, we acknowledge the people named in the methods section for providing seeds of the genotypes used in this chapte.





## MATERIALS AND METHODS

### Plant material and growth conditions

Plant material: *Arabidopsis thaliana* seeds of the ecotype Col-0 were obtained from the Nottingham Arabidopsis Stock Centre. Other germlines used in this study were kindly provided by the following individuals: Ler-0, *rap2.2-5* (Ler-0 background, AY201781/GT5336), *rap2.12-2* (SAIL_1215_H10), *rap2.2-5rap2.12-A* and *-B* (and mixed Ler-0 and Col-0 WT backgrounds) from Prof. Angelika Mustroph (Gasch *et al.*, 2016), University Bayreuth, Germany; *35S:δ13-RAP2.12-GFP* and *35S:RAP2.12-GFP* from Prof. Francesco Licausi, University of Pisa, Italy (Licausi *et al.*, 2011); *ora59* and *35S:ORA59* from Merel Steenbergen, Utrecht University, The Netherlands, (Pré *et al.*, 2008); and *acbp1* (SAIL_683_C03) from dr. Romy R. Schmidt, Aachen University, Germany (Schmidt *et al.*, 2018). The *35S::RAP2.3-HA* transgenic line, as well as *prt6-1* (SAIL_1278_H11), *rap2.3-1* (SAIL_1031_D10) and *hre1-1hre2-1* (SALK_039484 + SALK_052858) mutants were described previously (Gibbs *et al.*, 2011, 2014). All mutant and transgenic lines used in this chapter were confirmed by either conventional genotyping PCRs and/or antibiotic resistance selection (Primer and additional info in Appendix I). Growth conditions of adult rosettes and in vitro seedlings were similar as described in Chapter 2 of this thesis.

### Construction of transgenic plants.

The *promRAP2.12:MC-RAP2.12-GUS* protein fusion lines were constructed by amplifying the genomic sequence capturing 2 kb of sequence upstream of the translational start site, and removing the stop codon using the following primers: RAP2.12-fwd GGGGACAAGTTTGTAC AAAAAAGCAGGCTATTCAGATTGGATCGTGACATG and RAP2.12-rev GGGGACCACT TTGTACAAGAAAGCTGGGTAGAAGACTCCTCCAATCATG-GAAT. The PCR product was GATEWAY cloned into pDNR221 through a BP reaction, then transferred to pGWB433 creating an in-frame C-terminal fusion to the GUS reporter protein (Nakagawa *et al.*, 2007).

### Experimental setup and (pre-)treatments

Ethylene and hypoxia treatments were performed as described in Chapter 2 of this thesis.

Nitric oxide: Just before application, pure NO gas was diluted in ~60 ml glass vials with pure $N_2$ gas to minimize the oxidation of NO gas. For all but the optimization experiments, diluted NO gas was injected with a syringe into the air and ethylene treated desiccators at a final concentration of 10 $ul^{-1}$ NO, 1 hour prior to

the end of the (pre-)treatment. Timing and concentrations of NO application were optimized as described in the figure legend of Fig. S3.1A.

c-PTIO: Treatments with the NO-scavenging compound 2-(4-Carboxyphenyl)-4,5-dihydro-4,4,5,5-tetramethyl-1H-imidazol-1-yloxy-3-oxide potassium salt (cPTIO salt, Sigma Aldrich, Darmstadt, Germany) were performed ~1 hour prior to ethylene treatments to allow for treatment combinations. Droplets of 5µl cPTIO solution (250µM in autoclaved liquid ¼ MS) or mock solution (autoclaved liquid ¼ MS) were pipetted onto each individual root tip. Timing and concentrations of cPTIO application were optimized as described in the figure legend of Fig. S3.1B.

### Hypoxia tolerance assays

Hypoxia tolerance assays were performed as described in Chapter 2 of this thesis.

### RNA extraction and quantification, cDNA synthesis and RT-qPCR

Adult rosette (2 whole rosettes per sample) or seedling root tip (~500 root tips) samples were harvested by snap freezing in liquid nitrogen. RNA extraction, RNA quantification, cDNA synthesis and RT-qPCR were performed as described in Chapter 2 of this thesis. Primers used for RT-qPCR can be found in Appendix II.

### Histochemical staining for GUS activity

Seedlings of *promRAP2.12:RAP2.12-GUS* (10 days old) were harvested in GUS solution (100mM NaPO4 buffer, pH 7.0, 10mM EDTA, 2mM X-Gluc, 500 µM K3Fe(CN)6 and 500 µM K4Fe(CN)6) directly after treatments, vacuum infiltrated for 15 minutes and incubated for 2 days at 37°C before de-staining with 70% ethanol. Seedlings were kept and mounted in 50% glycerol and analyzed using a Zeiss Axioskop2 differential interference contrast (DIC) microscope (10× DIC objective) or regular light microscope with a Lumenera Infinity 1 camera (5 or 10× objective). GUS pixel intensity of the microscopy images was analyzed using ICY software (http://icy.bioimageanalysis.org/), by quantifying the pixel intensity of the red (ch0) and blue (ch2) channels of the tissues of interest relative to the respective channel background values of these images. GUS intensity of all treatments was expressed relatively to the Air-treated controls.

### Protein extraction, SDS-PAGE and Western Blotting

Protein was extracted on ice for 30 minutes from pulverized snap frozen samples in modified radio-immunoprecipitation assay (RIPA) lysis buffer as described in (Zhang *et al.*, 2018a). Protein concentration was quantified using and following the



protocol of a BCA protein assay kit (Pierce). Protein concentrations were equalized by dilution with RIPA buffer and incubated for 10 minutes with loading buffer (5x sample loading buffer, Bio Rad) + β-ME) at 70°C before loading (30 µg total protein per sample) on pre-cast Mini-PROTEAN Stain Free TGX Gels (Bio Rad) and ran by SDS-PAGE. Gels were imaged before and after transferring to PVDF membranes (Bio Rad) using trans-blot turbo transfer system (Bio Rad), to verify successful and equal protein transfer. Blots were blocked for at least 1 hour in blocking solution at RT (5% milk in 1xTBS) before probing with primary antibody in blocking solution (α-HA-HRP, 1:2500 (Roche); α-Actin, 1:2500 (Thermo Scientific) overnight at 4°C. Blots were rinsed 3 times with 1xTBS-T (0.1% Tween 20) for 10 minutes under gentle agitation before probing with secondary antibody (α-mouse IgG-HRP for Actin, 1:2500) and/or SuperSignal™ West Femto chemiluminescence substrate (Fisher Scientific) and blot imaging using Image Lab software in a chemi-gel doc (Bio-rad) with custom accumulation sensitivity settings for optimal contrast between band detection and background signal. To visualize RAP2.3 (~45 kDa) and Actin (~42 kDa) protein levels on the same blot, membranes were stripped after taking final blot images using a mild stripping buffer (pH 2,2, 1.5% (w/v) glycine, 0.1% SDS and 1.0% Tween 20) for 15 minutes and rinsed 3x in 1xTBS-T before blocking and probing with the 2nd primary antibody of interest.

### NO quantification

Intracellular NO levels were visualized using DAF-FM diacetate (7'-difluorofluorescein diacetate, Bio-Connect). Seedlings were incubated in the dark for 15 min under gentle agitation in 10mM Tris-HCl buffer (pH 7.4) containing 50µM DAF-FM DA and subsequently washed twice for 5 min 10mM Tris-HCl buffer (pH 7.4). Several roots of all treatments/genotypes were mounted in 10mM Tris-HCl buffer (pH 7.4) on the same microscope slide. Fluorescence was visualized using a Zeiss Observer Z1 LSM700 confocal microscope (oil immersion, 40x objective Plan-Neofluar N.A. 1.30) with excitation at 488 nm and emission at 490-555 nm. Roots incubated and mounted in 10mM Tris-HCl buffer (pH 7.4) without DAF-FM DA were used to set background values where no fluorescence was detected. Within experiments, laser power, pinhole, digital gain and detector offset were identical for all samples. Mean DAF-FM DA fluorescence pixel intensity in root tips was determined in similar areas of ~17000 µm$^2$ between epidermis layers using ICY software (http://icy.bioimageanalysis.org/).

### Confocal Microscopy

Transgenic Arabidopsis seedlings of *35S:RAP2.12-GFP* were visualized using confocal microscopy as described in Chapter 2 of this thesis.

### Statistical analyses

Statistical analyses were performed as described in Chapter 2 of this thesis.



## SUPPLEMENTAL FIGURES

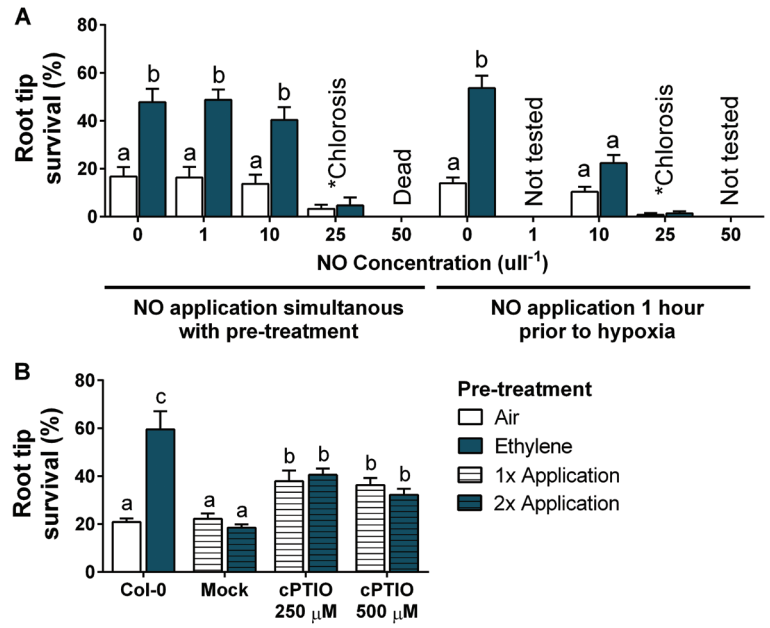


**Supplemental Figure 3.1. NO reduction prior to hypoxia enhances subsequent hypoxia survival.**

**(A)** Seedling root tip survival of Col-0 seedling root tips after 4 hours air or ~5µll⁻¹ ethylene in combination with application of several NO concentrations followed by hypoxia (4h) and 3 days recovery. On the left, NO treatments were given simultaneously with the pre-treatments (at 9:00). On the right, NO treatments were administered 3 hours into the pre-treatment (1 hour prior to hypoxia, at 12:00). Not all NO concentrations were tested in the latter experiment. Values are relative to control (normoxia) plants with NO application concentrations of 0-10µll⁻¹. *With 25 and 50 µll⁻¹ NO injections the control plants suffered either severe chlorotic damage in the green tissues and/or did not survive. **(B)** Seedling hypoxia root tip survival of Col-0 seedling root tips after pre-treatment with 4 hours of air, ~5µll⁻¹ ethylene or where 5µl cPTIO (2 concentrations) or mock (1/4 MS) solution was pipetted directly onto every single root tip, either once or twice (4 or 4+2 hours prior to hypoxia, respectively). Pre-treatments were followed by hypoxia (4h) and 3 days recovery. In both A and B letters indicate significant differences between pre-treatments ($p<0.05$, 2-way ANOVA, Tukey's HSD, n=8-16 rows of ~23 seedlings). All data shown are mean ± sem.

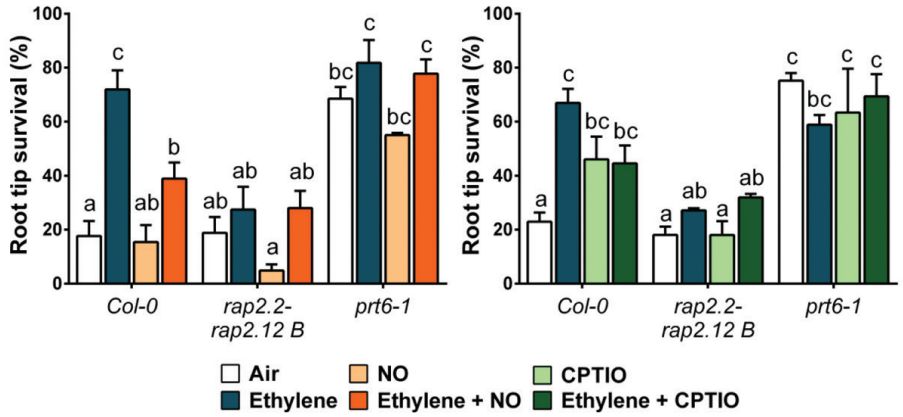


**Supplemental Figure 3.2. Ethylene-mediated NO depletion enhances subsequent hypoxia survival through RAP2.2, RAP2.12 and the PRT6 N-degron pathway.**
Seedling root tip survival of Col-0, *rap2.2rap2.12*-B and PRT6 N-degron pathway mutant *prt6-1* after indicated pre-treatments followed by hypoxia (4h) and 3 days recovery. Values are relative to control (normoxia) plants. Letters indicate significant differences ($p<0.05$, 2-way ANOVA, Tukey's HSD, n=4-8 rows of ~23 seedlings). All data shown are mean ± sem.



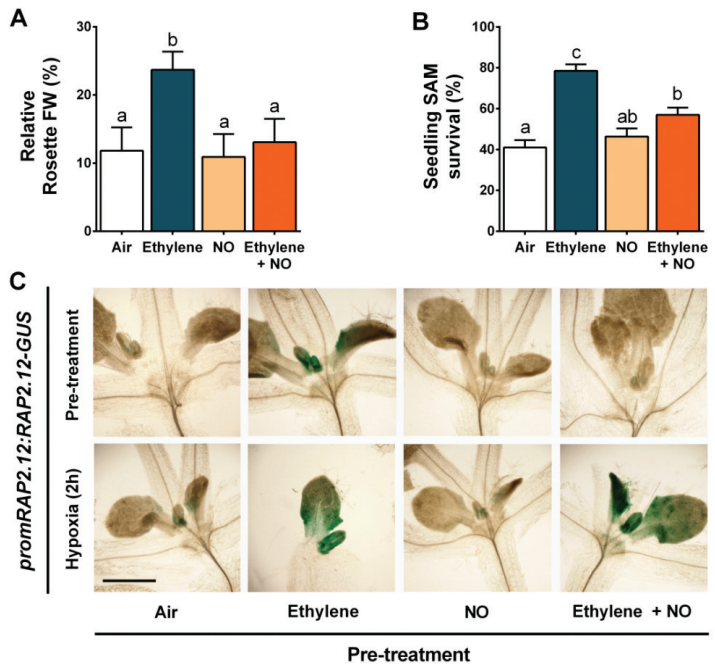


**Supplemental Figure 3.3. Ethylene-mediated NO depletion enhances shoot RAP2.12 stability and hypoxia acclimation.**
**(A, B)** Arabidopsis adult rosette fresh weight (FW) in **A**, or shoot apical meristem survival of 10-day old seedlings in **B**, after indicated pre-treatments followed by 7 hours of hypoxia and 7 days of recovery. Values are relative to control (normoxia) plants with the same pre-treatment. Letters indicate significant differences ($p<0.05$, 1-way ANOVA, Tukey's HSD, n=9 rosettes for A, n=16 rows of ~23 seedlings for B). All data shown are mean ± sem. **(C)** Representative light microscopy images of *promRAP2.12:RAP2.12-GUS* in 10-day old seedling shoots after indicated pre-treatments or subsequent (2h) hypoxia treatments (n=8-11 seedlings, Scale bars = 200μm).

# CHAPTER 4

## NO PROBLEM: ETHYLENE-INDUCED NITRIC OXIDE DEPLETION LIMITS ERFVII PROTEOLYSIS THROUGH PHYTOGLOBIN1


Sjon Hartman[1]
Emilie Reinen[1]
Jorge Vicente[2]
Michael J. Holdsworth[2*]
Rashmi Sasidharan[1*]
Laurentius A.C.J. Voesenek[1*]


**MODIFIED EXCERPTS OF THIS CHAPTER ARE PUBLISHED IN:**

- Sasidharan, R., Hartman, S., *et al.* (2018). Signal dynamics and interactions during flooding stress. Plant Physiology, 176(2), 1106-1117.
- Hartman S., *et al.* (2019) Ethylene-mediated nitric oxide depletion pre-adapts plants to hypoxia stress, Nature Communications, 10 (1), 4020.


1. Plant Ecophysiology, Institute of Environmental Biology, Utrecht University, Padualaan 8, 3584 CH, Utrecht, The Netherlands
2. School of Biosciences, University of Nottingham, Loughborough, LE12 5RD, United Kingdom

*Shared senior authors

## ABSTRACT

Ethylene is a crucial signal during plant submergence that acclimates plant tissues to impending low oxygen (O2) conditions (hypoxia). Previous work has shown that ethylene-mediated nitric oxide (NO) removal stabilized group VII Ethylene Response Factor (ERFVII) transcription factors prior to hypoxia by limiting NO-dependent ERFVII proteolysis in Arabidopsis thaliana. This ethylene-mediated NO depletion and ERFVII stability primes the hypoxia transcriptional response and enhances subsequent hypoxia survival. However, how ethylene reduces NO levels in plant tissues is currently unclear. To unravel how ethylene regulates NO levels, we explored the effects of ethylene on key NO biosynthesis and NO scavenging regulators. Our results reveal that ethylene enhances transcript levels of both NO biosynthesis and scavenging related genes, but that the induction of NO-scavenger PHYTOGLOBIN1 (PGB1) regulates NO depletion. In addition, we show that ethylene-mediated ERFVII stability, the enhanced hypoxia transcriptional response and subsequent hypoxia tolerance is PGB1 dependent. Our results reveal that PGB1-mediated NO depletion is indispensable for hypoxia survival and identifies PGB1 as a key regulatory target for early stress perception that could be pivotal for developing flood-tolerant crops.




## INTRODUCTION

Climate models predict that changing weather patterns will lead to a significant increase in the frequency and severity of global flooding events (Hirabayashi *et al.*, 2013). These floods have catastrophic effects on agricultural productivity and plant biodiversity (Hirabayashi *et al.*, 2013; Voesenek & Bailey-Serres, 2015a). Underwater diffusion of oxygen ($O_2$) in submerged plant tissues is severely impaired due to Fick's law, and terrestrial plants consequently suffer from $O_2$ deprivation (hypoxia). Therefore, plant survival during flooding greatly depends on molecular and physiological responses that enhance hypoxia tolerance (Shiono *et al.*, 2008; Voesenek & Bailey-Serres, 2015a). Interestingly, ethylene is rapidly entrapped in submerged plant tissues and was shown to drive enhanced hypoxia acclimation and survival in *Rumex palustris* and *Arabidopsis thaliana* (Chapter 2; van Veen *et al.*, 2013). Moreover, this ethylene-mediated hypoxia tolerance correlated with ethylene-enhanced induction of hypoxia adaptive genes upon hypoxia (Chapter 3; van Veen *et al.*, 2013). Transcriptional regulation of most hypoxia adaptive genes is under the control of the group VII Ethylene Response Factor transcription factors (ERFVIIs), which can bind to a conserved cis-regulatory motif called the Hypoxia Responsive Promoter Element (HRPE) (Hinz *et al.*, 2010; Gasch *et al.*, 2016). The ERFVIIs are part of a $O_2$ and nitric oxide (NO) sensing mechanism through the cysteine-branch of the PROTEOLYSIS 6 (PRT6) N-degron pathway (Gibbs *et al.*, 2011, 2014; Licausi *et al.*, 2011). All Arabidopsis ERFVIIs contain a conserved N-terminal sequence of Methionine-Cysteine (MC), which renders the proteins susceptible to N-degron targeted proteolysis when both $O_2$ and NO are present (Gibbs *et al.*, 2011, 2014; Licausi *et al.*, 2011). Therefore, a decline in either $O_2$ or NO stabilizes ERFVIIs and causes subsequent hypoxia adaptive gene expression (Gibbs *et al.*, 2011, 2014; Licausi *et al.*, 2011). Interestingly, we found that ethylene can stabilize ERFVIIs in ambient $O_2$ (normoxia), through active NO reduction, in turn limiting NO-dependent ERFVII proteolysis (Chapter 3). Moreover, this ethylene-mediated NO depletion and ERFVII stability prior to hypoxia was absolutely vital for subsequent enhanced hypoxia acclimation and survival. However, it is currently unclear how ethylene can reduce NO levels in plant tissues.

NO is a highly reactive, but short-lived molecule that affects a plethora of plant developmental and stress responses, including hypoxia and flooding tolerance (Libourel *et al.*, 2006; Astier *et al.*, 2011; Manjunatha *et al.*, 2012; Mur *et al.*, 2013; Pucciariello & Perata, 2017). NO homeostasis in plant cells is controlled through both NO biosynthesis and NO scavenging capacity. Pathways controlling NO biosynthesis in plants are plentiful and not yet fully understood. The majority of

studies suggest that the main source of NO production occurs through enzymatic and non-enzymatic reduction of nitrite (Chamizo-Ampudia *et al.*, 2017; León & Costa-Broseta, 2019). Nitrite production itself is highly dependent on nitrate reductase (NR) activity, making NRs the dominant enzymes for NO production in plants (Magalhaes *et al.*, 2000; Chamizo-Ampudia *et al.*, 2017; León & Costa-Broseta, 2019). Conversely, NO removal can occur via multiple reactions. Firstly, NO can leave the plant through passive diffusion (Hebelstrup *et al.*, 2012). Secondly, NO can react chemically with $O_2$ to produce nitrite and nitrate, or with reactive oxygen species (ROS) to form additional reactive nitrogen species (RNS) (Chamizo-Ampudia *et al.*, 2017; León & Costa-Broseta, 2019). Thirdly, NO can be scavenged by glutathione to produce S-nitrosylated glutathione (Frungillo *et al.*, 2014). Finally, phytoglobins, previously called non-symbiotic hemoglobins, can dioxygenate NO in an $O_2$ dependent manner, effectively scavenging any free NO in plant cells to form nitrate and preventing NO-induced nitrosative stress damage (Hebelstrup *et al.*, 2006, 2012; Voesenek *et al.*, 2016; Mot *et al.*, 2018).

Interestingly, phytoglobins have been shown to affect hypoxia and flooding tolerance in several plant species (Hunt *et al.*, 2002; Dordas *et al.*, 2003; Hebelstrup *et al.*, 2012; Mira *et al.*, 2016). While the Arabidopsis genome contains three genes coding for highly similar phytoglobins, *PHYTOGLOBIN1* (*PGB1*) was shown to be the most potent NO-scavenger and crucial for normal plant development and stress responses (Hebelstrup *et al.*, 2006, 2012; Mur *et al.*, 2013). In waterlogged maize root tips, over-expression of *PGB1* led to increased expression of fermentation genes, including the core hypoxia gene *ALCOHOL DEHYDROGENESE (ADH)* (Youssef *et al.*, 2019). In addition, ethylene rapidly enhanced *PGB1* transcript levels in both Arabidopsis and *Rumex. palustris* (Chapter 3; Veen *et al.*, 2013). In both species, this PGB1 induction prior to hypoxia correlated with subsequent ethylene-enhanced hypoxia gene expression upon hypoxia. In Arabidopsis, the *PGB1* induction correlated with NO depletion and enhanced ERFVII stability (Chapter 3). Therefore, we hypothesized that ethylene caused NO depletion through enhanced *PGB1* induction, in turn limiting NO-dependent ERFVII proteolysis and enhancing ERFVII stability under normoxia.

To unravel whether *PGB1* controls ethylene-mediated NO depletion, ERFVII stability and subsequent hypoxia tolerance, we studied these processes in both a knockdown and over-expression line of *PGB1*. The results reveal that ethylene enhances PGB1 protein levels and that PGB1 is crucial for ethylene-mediated NO depletion. In addition, we show that PGB1 is key for enhanced ERFVII stability, hypoxia



adaptive gene expression and subsequent hypoxia acclimation of Arabidopsis root tips. We conclude that early PGB1 induction during submergence is paramount for subsequent hypoxia acclimation and that the uncovered mechanism is a valuable tool to identify key players that confer flooding tolerance in plants.

## RESULTS

### Ethylene enhances protein abundance of NO-scavenger PGB1

To unravel how ethylene regulates NO levels under normoxia in Arabidopsis, we explored the effects of ethylene on key regulators that control NO biosynthesis and NO scavenging. To study changes in NO biosynthesis, we followed both *NR* transcript abundance and NR enzyme activity (Chamizo-Ampudia *et al.*, 2017). Surprisingly, ethylene led to small increases in *NR1* and *NR2* mRNA levels in seedling root tips and enhanced *NR1* mRNA abundance in adult rosettes (Fig. 4.1A, B). However, these ethylene-enhanced *NR* transcript levels did not influence total NR activity in Arabidopsis seedlings, whereas hypoxia did (Fig. 4.1C). Next, we assessed whether ethylene affected NO-scavenging through changes in the transcript levels of the three non-symbiotic phytoglobins (Hebelstrup *et al.*, 2006; Stasolla & Hill, 2017). Transcript abundance of *PGB1,* the most potent NO-scavenger (Hebelstrup *et al.*, 2012), but not *PGB2* and *PGB3*, increased in Arabidopsis root tips after ethylene treatment (Fig. 4.1A). The mRNA levels of *PGB1* also rapidly increased in adult rosette tissues upon ethylene fumigation (Fig. 4.1B, D). Finally, ethylene also led to enhanced PGB1 protein levels in Col-0 seedling root tips (Fig. 4.2D). Together these results suggest that ethylene could reduce NO levels through enhanced PGB1 levels.

Next, we explored which ethylene-mediated transcription factors are required for *PGB1* induction. In Arabidopsis, ethylene-dependent signaling is controlled by the transcription factors ETHYLENE INSENSITIVE 3 (EIN3) and EIN3 LIKE 1 (EIL1), that facilitate the downstream ethylene transcriptional response (Alonso *et al.*, 2003; Guo & Ecker, 2004; Chang *et al.*, 2013). In addition, EIN2 is required for EIN3 protein stability and nuclear localization (An *et al.*, 2010) whereas the transcription factor ERF1 functions directly downstream of EIN3 signaling and controls a large proportion of ethylene responses (Solano *et al.*, 1998). Ethylene was unable to enhance *PGB1* transcript levels in the ethylene signaling loss-of-function mutants *ein2-5* and *ein3eil1* (Fig. 4.1E). However, ethylene-mediated PGB1 induction did not require ERF1, as the *erf1-1* mutant still had enhanced *PGB1* transcripts (Fig. 4.1E). In addition, since *PGB1* is a known target of the ERFVII transcription factors RELATED TO APETALA2.2 (RAP2.2) RAP2.2 and RAP2.12 (Gasch *et al.*, 2016),

and ethylene could stabilize ERFVIIs under normoxia (Chapter 3), we assessed whether the ethylene-mediated *PGB1* mRNA increase is RAP2.2 and RAP2.12 dependent. However, transcript levels of *PGB1* were still enhanced by ethylene during normoxia in two loss-of-function *rap2.2 rap2.12* mutant lines (Fig. 4.1E). Together, these results illustrate that ethylene could modulate *PGB1* levels in an ERF1 and ERFVII-independent manner, but does require functional EIN2 and EIN3 signaling.

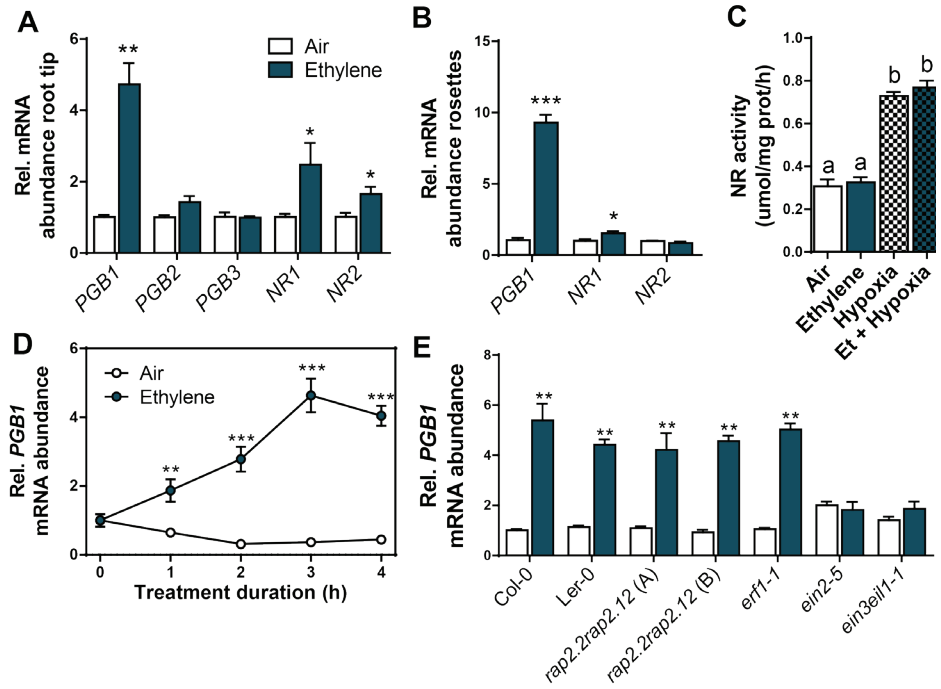


**Figure 4.1. The effects of ethylene on genes and proteins that mediate NO homeostasis.**
**(A, B)** Relative mRNA abundance of genes coding for enzymes involved in NO metabolism in seedling root tips **(A)** and adult rosettes **(B)** of Col-0 plants after 4 hours of treatment with air (white) or ~5µll$^{-1}$ ethylene (blue). Values are relative to Col-0 air treated samples. Asterisks indicate significant differences between air and ethylene (***p<0.001, **p<0.01, *p<0.05 Student's *t* test, n=3-4 replicates of ~400 root tips in A, n=5 replicates of 2 rosettes in B). **(C)** Nitrate reductase activity in whole Col-0 WT seedlings after 4 hours of pre-treatment with air (white) or ~5µll$^{-1}$ ethylene (blue), followed by (4h) hypoxia (dashed stripes). Statistically similar groups are indicated using the same letter (p<0.05, 1-way ANOVA, Tukey's HSD, n=2 replicates of ~200 seedlings). **(D)** Relative *PGB1* mRNA transcript abundance in rosettes of Col-0 plants during 4 hours of treatment with air (white) or ~5µll$^{-1}$ ethylene (blue). Asterisks indicate significant differences between air and ethylene (***p<0.001, ANOVA with planned comparisons, Tukey's HSD correction for multiple comparisons, n=5 replicates of 2 rosettes). **(E)** Relative *PGB1* mRNA transcript abundance in seedlings of Arabidopsis Col-0 and Ler-0 WT, 2 double *rap2.2rap2.12* mutants (Col-0 x Ler-0 background), and ethylene signaling mutants *erf1-1, ein2-5* and *ein3eil1* after 4 hours of treatment with air (white) or ~5µll$^{-1}$ ethylene (blue). Values are relative to Col-0 air treated samples. Asterisks indicate significant differences between air and ethylene (**p<0.01, ANOVA with planned comparisons, Tukey's HSD correction for multiple comparisons, n=2 replicates of ~400 root tips). All error bars are SEM.



## Ethylene-mediated hypoxia tolerance is PGB1-dependent

To unravel whether ethylene-induced *PGB1* levels enhance NO depletion, ERFVII stabilization, hypoxia-adaptive gene expression and hypoxia tolerance, we identified a T-DNA insertion line (SK_058388; hereafter *pgb1-1*). In *pgb1-1* the T-DNA is located exactly 300 nucleotides upstream of the *PGB1* start codon (Fig. 4.2A, B). In wild-type Arabidopsis seedling root tips, both ethylene and hypoxia treatment enhanced *PGB1* transcript and protein accumulation (Fig. 4.2C, D). However, in the *pgb1-1* mutant line *PGB1* transcript levels were reduced, and ethylene did not increase *PGB1* transcript or protein abundance, whereas hypoxia only affected transcript abundance slightly (Fig. 4.2C, D). A faint band of lower molecular weight than expected for PGB1 (18 kDa) was observed in some *pgb1-1* samples, but did not show any clear treatment effect (Fig. 4.2D). Together these data suggest that the T-DNA insertion in the promoter of *pgb1-1* uncouples *PGB1* expression from ethylene regulation. Finally, a *35S:PGB1* line showed constitutively elevated *PGB1* transcript and protein levels (Fig. 4C, D, (Hebelstrup *et al.*, 2012)).

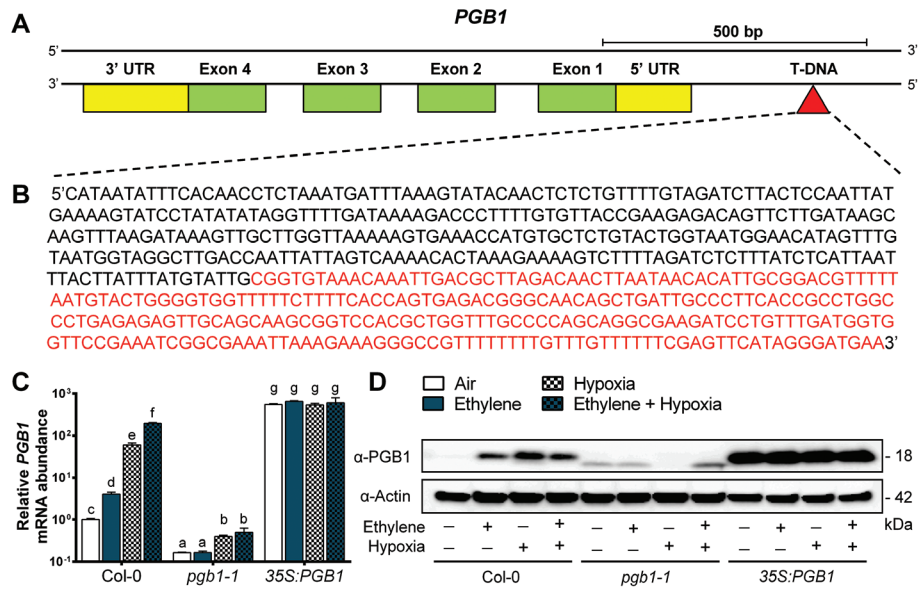


**Figure 4.2. The regulation *PGB1* transcript and PGB1 protein abundance by ethylene and hypoxia.**
**(A)** Schematic map of genomic *PGB1* gene region including the 4 *PGB1* exons (green) and the location of the t-DNA insertion (red triangle) of *pgb1-1* line *SK_058388.* **(B)** Partial DNA sequencing reaction of *pgb1-1* aligned with genomic *PGB*1 gene region. The aligned native *PGB1* sequence (black) ends and the T-DNA sequence (red) starts exactly 300bp upstream of the *PGB1* start codon. **(C)** Relative transcript abundance of *PGB1* in root tips of Col-0, *pgb1-1* and *35S:PGB1* after 4 h air or ~5µll$^{-1}$ ethylene followed by (4h) hypoxia. Values are relative to Col-0 air treated samples. Letters indicate significant differences (p<0.05, 2-way ANOVA, n=3 replicates of ~200 root tips each). **(D)** PGB1 protein levels in Col-0, *pgb1-1* and *35S::PGB1* root tips after 4 h air or ~5µll$^{-1}$ ethylene followed by (4h) hypoxia.

Next, we assessed whether ethylene-mediated *PGB1* induction was required for NO depletion, using the NO fluorescent probe 4-amino-5-methylamino-2′,7′-difluorofluorescein (DAF-FM) diacetate (Planchet & Kaiser, 2006). The ethylene-mediated NO decline observed in Col-0 root tips was fully abolished in *pgb1-1*, demonstrating the requirement of *PGB1* induction for local NO removal upon ethylene exposure (Fig. 4.3A, B). Moreover, lack of NO removal by ethylene in *pgb1-1* resulted in the inability to stabilize RAP2.3 levels and reduced hypoxia survival (Fig. 4.3C, D). Interestingly, these effects could be rescued through active NO depletion prior to hypoxia, using the NO-scavenging compound 2-(4-carboxyphenyl)-4,4,5,5-tetramethylimidazoline-1-oxyl-3-oxide (cPTIO) (Fig. 4.3C, D). In addition, the reduced ethylene-induced hypoxia tolerance in *pgb1-1* was accompanied by an absence of ethylene-enhanced hypoxia adaptive gene expression upon hypoxia (Fig. 4.4). In contrast, *35S:PGB1* showed constitutively low NO levels in root tips (Fig. 4.3A, B, (Hebelstrup *et al.*, 2012)). Moreover, this ectopic *PGB1* over-expression increased RAP2.3 stability under normoxia and showed enhanced hypoxia tolerance without an ethylene pre-treatment (Fig. 4.3C, D). Both the constitutive RAP2.3 stability and enhanced hypoxia survival in *35S:PGB1* were abolished when an NO pulse was applied during the air and ethylene pre-treatments (Fig. 4.3C, D). Furthermore, elevated mRNA levels for several hypoxia adaptive genes accompanied the constitutive hypoxia tolerance in *35S:PGB1* root tips (Fig. 4.4). Importantly, both *pgb1-1* and *35S:PGB1* showed mostly similar ethylene responses in abundance of perception (*ETR2*) and biosynthesis (*ACO1*) transcripts compared to wild-type during normoxia (Fig. 4.4), indicating that the observed effects are unlikely to be caused by altered ethylene biosynthesis and signaling in these mutants. Together these results demonstrate that active reduction of NO levels by ethylene-induced *PGB1* prior to hypoxia can precociously enhance ERFVII stability to prepare cells for impending hypoxia (Summarizing model, Fig. 4.5).

## DISCUSSION

Ethylene is an important early signal for submergence that mediates subsequent hypoxia acclimation in Arabidopsis through active NO removal (Chapter 3). To uncover how ethylene controls NO levels and downstream effects, we tested the effects of ethylene treatment on genes involved in both NO biosynthesis and scavenging. Our results revealed that ethylene enhanced transcript levels of both NO biosynthesis and scavenging genes, but that enhanced PGB1 levels are crucial for NO depletion and subsequent hypoxia acclimation.



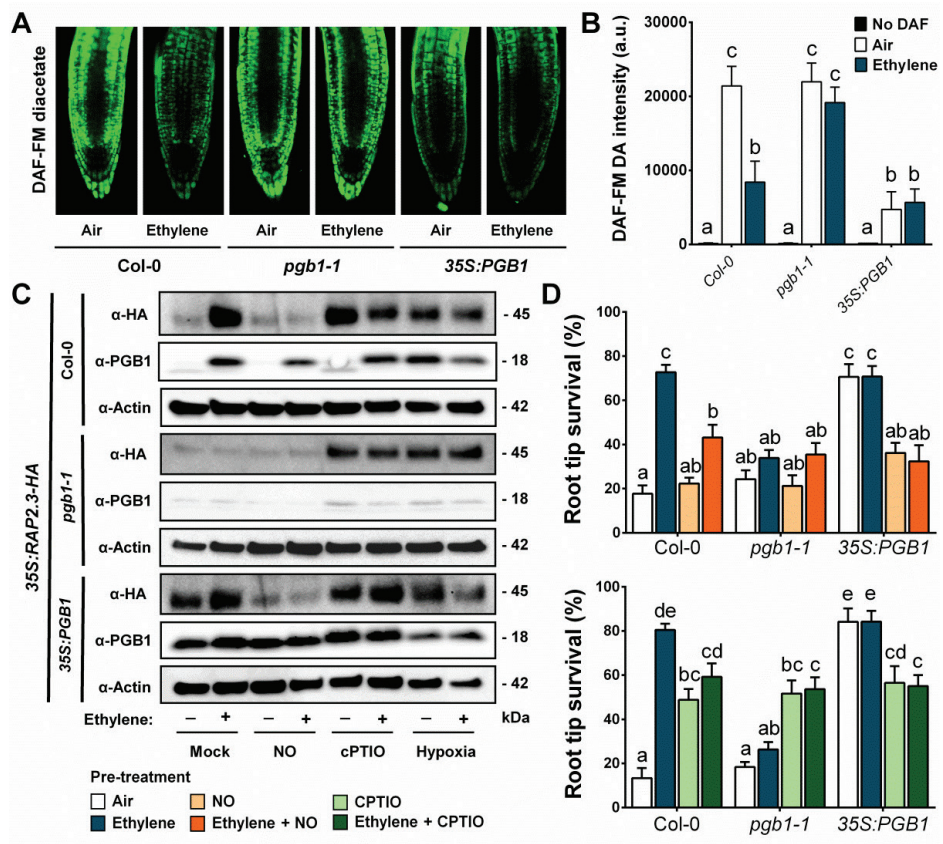


**Figure 4.3. Ethylene enhances NO depletion, ERFVII stability and hypoxia survival through PGB1.**

**(A, B)** Representative confocal images visualizing (A) and quantifying (B) NO using fluorescent probe DAF-FM diacetate in Col-0, *pgb1-1* and *35S:PGB1* seedling root tips after 4h air or ~5µl l$^{-1}$ ethylene (scale bar = 50µm). Letters indicate significant differences ($p<0.05$, 2-way ANOVA, Tukey's HSD, n=5) **(C)** RAP2.3 and PGB1 protein levels in *35S:MC-RAP2.3-HA* (in Col-0, *pgb1-1* and *35S:PGB1* backgrounds) seedling root tips after indicated pre-treatments and subsequent hypoxia (4h). **(D)** Seedling root tip survival of Col-0, *pgb1-1* and *35S:PGB1* after indicated pre-treatments followed by 4 h hypoxia and 3 days recovery. Values are relative to control (normoxia) plants. Letters indicate significant differences ($p<0.05$, 2-way ANOVA, Tukey's HSD, n=12 rows of ~23 seedlings). All data shown are mean ± sem.

Interestingly, induction of *NR1* and *NR2* transcripts upon ethylene exposure did not alter total NR activity (Fig. 4.1A, B), suggesting that enhanced *NR* mRNAs either do not lead to more NR proteins, or that NR protein abundance does not determine NR activity. Previous research has shown that NR activity is indeed highly dependent on its phosphorylation state (Kaiser *et al.*, 1993). In multiple plant species, a decline in both cytosolic ATP levels and pH were shown to increase NR phosphorylation and subsequently enhance NR activity and NO levels under

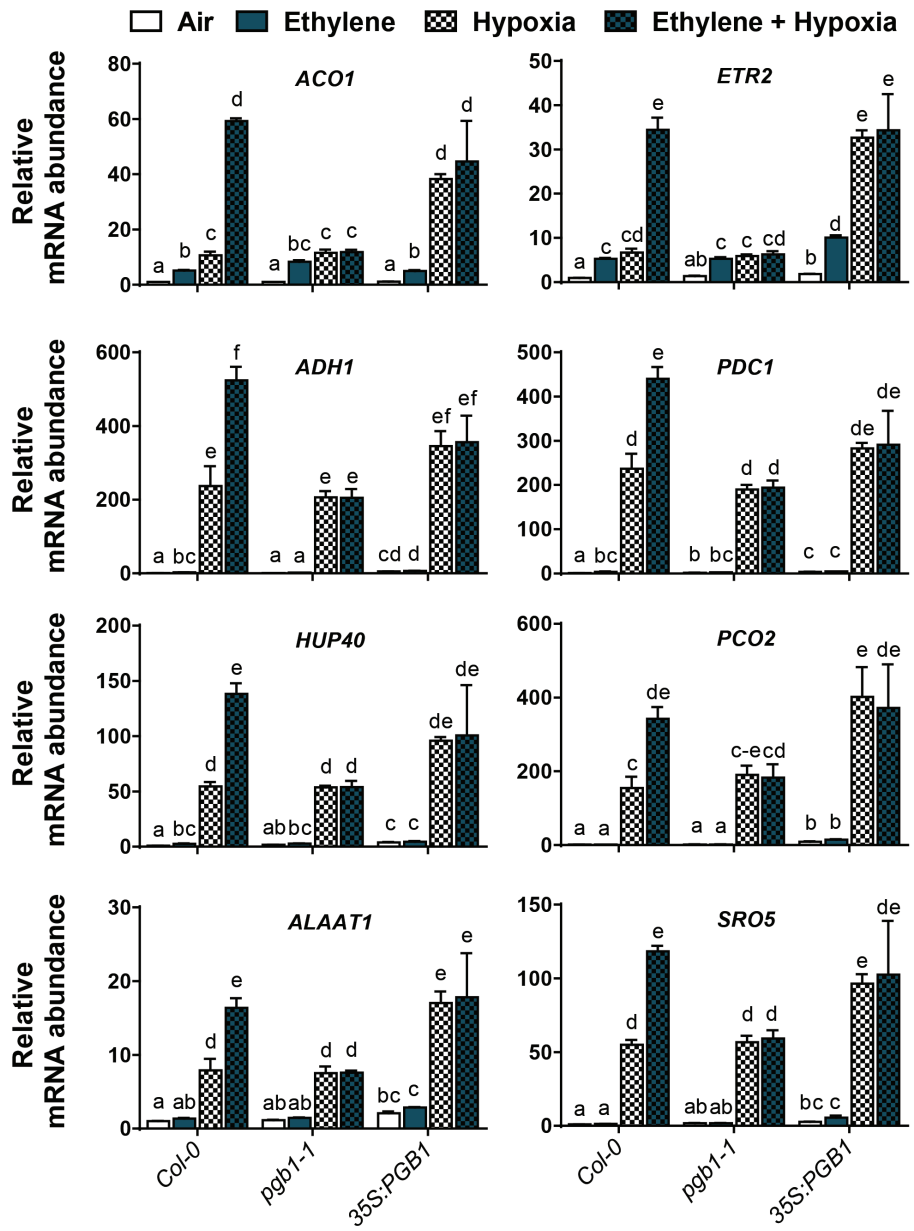


**Figure 4.4. Hypoxia adaptive gene expression in *PGB1* knock-down and over-expression lines.**

Relative mRNA transcript abundance of 8 hypoxia adaptive genes in seedling root tips of Col-0, *pgb1-1* and *35S:PGB1* after 4 hours of pre-treatment with air (white) or ~5µll⁻¹ ethylene (blue), followed by (4h) hypoxia (blocked pattern). Values are relative to Col-0 air treated samples. Different letters indicate significant differences (Error bars are SEM, $p<0.05$, 2-way ANOVA, Tukey's HSD, n=3 replicates containing ~200 root tips).



hypoxia (Kaiser *et al.*, 1993; Botrel & Kaiser, 1997; Shi *et al.*, 2008). These reports are consistent with our results that show enhanced NR activity in response to hypoxia treatments (Fig. 4.1C). The resulting NO burst during hypoxia is thought to be beneficial through S-nitrosylation and modification of key proteins involved in respiration, metabolism, signaling, and stress responses (Astier *et al.*, 2011; León *et al.*, 2016). In addition, this NR-dependent hypoxic NO burst is thought to enhance hypoxia acclimation by maintaining fermentation and ATP synthesis in 'anoxic cores' of Maize root meristems (Igamberdiev *et al.*, 2005; Mugnai *et al.*, 2012; Armstrong *et al.*, 2019). Phytoglobins facilitate $NAD^+$ regeneration under hypoxia via the so-called phytoglobin/NO cycle and are suggested to play a crucial role in maintaining the energy charge in the 'anoxic core' as long as carbohydrates and nitrate are sufficiently available (Igamberdiev *et al.*, 2005; Gupta & Igamberdiev, 2016; Armstrong *et al.*, 2019). These reports suggest that the NO burst during hypoxia is adaptive and partially mediated by high PGB1 levels during hypoxia. However, our results demonstrate that ethylene-enhanced hypoxia acclimation is dependent on PGB1-mediated NO removal prior to hypoxia, as the beneficial hypoxia response was abolished when NO was applied prior to hypoxia (Fig. 4.3C, D). Taken together, we suggest that ethylene-mediated NO depletion prior to hypoxia, followed by an NO burst during hypoxia are both crucial for enhanced hypoxia acclimation and survival of plants.

In addition, our results imply that PGB1-controlled hypoxia acclimation is not caused by enhanced PGB1-dependent NO scavenging during hypoxia (Gupta *et al.*, 2011), but by increased NO-scavenging and ERFVII stability prior to hypoxia (Fig. 4.3C, D). Indeed, we show that over-expression of PGB1 leads to ERFVII stability under normoxia and enhanced hypoxia acclimation and depends on NO-removal (Fig. 4.3C, D). As observed in *35S:PGB1*, ERFVII stability was also enhanced under normoxic conditions in *NR*-double mutants that have constitutively low NO levels (Gibbs *et al.*, 2014; Vicente *et al.*, 2017). Moreover, our results are consistent with earlier reports where *PGB1*-impaired mutants showed reduced hypoxia tolerance, while over-expression enhanced tolerance in multiple plant species (Hunt *et al.*, 2002; Dordas *et al.*, 2003; Hebelstrup *et al.*, 2012; Mira *et al.*, 2016). Interestingly, variation for ethylene-induced hypoxia adaptation was also observed in wild *Rumex* species and correlated with *PGB1* induction (van Veen *et al.*, 2013). Finally, natural variation for flooding tolerance in *Brachypodium distachyon* ecotypes was suggested to be dependent on NO removal and correlated with constitutive *PGB1* orthologue up-regulation and active down-regulation of NR during submergence (Rivera-Contreras *et al.*, 2016). Our discovery of PGB1-mediated ERFVII stability

and hypoxia acclimation provides a molecular explanation for the protective role of PGB1 during hypoxia and submergence described in these studies.

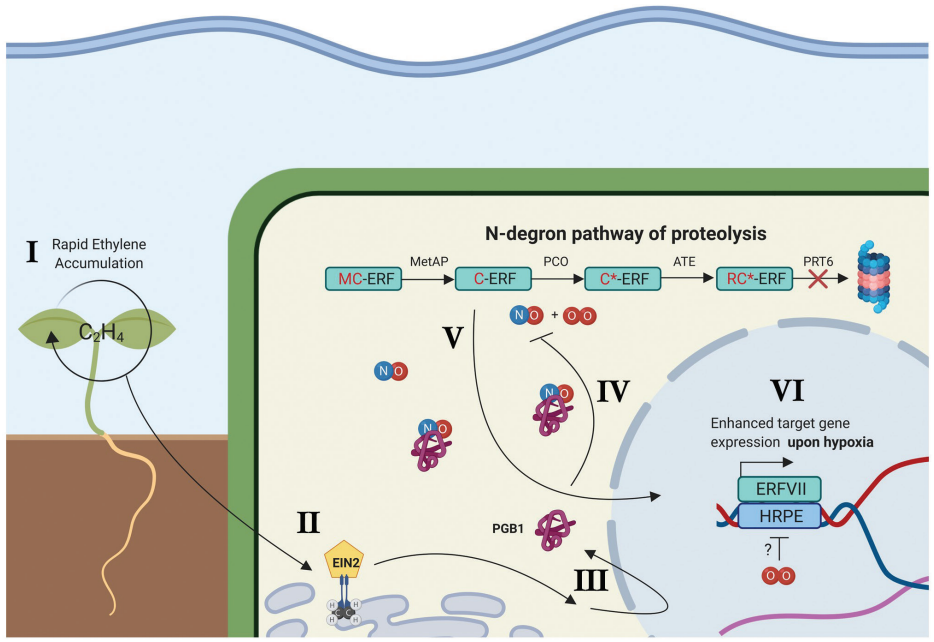


**Figure 4.5. Proposed mechanism of ethylene-induced hypoxia tolerance upon submergence.**
**(I)** Upon submergence ethylene ($C_2H_4$) accumulates within minutes in plant tissues due to restricted gas diffusion. **(II+III)** Ethylene perception leads to EIN2 and EIN3EIL1 dependent signaling and enhanced production of NO-scavenger PHYTOGLOBIN1 (PGB1) within 1 hour of ethylene signaling. **(IV+V)** Within 4 hours, these enhanced PGB1 levels lead to NO depletion, in turn limiting PRT6 N-degron pathway targeted proteolysis of constitutively expressed group VII Ethylene Response Factor transcription factors (ERVIIs). **(V+VI)** Stabilized ERFVIIs translocate to the nucleus where they induce enhanced hypoxia gene expression only when $O_2$ deprivation occurs. This amplified hypoxia response increases hypoxia tolerance of Arabidopsis root and shoot apical meristems (created with BioRender.com).

One remaining question is how ethylene enhances *PGB1* transcript levels in Arabidopsis. Our results show that *PGB1* induction is controlled by the conventional EIN3-dependent ethylene-signaling pathway (Fig. 4.1E). Interestingly, the *PGB1* promoter does not contain typical ethylene-regulated cis-elements and was shown not to be a direct target of EIN3 and is therefore likely indirectly regulated downstream of EIN3 (Chang *et al.*, 2013; Stasolla *et al.*, 2019). Possible crosstalk of ethylene with the plant hormones abscisic acid (ABA) and jasmonic acid (JA) could potentially facilitate *PGB1* induction (Qu *et al.*, 2005; Bustos-Sanmamed *et al.*, 2011; Stasolla *et al.*, 2019). Future research is required to unravel the transcription



factors and the regulatory promoter elements that control ethylene-induction of *PGB1* transcripts.

In conclusion, we show that plants have the remarkable ability to quickly detect submergence through passive ethylene entrapment and use this signal to acclimate to forthcoming hypoxic conditions. This early ethylene signal prevents N-degron targeted ERFVII proteolysis by increased production of the NO-scavenger PGB1 and in turn primes the plant's hypoxia response (Summarizing model, Fig. 4.5). The proposed mechanism could be instrumental in enhancing conditional flooding tolerance in crops via manipulation of ethylene responsiveness of *PGB1* genes and its downstream signaling targets.

## ACKNOWLEDGEMENTS
We thank Frederica Theodoulou and Hongtao Zhang for feedback and optimization of the PGB1 antibody. We also thank Kim Hebelstrup, Daniel Gibbs, Femke Bosman, Nienke van Dongen, Ankie Ammerlaan and Rob Welschen for technical advice and assistance. Finally, we kindly acknowledge the people named in the methods section for providing seeds of the genotypes used in this chapter.

## MATERIALS AND METHODS
### Plant material and growth conditions
Plant material: *Arabidopsis thaliana* seeds of the ecotype Col-0 and mutants, *pgb1-1* (SK_058388), *ein2-5* and *ein3eil1-1* (Col-0 Background) (Alonso *et al.*, 1999, 2003) were obtained from the Nottingham Arabidopsis Stock Centre. Other germlines used in this study were kindly provided by the following individuals: Ler-0, *rap2.2-5rap2.12-A* and *-B* (and mixed Ler-0 and Col-0 WT backgrounds) from Prof. Angelika Mustroph (Gasch *et al.*, 2016), University Bayreuth, Germany; *35S:PGB1* (Col-0 background) from Prof. Kim H. Hebelstrup (Hebelstrup *et al.*, 2006), Aarhus University, Denmark, and *erf1-1* from Prof. Corné Pieterse, Utrecht University, The Netherlands. The *35S:RAP2.3-HA* transgenic line was described previously (Gibbs *et al.*, 2011, 2014). Additional mutant combinations used in this study were generated by crossing, and all lines were confirmed by either conventional genotyping PCRs and/or antibiotic resistance selection (Primer and additional info in Appendix I). Growth conditions for adult rosettes and in vitro seedlings were similar as described in Chapter 2 of this thesis.

### Experimental setup and (pre-)treatments and hypoxia tolerance assays

Ethylene, NO, cPTIO and hypoxia treatments and tolerance assays were performed as described in Chapter 2 and Chapter 3 of this thesis.

### RNA extraction and quantification, cDNA synthesis and RT-qPCR

Adult rosette (2 whole rosettes per sample) or seedling root tip (~500 root tips) samples were harvested by snap freezing in liquid nitrogen. RNA extraction, RNA quantification, cDNA synthesis and RT-qPCR were performed as described in Chapter 2 of this thesis. Primers used for RT-qPCR can be found in Appendix II.

### Nitrate reductase activity assay

The NR activity was assessed using a mix of 20 whole 10-day-old seedlings with 2 replicates per treatment. Snap frozen samples were ground and homogenized in extraction buffer (100mM HEPES (pH7.5), 2mM EDTA, 2mM di-thiothreitol, 1% PVPP). After centrifugation at 30.000g at 4C for 20 min, supernatants were collected and added to the reaction buffer (100mM HEPES (pH7.5), 100mM $NaNO_3$, 10mM Cysteine, 2mM NADH and 2mM EDTA). The reaction was stopped by the addition of 500mM zinc acetate after incubation for 15min at 25°C. Total nitrite accumulation was determined following addition of 1% sulfanilamide in 1.5M HCl and 0.02% naphthylethylenediamine dihydrochloride (NNEDA) in 0.2M HCl by measuring the absorbance of the reaction mixture at 540 nm.

### Protein extraction, SDS-PAGE and Western Blotting

Protein extraction and SDS-PAGE were performed as described in chapter 3. Blots were blocked for at least 1 hour in blocking solution at RT (5% milk in 1xTBS) before probing with primary antibody in blocking solution (α-HA-HRP, 1:2500 (Roche, Cat. No. 12 013 819 001); α-PGB1, 1:500 (produced for this study using full length protein as antigen by GenScript); α-Actin, 1:2500 (Thermo Fisher Scientific, Cat. No. MA1-744) overnight at 4°C. Blots were rinsed 3 times with 1xTBS-T (0.1% Tween 20) for 10 minutes under gentle agitation before probing with secondary antibody (α-rabbit IgG-HRP, Cat. No. 7074, for PGB1, 1:3000; α-mouse IgG-HRP, Cat. No. 7076, for Actin, 1:2500) and/or SuperSignal™ West Femto chemiluminescence substrate (Fisher Scientific) and blot imaging using Image Lab software in a chemigel doc (Bio-rad) with custom accumulation sensitivity settings for optimal contrast between band detection and background signal. To visualize RAP2.3 (~45 kDa) and ACTIN (~42 kDa) protein levels on the same blot, membranes were stripped after taking final blot images using a mild stripping buffer (pH 2,2, 1.5% (w/v) glycine, 0.1% SDS and 1.0% Tween 20) for 15 minutes and rinsing 3x in 1xTBS-T before blocking and probing with the 2nd primary antibody of interest.



### NO quantification

NO quantification was visualized using confocal microscopy as described in Chapter 3 of this thesis.

### Statistical analyses

Statistical analyses were performed as described in Chapter 2 of this thesis.

# CHAPTER 5

## ETHYLENE REGULATES PROTEINS INVOLVED IN HYPOXIA ACCLIMATION, MITOCHONDRIAL RESPIRATION AND ROS HOMEOSTASIS


Sjon Hartman[1]
Femke Bosman[1]
Hongtao Zhang[2]
Florian de Deugd[1]
Frederica L. Theodoulou[2]
Rashmi Sasidharan[1]*
Laurentius A.C.J. Voesenek[1]*

1. Plant Ecophysiology, Institute of Environmental Biology, Utrecht University, Utrecht, The Netherlands
2. Plant Sciences Department, Rothamsted Research, Harpenden, United Kingdom

*Shared senior authors

## ABSTRACT

Submerged plants suffer from impaired gas diffusion underwater, ultimately leading to oxygen deprivation (hypoxia). The gaseous plant hormone ethylene is rapidly entrapped in submerged plant tissues and instrumental for hypoxia acclimation. To identify ethylene-regulated proteins that are potentially involved in hypoxia acclimation, we performed quantitative proteomics on root tips of ethylene-treated Arabidopsis seedlings. The results revealed that ethylene increased abundance of several proteins localized in the mitochondria, including subunits of electron transport chain complexes. Ethylene also down-regulated ribosomal subunits and possibly translation. In addition, we uncovered that ethylene upregulates proteins involved in hypoxia responses and the homeostasis of reactive oxygen species (ROS). Furthermore, we show that ethylene is crucial for amelioration of the ROS burst during hypoxia and subsequent re-oxygenation. Finally, we demonstrate that ethylene enhances oxidative stress tolerance and propose that this could be a universal response for abiotic stress tolerance in plants.




## INTRODUCTION

The increasing frequency and severity of global flooding events seriously impairs sustainable crop production (Hirabayashi *et al.*, 2013; Voesenek & Bailey-Serres, 2015a). Submerged plants ultimately experience a cellular lack of oxygen ($O_2$) availability (hypoxia) under light-limited conditions as a result of impaired gas diffusion underwater and high water turbidity (Voesenek & Bailey-Serres, 2015a). Hypoxia ultimately arrests mitochondrial respiration and leads to a life-threatening energy crisis. It is therefore of crucial importance for plants to quickly detect submergence in order to acclimate to, or escape from, severe hypoxia.

Previous research has shown that the gas ethylene is rapidly entrapped and perceived in submerged plant tissues (Voesenek & Sasidharan, 2013) (Chapter 2 of this thesis). Ethylene mediates a plethora of flooding adaptive responses and facilitates metabolic acclimation to hypoxia in plants (Voesenek & Sasidharan, 2013; van Veen *et al.*, 2013; Yamauchi *et al.*, 2014). In addition, ethylene was shown to be necessary for full induction of ethanolic fermentation under hypoxia (Peng, 2001; Tesniere *et al.*, 2004; Yamauchi *et al.*, 2014). In chapters 3 and 4 of this thesis we show that ethylene mediates hypoxia acclimation through enhancing the stability of group VII Ethylene Response Factor transcription factors (ERFVIIs). The ERFVIIs are responsible for $O_2$ and nitric oxide level (NO) sensing through the PROTEOLYSIS6 (PRT6) N-degron pathway of proteolysis and are the principal activators of the adaptive transcriptional hypoxia response (Gibbs *et al.*, 2011, 2014; Licausi *et al.*, 2011; Bui *et al.*, 2015; Gasch *et al.*, 2016; Varshavsky, 2019). The ERFVIIs are substrates of the PRT6 N-degron pathway through a conserved amino acid sequence of MCGGAII/L at the N-terminus (Gibbs *et al.*, 2011; Licausi *et al.*, 2011; Varshavsky, 2019). The fate of ERFVII turnover is defined by the presence of the $Met_1$-$Cys_2$ (MC) residues, which function as part of an N-degron and render these proteins susceptible to PRT6-dependent ubiquitination and proteolysis (Tasaki *et al.*, 2012; Varshavsky, 2019). We showed that ethylene can stabilize ERFVIIs through enhanced NO depletion in ambient $O_2$ (normoxia) and consequently prime the hypoxia response when $O_2$ levels diminish. This enhanced ERFVII stability is mediated through the non-symbiotic PHYTOGLOBIN1 (PGB1), which facilitates NO-depletion and impairs NO-dependent ERFVII proteolysis. Additionally, the MC-initiating proteins and PRT6 N-degron pathway targets VERNALIZATION2 (VRN2) and LITTLE ZIPPER2 (ZPR2) were identified and shown to be involved in hypoxia-mediated developmental processes and tolerance (Gibbs *et al.*, 2018; Weits *et al.*, 2019). Together, these results show that ethylene is an important early

signal that regulates key proteins during flooding acclimation and that ethylene has the potential to stabilize MC-initiating proteins through active NO-depletion.

To uncover novel ethylene-regulated proteins that contribute to hypoxia acclimation, we performed quantitative proteomics on root tips of ethylene-treated Arabidopsis seedlings. Ethylene treatment increased the abundance of multiple proteins associated with mitochondria, including proteins that are components of the electron transport chain (ETC). Surprisingly, MC-initiating proteins with increased abundance were not detected in the root tips of ethylene treated seedlings, but levels of 3 MC-proteins were reduced. However, a partial overlap was found between ethylene-regulated proteins and those upregulated in mutants of the PRT6 N-degron pathway. Furthermore, ethylene down-regulated proteins involved in translation. Finally, several proteins involved in hypoxia acclimation and ROS tolerance were increased in response to ethylene. This led us to investigate and demonstrate that ethylene is important for amelioration of the mitochondrial ROS burst during hypoxia and subsequent re-oxygenation. We conclude that ethylene increases proteins involved in mitochondrial respiration, hypoxia acclimation and ROS homeostasis and in this way contributes to subsequent hypoxia and post-hypoxia tolerance.

## RESULTS

To be able to perform quantitative proteomics on Arabidopsis root tips, a substantial amount of root tip sample material is required (100-200 mg fresh weight per sample). To retrieve enough root tip material, seedlings had to be grown at significantly higher (~8x higher) densities compared to prior studies (Chapter 2-4 of this thesis). At this higher density, root tips showed enhanced basal root tip survival after hypoxia, but still responded to ethylene (Fig. S5.1A). The increased root tip survival of air pre-treated seedlings grown at higher densities was not caused by differences in basal ethylene levels, as blocking ethylene signaling with antagonist 1-methylcyclopropene (1-MCP) did not reduce the density-enhanced survival (Fig. S5.1A). Furthermore, the ethylene responsive genes *ETHYLENE RESPONSE 2* (*ETR2*) and *ACC OXIDASE 2* (*ACO2*) behaved similarly in experiments comparing seedlings grown at low and high densities (Fig. S5.1B). Therefore, we performed 5 independent ethylene-treatment experiments in which the seedlings were grown at higher densities to enable the harvest of enough root tip material for quantitative proteomics.



### Ethylene enhances proteins involved in the mitochondrial electron transport chain, ROS homeostasis and anaerobic respiration

We used isobaric multiplex tandem mass tag (TMT™)-based quantitative mass spectrometry (MS) to quantify protein abundance differences in root tips of 5-day old seedlings treated with ethylene or air. With a cut-off of 2 or more detected peptides for protein recognition, 6525 annotated Arabidopsis proteins were identified and quantified. 729 proteins were differentially regulated ($p<0.05$) by an ethylene treatment of 4 hours. Ethylene enhanced the abundance of 375 proteins and decreased the abundance of 354 proteins (the 30 most differentially regulated proteins are shown in Table S5.1 & S5.2). To identify molecular and cellular processes that are regulated by ethylene-mediated proteins, we performed gene ontology (GO) term enrichment analysis using the ranked list of the normalized protein fold change between ethylene and air treatments. GO terms were divided into three categories for both up-regulated and down-regulated proteins: cellular component, molecular function and biological process (Eden *et al.*, 2009). Firstly, GO term enrichment for cellular components revealed that ethylene strongly enhanced abundance of proteins associated with mitochondria, including mitochondrial respiratory chain complex I (Table 5.1). Moreover, GO terms for molecular function show that ethylene may control reactive oxygen species (ROS) homeostasis through enhanced abundance of proteins involved in oxidoreductase, peroxidase, antioxidant and catalase activity (Table 5.1). In addition, ethylene strongly enriched the GO terms for biological processes 'oxidation-reduction process', 'hydrogen peroxide catabolic process' and "anaerobic respiration", of which the last term consisted of the hypoxia responsive proteins HYPOXIA-RESPONSIVE UNKNOWN PROTEIN (HUP) 36 and HUP26 (Table 5.1 & S5.1) (Mustroph *et al.*, 2010). Finally, GO term enrichment for most down-regulated proteins reveals that ethylene may restrict translation through a reduction in ribosomal subunit proteins (Table 5.2 & S5.2).

**Table 5.1 Gene ontology analysis of proteins up-regulated by ethylene in Arabidopsis root tips.**
Table showing the overrepresented cellular component, molecular function and biological process gene ontology (GO) terms of ethylene-up-regulated proteins in Arabidopsis seedling root tips. Analysis was performed using *GOrilla*, a web-based software tool that identifies enriched GO terms, using the ranked list (highest to lowest) of the normalized protein fold change (ethylene compared to air, p <0.05, minimum hypergeometric test, Benjamini and Hochberg correction) (Eden *et al.*, 2009). GO term results were only included in the analysis if they had an enrichment score of 2 or higher and the GO term group consisted of at least 2 proteins that were present in the dataset. GO terms indicated in bold are discussed in the results section.

**CELLULAR COMPONENT**

| GO term | Description | P-value | Enrichment Score |
|---|---|---|---|
| GO:0098800 | **Inner mitochondrial membrane protein complex** | 0.000 | 3.01 |
| GO:0044455 | **Mitochondrial membrane part** | 0.000 | 2.76 |
| GO:0098798 | **Mitochondrial protein complex** | 0.000 | 2.47 |
| GO:0044429 | **Mitochondrial part** | 0.003 | 11.46 |
| GO:0098803 | **Respiratory chain complex** | 0.003 | 2.96 |
| GO:1990204 | **Oxidoreductase complex** | 0.003 | 20.14 |
| GO:0030964 | **NADH dehydrogenase complex** | 0.004 | 3.27 |
| GO:0045271 | **Respiratory chain complex I** | 0.004 | 3.27 |
| GO:0005747 | **Mitochondrial respiratory chain complex I** | 0.004 | 3.27 |
| GO:0019866 | Organelle inner membrane | 0.014 | 11.66 |
| GO:0098796 | Membrane protein complex | 0.026 | 8.68 |
| GO:0042170 | Plastid membrane | 0.031 | 9.09 |
| GO:0031969 | Chloroplast membrane | 0.029 | 9.09 |
| GO:0009505 | Plant-type cell wall | 0.029 | 3.2 |

**MOLECULAR FUNCTION**

| GO term | Description | P-value | Enrichment Score |
|---|---|---|---|
| GO:0004601 | **Peroxidase activity** | 0.002 | 8.61 |
| GO:0016684 | **Oxidoreductase activity, acting on peroxide as acceptor** | 0.001 | 8.4 |
| GO:0016209 | **Antioxidant activity** | 0.001 | 7.81 |
| GO:0020037 | **Heme binding** | 0.003 | 25.05 |
| GO:0046906 | **Tetrapyrrole binding** | 0.003 | 25.05 |
| GO:0004096 | **Catalase activity** | 0.004 | 180.37 |
| GO:0003700 | DNA-binding transcription factor activity | 0.008 | 2.16 |
| GO:0016491 | **Oxidoreductase activity** | 0.044 | 4.83 |

**BIOLOGICAL PROCESS**

| GO term | Description | P-value | Enrichment Score |
|---|---|---|---|
| GO:0055114 | **Oxidation-reduction process** | 0.002 | 7.58 |
| GO:0009061 | **Anaerobic respiration** | 0.009 | 214.19 |
| GO:0042744 | **Hydrogen peroxide catabolic process** | 0.045 | 3.41 |



**Table 5.2 Gene ontology analysis of proteins down-regulated by ethylene in Arabidopsis root tips.**
Table showing the overrepresented cellular component, molecular function and biological process gene ontology (GO) terms of ethylene-down-regulated proteins in Arabidopsis seedling root tips. Analysis was performed using *GOrilla*, a web-based software tool that identifies enriched GO terms, using the ranked list (lowest to highest) of the normalized protein fold change (ethylene compared to air, p <0.05, minimum hypergeometric test, Benjamini and Hochberg correction) (Eden *et al.*, 2009). GO term results were only included in the analysis if they had an enrichment score of 2 or higher and the GO term group consisted of at least 2 proteins that were present in the dataset. GO terms indicated in bold are discussed in the results section.

**CELLULAR COMPONENT**

| GO term | Description | P-value | Enrichment Score |
|---|---|---|---|
| GO:0022625 | **Cytosolic large ribosomal subunit** | 0.00 | 3.92 |
| GO:0044391 | **Ribosomal subunit** | 0.00 | 3.02 |
| GO:0015934 | **Large ribosomal subunit** | 0.00 | 3.53 |
| GO:0044445 | Cytosolic part | 0.00 | 2.61 |
| GO:0022626 | **Cytosolic ribosome** | 0.00 | 2.97 |
| GO:0005840 | **Ribosome** | 0.00 | 2.48 |

**MOLECULAR FUNCTION**

| GO term | Description | P-value | Enrichment Score |
|---|---|---|---|
| GO:0003735 | **Structural constituent of ribosome** | 0.00 | 2.83 |
| GO:0005198 | Structural molecule activity | 0.00 | 2.24 |
| GO:0042973 | Glucan endo-1,3-beta-D-glucosidase activity | 0.04 | 9.31 |

**BIOLOGICAL PROCESS**

| GO term | Description | P-value | Enrichment Score |
|---|---|---|---|
| GO:0006518 | **Peptide metabolic process** | 0.00 | 2.94 |
| GO:0006412 | **Translation** | 0.00 | 2.65 |
| GO:0043043 | **Peptide biosynthetic process** | 0.00 | 2.65 |
| GO:0043604 | Amide biosynthetic process | 0.00 | 2.87 |
| GO:0043603 | Cellular amide metabolic process | 0.00 | 2.41 |
| GO:0044271 | Cellular nitrogen compound biosynthetic process | 0.00 | 2.08 |
| GO:0009059 | Macromolecule biosynthetic process | 0.00 | 1.92 |
| GO:0045739 | Positive regulation of DNA repair | 0.01 | 8.9 |

In an alternative analysis, we investigated if ethylene could enhance MC-initiating proteins and whether there are indications that ethylene universally impairs the PRT6 N-degron pathway. We detected 29 MC-initiating proteins using quantitative proteomics, but none of these proteins were enriched after an ethylene treatment (Table S5.3). Interestingly, ethylene did reduce the abundance of three MC-proteins with unknown biological function (Table S5.3). Moreover, comparison with proteins stabilized in both the PRT6 N-degron loss-of-function mutants *prt6* and *ate1ate2* showed that at least 3 proteins were regulated in a similar fashion by ethylene (Table S5.4, (Zhang *et al.*, 2015)). It is, however, not clear whether these proteins are regulated by ethylene through impairment of the PRT6 N-degron pathway, as at least one of these proteins is also a direct target of the ethylene transcriptional regulator ETHYLENE INSENSITIVE3 ((EIN3), Table S5.4, (Chang *et al.*, 2013)).

In a final analysis, we screened the dataset for ethylene-enhanced proteins that could play a role in hypoxia acclimation. Interestingly, PGB1 was the most enriched protein in response to ethylene (6.4-fold, Table S5.1). Furthermore, HUP36 (4.05-fold), HUP26 (1.47-fold) and HUP54 (1.21-fold) abundance were increased in response to ethylene (Table S5.1 (Mustroph *et al.*, 2010)). Additional interesting proteins that were more abundant and previously linked to hypoxia responses include BRANCHED CHAIN ALPHA-KETO DE-HYDROGENASE COMPLEX SUBUNIT E1-ALPHA ((BCKDE1A), 2.18-fold (Schertl & Braun, 2014; Peng *et al.*, 2015)) and NITRATE REDUCTASE 1 ((NR1), 1.83-fold, Table S5.1, (Igamberdiev *et al.*, 2005; Gupta *et al.*, 2012)). Finally, PGB2, PGB3 and NR2 were also present in the dataset but not affected by ethylene treatment (data not shown). Next, we aimed to unravel whether the observed ethylene-regulated processes and proteins were important for hypoxia acclimation.



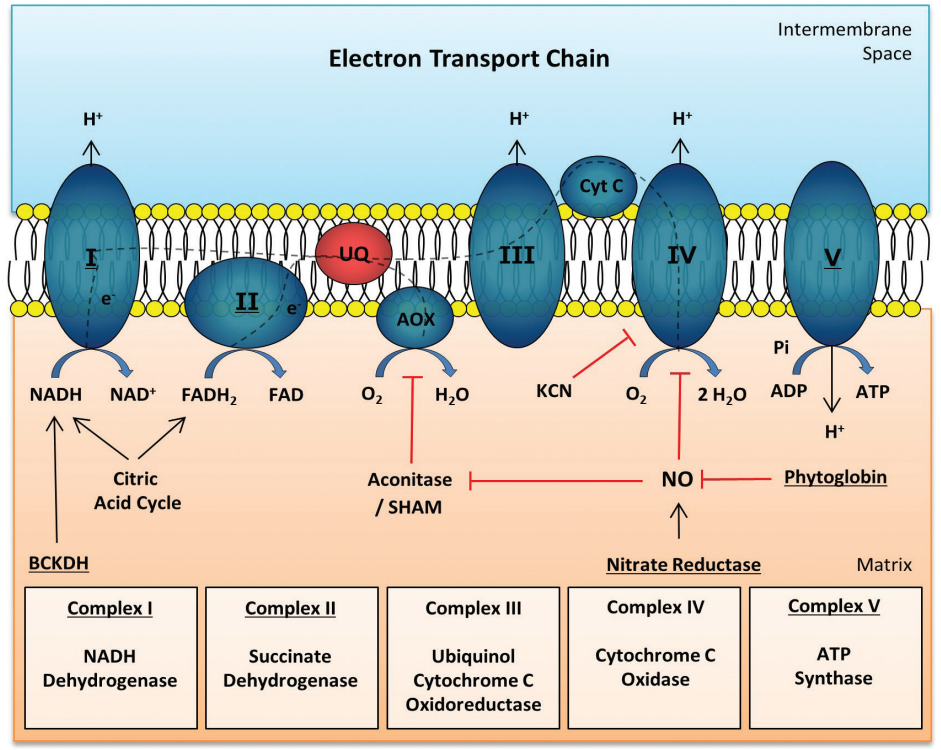


**Figure 5.1 Overview of the mitochondrial electron transport chain and ethylene-regulated proteins.**
A simplified overview of the mitochondrial election transport chain (ETC) showing the five respiratory chain complexes (**I-V**) of oxidative phosphorylation, two mobile electron transporters (**UQ:** ubiquinone, **Cyt C**: Cytochome c), alternative oxidase (**AOX**) and (ethylene-mediated) proteins known to influence these complexes. Generally, the electron ($e^-$) flow (dashed line) is established through the transfer of electrons from NADH at complex I or $FADH_2$ at complex II. The electrons can ultimately be transferred to $O_2$, which is reduced to water at cytochrome c oxidase (COX) or AOX. At complex I, III and IV the electron transfer generally leads to proton translocation across the inner mitochondrial membrane. This proton translocation supplies ATP synthase (complex V) with the required proton gradient for the phosphorylation of ADP, synthesizing ATP through oxidative phosphorylation. Ethylene leads to significant enhanced protein abundance of subunits in complexes I, II and V. Ethylene also increased protein abundance of several other proteins known to play a role in the ETC or mitochondrial respiration (underscored in figure). **BCKDH** subunit E1- alpha (BCKDE1A) is present in the mitochondria and can deliver electrons to complex I . Aconitase inhibits AOX activity, stimulating electron transfer through Cyt c. However, NO inhibits **aconitase** activity and cytochrome c oxidase, and cellular NO homeostasis is regulated by **nitrate reductases** and **phytoglobins**. Finally, potassium cyanide (**KCN**) prevents the reduction of $O_2$ at complex IV, whereas salicylhydroxamic acid (**SHAM**) inhibits AOX.

### Ethylene may improve hypoxia tolerance through changes in COX and AOX activity

Ethylene increased the GO enrichment term of ETC complex I (Table 5.1), several subunits of ETC complexes (I, II, V) and proteins involved in NO homeostasis (Fig. 5.1, Table S5.1). Moreover, NO was previously shown to increase the activity of ALTERNATIVE OXIDASE (AOX) through impairment of aconitase but also to restrict CYTOCHROME C OXIDASE (COX) activity (Fig. 5.1, (Gupta *et al.*, 2012; Schertl & Braun, 2014; Konert *et al.*, 2015)). Finally, BCKDE1A was one of the most differentially abundant proteins in response to ethylene and was shown to stimulate electron transfer into the ETC through enhanced NADH production (Fig. 5.1, Table S5.1, (Schertl & Braun, 2014; Peng *et al.*, 2015)). Since both mitochondrial energy production and $O_2$ consumption are crucial for hypoxia survival, we explored whether ethylene could regulate hypoxia acclimation through changes in homeostasis of the ETC or mitochondrial respiration.

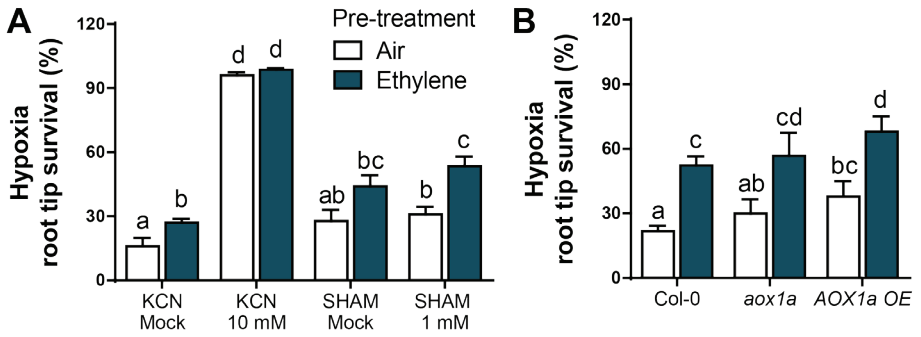


**Figure 5.2 Impairment of COX and stimulation of AOX benefits hypoxia root tip survival.**
**(A)** Seedling root tip survival of Col-0 after 4 hours of pre-treatment with air (white) or ~5µll$^{-1}$ ethylene (blue) in combination with 10mM KCN (chemical inhibitor of COX) or 1mM SHAM (chemical inhibitor of AOX), followed by 4.5 hours of hypoxia and 4 days of recovery. KCN was diluted in autoclaved water (KCN mock), whereas SHAM was diluted in 10% EtOH (v/v, final concentration) and autoclaved water (SHAM mock). Values are relative to control (normoxia) plants. Statistically similar groups are indicated using the same letter (Error bars are SEM, p<0.05, 2-way ANOVA, Tukey's HSD, n=8-16 rows of ~23 seedlings). **(B)** Seedling root tip survival of Col-0, an AOX anti-sense (*aox1a* AS, N6591) and AOX over-expression (N6707) line after 4 hours of pre-treatment with air (white) or ~5µll$^{-1}$ ethylene (blue) followed by 3.5 hours of hypoxia and 4 days of recovery. Values are relative to control (normoxia) plants. Statistically similar groups are indicated using the same letter (Error bars are SEM, p<0.05, 2-way ANOVA, Tukey's HSD, n=4-16 rows of ~23 seedlings).

To unravel whether ethylene affects hypoxia tolerance through COX or AOX functioning, we used chemical inhibitors of these complexes. Potassium cyanide (KCN) prevents the reduction of $O_2$ at complex IV by binding in the center of COX (Schertl & Braun, 2014; Zubo *et al.*, 2014), whereas salicylhydroxamic acid (SHAM) inhibits AOX (Fig. 5.1, (Gupta *et al.*, 2012; Vanlerberghe *et al.*, 2013)). Firstly, we investigated what concentrations of KCN and SHAM impaired primary root growth and survival of Arabidopsis seedlings under normoxic conditions. KCN concentrations of 5mM or 10mM reduced root growth but did not affect root tip survival (Fig. S5.2). SHAM already reduced root growth at 1mM and impaired survival at concentrations of 5mM and higher (Fig. S5.2). We therefore selected inhibitor concentrations that clearly affected physiology but did not impair survival of root tips; 10mM and 1mM for KCN and SHAM, respectively. Interestingly, mock treatments already slightly increased survival compared to previous experiments and the hypoxia duration therefore had to be increased to uncover root tip survival differences in these experiments (Fig. 2.4, 5.2A). Surprisingly, KCN application prior to hypoxia drastically increased hypoxia tolerance of root tip meristems, with 100% of root tips still surviving after 4.5h of hypoxia. Ethylene pre-treatment could only mildly increase survival at these hypoxia durations (Fig. 5.2A). Both pharmaceutical (SHAM) and genetic impairment (*aox1a* anti-sense) of AOX did not affect basal or ethylene-mediated hypoxia tolerance of root tips (Fig. 5.2). However, over-expression of AOX did slightly increase basal and ethylene-induced hypoxia survival compared to Col-0 (Fig. 5.2B). Finally, we observed that a T-DNA line of BCKDE1A did not alter ethylene-induced hypoxia tolerance in root tips compared to the wild type Col-0 (Fig. 5.3A). Together, these results suggest that both enhanced AOX functioning and reduced COX action could play a role in hypoxia acclimation.

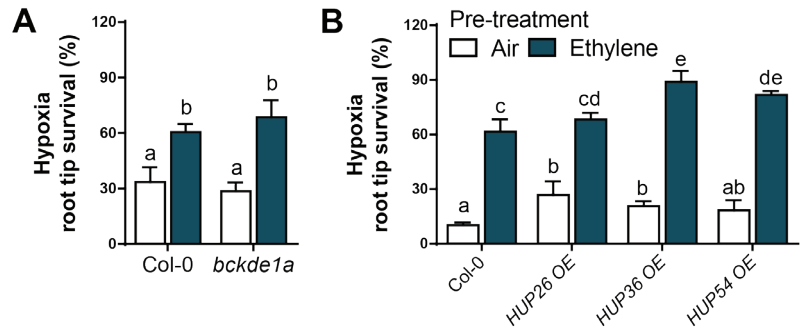


**Figure 5.3 Several ethylene-mediated proteins affect hypoxia survival of Arabidopsis root tips.**
**(A, B)** Seedling root tip survival of Col-0 and a T-DNA line (in 3'UTR) of BCKDE1A **(A)** or Col-0, and 3 over-expression lines of *HUP26, HUP36* and *HUP54* **(B)** or after 4 hours of pre-treatment with air (white) or ~5µll$^{-1}$ ethylene (blue) followed by 3.5 hours of hypoxia and 4 days of recovery. Values are relative to control (normoxia) plants. Statistically similar groups are indicated using the same letter (Error bars are SEM, p<0.05, 2-way ANOVA, Tukey's HSD, n=6-12 rows of ~23 seedlings).

### The ethylene-regulated proteins HUP26 and HUP36 enhance hypoxia tolerance

In addition to regulating mitochondrial specific proteins, ethylene enhanced abundance of several proteins involved in anaerobic respiration and ROS homeostasis (Table 5.1). PGB1 and NR1 were more abundant after ethylene treatment and were previously shown to play an important role in (ethylene-mediated) hypoxia tolerance through enhanced NO metabolism (Table S5.1, Chapter 4, (Hunt *et al.*, 2002; Sanz *et al.*, 2014)). We also found that the proteins encoded by the hypoxia-regulated genes *HUP26*, *HUP36* and *HUP54* were more abundant after ethylene treatment (Table S5.1). In order to uncover whether these proteins are indeed involved in ethylene-regulated hypoxia acclimation, we performed hypoxia root tip survival assays with a selection of transgenic lines. Over-expression lines of *HUP26* and *HUP36*, but not *HUP54*, had higher basal hypoxia tolerance, whereas *HUP36* and *HUP54* over-expressors showed increased ethylene-induced hypoxia tolerance compared to the wild-type (Fig. 5.3B). Together these data suggest that the ethylene-regulated proteins HUP26 and HUP36 may play a role in ethylene-mediated hypoxia acclimation of Arabidopsis root tips.

### Ethylene ameliorates ROS damage in the mitochondria in response to hypoxia and post-hypoxia

Analysis for GO term enrichment showed that ethylene could potentially affect ROS homeostasis through changes in oxidoreductase, peroxidase, antioxidant and catalase activity (Table 5.1). ROS are highly reactive oxygen species produced either enzymatically or non-enzymatically by the reduction of molecular $O_2$ and include radicals such as superoxide, singlet oxygen and hydrogen peroxide ($H_2O_2$) (Mittler, 2017). While ROS are important signaling molecules required for basic biological processes in the cell, excessive ROS as a result of stress is highly destructive for cell integrity (Mittler, 2017). Since ROS amelioration is also suggested to play a crucial part in conferring flooding and hypoxia tolerance (Sasidharan *et al.*, 2018; Yeung *et al.*, 2018), we investigated whether ethylene affects ROS homeostasis and oxidative stress tolerance in Arabidopsis root tips. Accordingly, we used the recently published transgenic $H_2O_2$-reporter line *roGFP2-Orp1* (Nietzel *et al.*, 2018). This fluorescent protein sensor allows the *in vivo* visualization and quantification of $H_2O_2$ in specific organelles at a subcellular level. Since a large portion of ROS is formed inside mitochondria through excessive electron flow through the ETC, we decided to study the mitochondrion-specific (mt-)*roGFP2-Orp1* line (Vanlerberghe *et al.*, 2013; Nietzel *et al.*, 2018). Application of $H_2O_2$ to root tips prior to imaging functioned as a positive control and showed an enhanced *roGFP2-Orp1* oxidation



state, indicative of higher $H_2O_2$ levels (Fig. 5.4A, B). The results show, through an increase in the oxidation state of *roGFP2-Orp1,* that ethylene pre-treatment slightly increased mitochondrial $H_2O_2$ levels in Arabidopsis root tips (Fig. 5.4A, B). However, after 4 hours of hypoxia and 1 hour of re-oxygenation, $H_2O_2$ levels increased drastically inside root tips. This excessive ROS burst inside mitochondria was strongly limited after an ethylene pre-treatment (Fig. 5.4A, B).

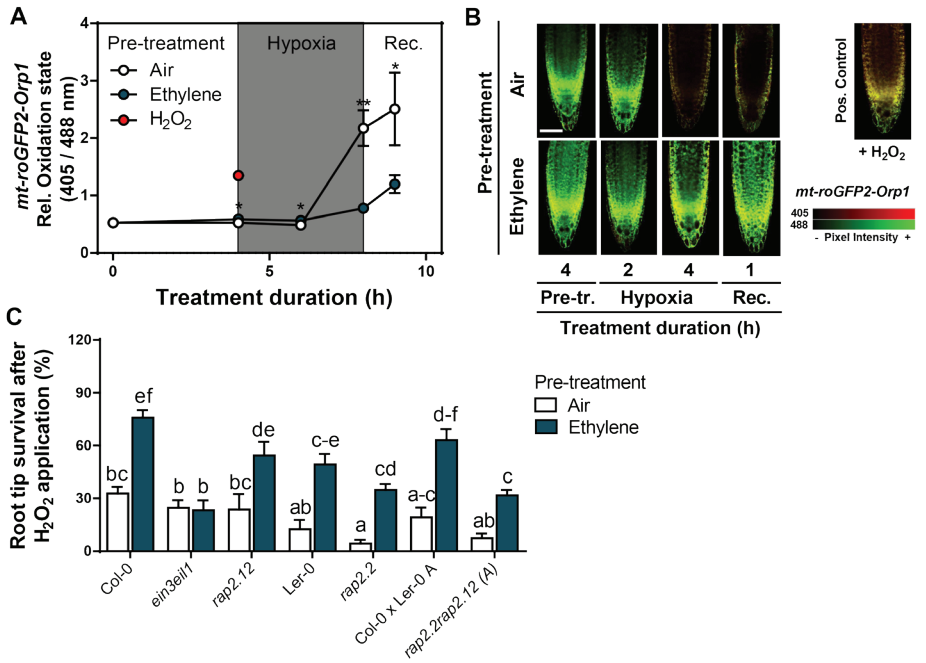


**Figure 5.4 Ethylene limits mitochondrial $H_2O_2$ levels during hypoxia and recovery and acclimates root tips to $H_2O_2$ stress.**

**(A, B)** Quantification (**A**) and representative overlay images (**B**, excitation 405 (red) and 488 (green), emission 520) of the oxidation state of mitochondrial targeted roGFP2-Orp1 in 5 day old Arabidopsis root tips after 4 hours of pre-treatment with air (white) or ~5µll$^{-1}$ ethylene (blue) followed by 2 and 4 hours of hypoxia and 1 hour of recovery. The oxidation state of roGFP2-Orp1 is calculated from 405nm/488 excitation ratios, where a higher oxidation rate corresponds to elevated $H_2O_2$ in mitochondrial matrix (Nietzel *et al.*, 2018). A positive control was included at the 4 hour time-point by adding 200mM $H_2O_2$ to the root tip, 30 minutes prior to imaging. Asterisks indicate significant differences between air and ethylene (Error bars are SEM, *p<0.05, **p<0.01, ANOVA with planned comparisons, Tukey's HSD, n=6-16 root tips). **(C)** Seedling root tip survival of Col-0, Ler-0, ethylene insensitive mutant *ein3eil1*, *rap2.2* (Ler-0 background) and *rap2.12* (Col-0 background) single or double knock-out lines (including WT background mix) after 4 hours of pre-treatment with air (white) or ~5µll$^{-1}$ ethylene (blue) followed by application of 5µl of $H_2O_2$ (6mM) on each single root tip and 3 days of recovery. Values are relative to control (normoxia) plants. Statistically similar groups are indicated using the same letter (Error bars are SEM, p<0.05, 2-way ANOVA, Tukey's HSD, n=6-12 rows of ~23 seedlings).

Previous research showed that a large portion of root tips of Arabidopsis seedlings do not survive 4 hours of severe hypoxia treatment (i.e. Fig. 5.3). We therefore wondered whether the drastic increase in $H_2O_2$ during hypoxia leads to oxidative stress and reduced survival in these root tips, or conversely, that cell death through impaired cell integrity leads to elevated $H_2O_2$ levels. To untangle this question, we assessed whether ethylene could ameliorate excessive ROS damage without the hypoxia treatment. We show that root tips of wild-type seedlings pre-treated with ethylene have enhanced survival when subsequently treated with $H_2O_2$ (Fig. 5.4C). This increased tolerance was absent in the ethylene signaling mutant *ein3eil*. Since previous research has showed that ethylene-regulated hypoxia tolerance is modulated through the enhanced stability of the ERFVIIs RELATED TO APETALA2.2 (RAP2.2) and RAP2.12 (Chapter 3), we assessed whether these ERFVIIs also contributed to the ethylene-mediated oxidative stress tolerance. Our results reveal that single mutants of RAP2.2 and RAP2.12 did not show a clear reduction in $H_2O_2$ tolerance after ethylene pre-treatment, compared to their respective wild types (Fig. 5.4C). However, the double null mutant *rap2.2rap2.12* did show a reduction in ethylene-mediated $H_2O_2$ tolerance compared to its wild-type double background (Ler-0 x Col-0, Fig. 5.4C). In summary, these results demonstrate that ethylene is an important early signal to limit the ROS burst during hypoxia and re-oxygenation.

## DISCUSSION

Ethylene is a reliable early signal for submergence recognition and indispensable for hypoxia acclimation (Chapter 2, (Sasidharan *et al.*, 2018)). We performed quantitative proteomics to reveal novel ethylene-regulated proteins that could facilitate hypoxia acclimation. The main results show that ethylene enhances the abundance of many proteins that are localized in the mitochondria and ETC (Table 5.1). In addition, ethylene increased the presence of several proteins that control hypoxia acclimation and ROS homeostasis and reduced proteins associated with translation and ribosomal subunits (Table 5.1, 5.2).

While quantitative proteomics is a powerful tool to uncover functional proteins involved in any biological process of interest, we also observed technical limitations that include low coverage of the Arabidopsis proteome, limited differential fold changes and high variability for many proteins among biological replicates. Indeed, with 6525 proteins detected and quantified, only ~17% of the Arabidopsis proteome was captured in the current dataset (Cheng *et al.*, 2017). This level of coverage is common for shotgun quantitative proteomics using the current generation of mass spectrometers (Rauniyar & Yates, 2014), but only represents the most



abundant proteins. This provides an explanation why we did not detect expected, but low abundance proteins such as ERFVIIs or ethylene-responsive transcription factors such as EIN3 (Chapter 3, (Alonso *et al.*, 2003; Chang *et al.*, 2013)). Additionally, ethylene-regulated fold changes in protein abundance were relatively small, with only 6 proteins having higher than a 2-fold change after ethylene treatment (Table S5.1). It is possible that a treatment of only 4 hours of ethylene is insufficient to lead to larger differences of protein abundance, and that longer treatment would enhance these differences and reduce variation across biological replicates. However, it is well known that quantitative proteomics using isobaric labelling underestimates changes in relative protein abundance due to technical limitations of mass spectrometry (Rauniyar & Yates, 2014), indicating that the actual fold changes could be significantly higher. Finally, we observed that ethylene strongly down-regulated ribosomal subunit proteins and the GO term 'translation', suggesting that the limited differences could be caused by active down-regulation of translation (Table 5.2, S5.2). Moreover, as translation is a highly energy-demanding process, it could be beneficial for plants to selectively down-regulate this process in anticipation of energy deficit during severe stress (Juntawong & Bailey-Serres, 2012; Juntawong *et al.*, 2014). Further research is required to assess whether ethylene truly reduces translation, whether this is through a reduction in ribosomal subunits and beneficial for subsequent stress survival.

Despite the limitations mentioned above, we uncovered enriched GO terms related to mitochondria and ROS signaling in response to ethylene. Since ethylene enhanced abundance of many proteins in the mitochondria including the ETC, it would be interesting to uncover whether ethylene affects respiration and ATP synthesis or even biogenesis of mitochondria. Pharmaceutical impairment of the ETC complex IV using KCN showed a tremendous positive effect on root tip hypoxia survival (Fig. 5.2A). KCN completely blocks oxidative phosphorylation (Dahan *et al.*, 2014), which on the one hand would conserve $O_2$ but on the other hand also seriously hamper ATP synthesis. One hypothesis could be that KCN therefore limits oxygen consumption before and during mild hypoxia, saving valuable molecular $O_2$ and thus delaying the complete depletion of $O_2$ (anoxia). Alternatively, chemical impairment of the ETC was previously shown to reduce NO production, potentially stabilizing ERFVIIs prior to hypoxia through impairment of the PRT6 N-degron pathway (Horchani *et al.*, 2011; Gibbs *et al.*, 2014). This hypothesis is in line with a recent report showing that impairment of mitochondrial respiration and a decline in mitochondrial ATP levels led to increased transcript levels of hypoxia adaptive genes under normoxia (Wagner *et al.*, 2019). Furthermore,

blocking complex IV with KCN could also force the electron flow from ubiquinone through AOX instead of complex III (Fig. 5.1 (Zhang *et al.*, 2012; Vanlerberghe *et al.*, 2013)). This is in accordance with the observation that over-expression of AOX had slightly enhanced hypoxia tolerance. Interestingly, previous work has shown that enhanced AOX functioning is in fact crucial for hypoxia acclimation, possibly through maintaining ROS and NO homeostasis in the mitochondrion (Gupta *et al.*, 2012; Konert *et al.*, 2015; Vishwakarma *et al.*, 2018). However, in our experiments, blocking AOX through either SHAM or genetic silencing did not alter basal or ethylene-regulated hypoxia tolerance in root tips (Fig. 5.2A, B). Finally, it is known that long-term hypoxia actually leads to a down-regulation of multiple ETC complexes, COX and AOX in rice, but it is unclear whether the down-regulation of all these proteins is beneficial for hypoxia tolerance (Shingaki-Wells *et al.*, 2014). Taken together, these results illustrate that further research is needed to pinpoint what mechanism drives the enhanced hypoxia tolerance after KCN application, and whether ethylene signaling is involved or acts independently.

It is possible that the observed effects could be attributed by side-effects of KCN and SHAM application, such as S-cyanylation of other proteins involved in mitochondrial respiration and glycolysis (Sunil & Raghavendra, 2017; García *et al.*, 2019). Therefore, we propose that it would be useful in future studies to use alternative inhibitors of specific mitochondrial complexes such as antimycin A or n-propyl gallate in combination with an ethylene pre-treatment (Ikuma & Bonner, 1967; Yamasaki *et al.*, 2001). Finally, to get a better understanding of mitochondrial functioning, it would be valuable to measure root tip respiration and local (cytosolic and mitochondrial) ATP levels in response to ethylene treatment and subsequent hypoxia. At the root tip level, this could be realized using $O_2$ micro-electrodes and organelle-specific transgenic ATP sensors (De Col *et al.*, 2017; Pedersen *et al.*, 2018).

In addition to uncovering mitochondrial proteins, we discovered that HUP26, HUP36 and HUP54 protein levels were enhanced in response to ethylene treatment (Table S5.1). Whether ethylene mediates enhanced abundance of these proteins through transcription, translation or post-translational modification is unclear. The promoters of *HUP36* and *HUP54* are, however, direct targets of EIN3, so enhanced protein abundance in response to ethylene could in these cases be driven by enhanced expression (Chang *et al.*, 2013). Previous reports showed that seedlings over-expressing HUP36 and HUP54 were slightly more tolerant to prolonged hypoxia (Mustroph *et al.*, 2010). Our results also demonstrate that over-expression



lines of HUP26 and HUP36, but not HUP54, have slightly enhanced basal hypoxia tolerance in seedlings root tips. Since it is currently unclear what the exact function of these proteins is, future research could focus on using knock-out lines to unravel whether these proteins are indeed required for ethylene-regulated hypoxia tolerance.

Perhaps the most striking result of this chapter is the discovery that ethylene prevents excessive mitochondrial ROS formation during hypoxia and re-oxygenation (Fig. 5.4A, B). Additionally, we showed that ethylene pre-treatment enhanced oxidative stress tolerance of Arabidopsis root tips and that this is partly regulated through the ERFVIIs RAP2.2 and RAP.12 (Fig. 5.4C). These results indicate that the observed RAP2.2- and RAP2.12-dependent ethylene-mediated hypoxia tolerance described in Chapter 3 may partially depend on enhanced ROS amelioration during hypoxia and re-oxygenation. While controlled ROS homeostasis and amelioration were shown to be crucial for hypoxia, re-oxygenation and flooding tolerance, the involvement of ethylene in ameliorating excessive ROS levels has hardly been studied (Fukao & Bailey-Serres, 2004; Yeung *et al.*, 2018). One study suggests that ethylene could indeed play a role during re-oxygenation in Arabidopsis (Tsai *et al.*, 2014). However, ethylene-regulated oxidative stress tolerance has been extensively studied in several plant species for a plethora of other abiotic stresses, including: drought, heat, freezing and especially salt stress (Wu *et al.*, 2008; Peng *et al.*, 2014; Müller & Munné-Bosch, 2015). Moreover, heat, drought and salt stress tolerance were also shown to be dependent on enhanced ERFVII stability (Vicente *et al.*, 2017), and ERFVIIs were shown to regulate several oxidative stress genes and confer oxidative stress tolerance (Borsani *et al.*, 2005; Gonzali *et al.*, 2015; Papdi *et al.*, 2015; Gasch *et al.*, 2016). Taken together, it is likely that ethylene contributes to abiotic stress tolerance through enhanced oxidative stress tolerance and that this process is partially regulated through ERFVIIs. Future research is required to unravel the functional proteins required for actual ethylene-mediated ROS amelioration. Summarizing, we show through quantitative proteomics that ethylene upregulates a plethora of proteins involved in mitochondrial respiration and ROS homeostasis, enhances oxidative stress amelioration during subsequent hypoxia and re-oxygenation and possibly down-regulates translation.

## ACKNOWLEDGEMENTS

We acknowledge Dr. Michael Deery of Cambridge Centre for Proteomics, Cambridge University, for assistance with mass spectrometry and Dr. Kirsty Hassall of

Rothamsted Research for statistical analysis of the raw proteomics data. We thank Emilie Reinen and Ankie Ammerlaan for technical assistance.

## METHODS

### Plant growth material and conditions used for proteomics harvest

Seedlings grown for proteomics harvests (*Arabidopsis thaliana* seeds of ecotype Col-0) were sown in 3 rows at high density (~15-20 seeds/cm) on sterile square petri dishes containing 40 ml autoclaved and solidified ¼ MS, 1% plant agar without additional sucrose, using a pipette after wet surface seed sterilization (incubation in 50% EtOH, 5% Bleach for 10 minutes, followed by 7 washing rounds with Autoclaved MQ water). The plates were left to dry for 30 minutes after sowing. Petri dishes were sealed with gas-permeable tape (Leukopor, Duchefa) and stratified at 4°C in the dark for 4 days. Seedlings were grown vertically on the agar plates under short day conditions (9:00 – 17:00, T= 20°C, Photon Flux Density = ~120 µmol $m^{-2}s^{-1}$, RH= 70%) for 5 days. Samples were harvested in 5 different experiments; 10 plates were pooled per biological replicate. Air and ethylene treatments were performed as described in Chapter 2 of this thesis. Experimental samples were verified by checking the induction of marker genes *ETR2*, *PGB1* and *RAP2.2* using the protocols of RNA extraction, RNA quantification, cDNA synthesis and RT-qPCR as described in Chapter 2 of this thesis.

### Quantitative proteomics: sample preparation, TMT labeling and data analysis

Protein extraction, quantification, reduction and alkalization was done as described previously (Zhang *et al.*, 2015). Protein precipitation was done by the methanol/chloroform method described by (Zhang *et al.*, 2018a). Sequential trypsin digestion was done according to (Zhang *et al.*, 2015). Peptide concentration was determined using a PierceTM Quantitative Colorimetric Peptide Assay kit (23275, Thermo Scientific). 100µg peptide aliquots were labelled using TMT10plex™ (90110, Thermo Scientific). 5 biological replicates were performed: Air-treated samples were labelled with TMT10 -126, -127N, -127C, -128N, -128C and ethylene-treated samples were labelled with -129 N, -129C, -130N, -130C, -131. Peptides were mixed equally and an aliquot corresponding to half of peptides was separated by high pH reverse-phase chromatography using a Waters reverse-phase Nano column as described in (Zhang *et al.*, 2015). All LC-MS/MS experiments were performed as previously (Zhang et al. 2018) using a Dionex Ultimate 3000 RSLC nanoUPLC (Thermo Fisher Scientific Inc, Waltham, MA, USA) system and a Orbitrap Fusion Lumos Tribrid Mass Spectrometer (Thermo Fisher Scientific Inc, Waltham, MA, USA).



Raw data were searched against the TAIR10 database using MASCOT v.2.4 (Matrix Science, London, UK) and PROTEOME DISCOVERER™ v.1.4.1.14 as described previously (Zhang *et al.*, 2015), employing Top 10 peaks filter node and percolator nodes and reporter ions quantifier with Trypsin enzyme specificity with a maximum of one missed cleavage. Carbamidomethylation (+57.021 Da) of cysteine and TMT isobaric labelling (+229.162 Da) of lysine and N-termini were set as static modifications while the methionine oxidation (+15.996) were considered dynamic. Mass tolerances were set to 20 ppm for MS and 0.6 Da for MS/MS. For quantification, TMT 10plex method was used and integration tolerance was set to 2mmu, Integration Method was set as centroid sum. Purity correction factor were set according the TMT10plex (90110) product sheet (Lot number: SA239883). Each reporting ion was divided by the sum of total ions and normalized by medians of each sample. Log transformation ensured a homogeneity and normal distribution of the variances. Statistical differences between air and ethylene samples were obtained using two-sample t-test of $\log_2$ transformed data, considering variation of quantification as a weighting factor. Only proteins represented by two or more peptides were considered for further analysis. All proteomics data is available in Supplemental Data File 1 upon request.

### Gene ontology (GO) term enrichment analysis

Gene ontology (GO) term enrichment analysis was performed using GOrilla, a web-based software tool that identifies enriched GO terms, using the ranked list of the normalized protein fold change (Eden *et al.*, 2009). The software associated 3427 out of the entered 6525 genes with a GO term. GO term results were only included in the analysis if they had an enrichment score of 2 or higher and the GO term group consisted of at least 2 proteins (B, as defined below) that were present in the dataset. Enrichment is defined as: (b/n) / (B/N), with N; total number of genes, B; total number of genes associated with a specific GO term, n; number of genes in the top of the ranked based list and b; number of genes in the intersection (ethylene compared to air, $p < 0.05$, minimum hypergeometric test, Benjamini and Hochberg correction).

### Plant growth material and conditions root tip survival assays

Plant material: *Arabidopsis thaliana* seeds of ecotypes Col-0, *bckde1a* (SK_48037) and *ein3eil1-1* (Alonso *et al.*, 1999, 2003) were obtained from the Nottingham

Arabidopsis Stock Centre. Other germlines used in this chapter were kindly provided by the following individuals: Ler-0, *rap2.2-5* (Ler-0 background, AY201781/GT5336), *rap2.12-2* (SAIL_1215_H10), *rap2.2-5rap2.12-A* and mixed Ler-0 x Col-0 WT background from Prof. Angelika Mustroph, University Bayreuth, Germany (Gasch *et al.*, 2016); *mt-roGFP2-Orp1* from Prof. Markus Schwarzländer (Nietzel *et al.*, 2018), University of Münster, Germany; AOX antisense *aox1a* and over-expression line *35S:AOX1a* from Dr. Jagadish Gupta (Vishwakarma *et al.*, 2018), National Institute Of Plant Genome Research, New Delhi, India; and *35S:HUP26* (35S:3g10020FH), *35S:HUP36* (35S:1g19530FH), *35S:HUP54* (35S:4g27450FH) from Prof. Julia Bailey-Serres (Mustroph *et al.*, 2010), University of California, USA.

**Experimental setup and (pre)treatments**

Ethylene and hypoxia treatments were performed as described in Chapter 2 of this thesis.

KCN and SHAM treatments: Treatments with COX inhibitor KCN and AOX inhibitor SHAM were applied ~30 minutes prior to the air and ethylene pre-treatments. Treatment concentrations were first optimized to ensure that they had no effect on root tip survival (Fig. S5.2). KCN (10 mM) was diluted in autoclaved water (mock), whereas SHAM (1 mM) was diluted in 10% EtOH (v/v, final concentration) and autoclaved water. Droplets of 5µl inhibitor solution or mock were pipetted onto each individual root tip.

$H_2O_2$ treatments: $H_2O_2$ was diluted in autoclaved water to a concentration of 6mM and applied subsequently to seedling root tips in air and ethylene pre-treatments by pipetting 5µl onto each individual root tip. Agar plates were closed after 30 minutes and sealed with Leukopor tape and the location of root tips was marked at the back of the agar plate using a marker pen (0.8mm fine tip). Plates were then placed back vertically under short day growth conditions (in the dark, at 17:00) for recovery. After 3-4 days of recovery, seedling root tips were scored as either alive or dead based on clear root tip re-growth beyond the line on the back of the agar plate. Primary root tip survival was calculated as the percentage of seedlings that showed root tip re-growth out of a row of 23 seedlings. Root tip survival was expressed as the relative survival compared to control plates that received similar pre-treatments but no $H_2O_2$. Droplets of 200 µM $H_2O_2$ were applied to RoGFP2-Orp1 seedling root tips 1h prior to confocal imaging and served as a positive control to verify full oxidation state of *Orp1*.



**Confocal microscopy**

To visualize subcellular levels of $H_2O_2$, confocal imaging of 5-day old *mt-roGFP2-Orp1* Arabidopsis seedlings was performed right after experimental time-points with a Zeiss Observer Z1 LSM700 confocal microscope (oil immersion, 40x objective Plan-Neofluar N.A. 1.30). RoGFP2-Orp1 was excited sequentially at 405 and 488 nm and emission was recorded at 505–535 nm. Within the experiments, laser power, pinhole, digital gain and detector offset were identical for each sample. The 405/488 ratio within root tips was determined in similar areas of ~5000 µm$^2$ using ICY software (http://icy.bioimageanalysis.org).

**Statistical analyses**

Data was plotted using Graphpad Prism software, tables were constructed using Microsoft Excel, Figure 5.1 was constructed using Microsoft Powerpoint. The statistical tests were performed using either Microsoft Excel, Graphpad Prism or R software and the "LSmeans and "multmultcompView" packages. Survival data was generally analyzed with an ANOVA after arcsin transformation of the surviving fraction. Arcsin transformation ensured a homogeneity and normal distribution of the variances, especially for data that did not have treatments with all living or all death responses. The remaining data were analyzed with either Students t-test, 1-way or 2-way ANOVAs. Here data were log transformed if necessary to adhere to ANOVA prerequisites. Multiple comparisons were corrected for with Tukey's HSD.

## SUPPLEMENTAL FIGURES AND TABLES

**Table S5.1 Most up-regulated proteins by ethylene in Arabidopsis root tips.**

Table showing the normalized ratios of the 30 most enhanced differentially regulated proteins in seedling root tips by ethylene, expressed as the protein fold change ratio of ethylene treated seedlings compared to air ($p<0.05$, Student's t-Test, n=5). In addition, HUP54 is added to this table to show its relative protein fold change.

| GENE | Description | Ratio ethylene vs air | p value |
|---|---|---|---|
| AT2G16060.1 | Phytoglobin 1 | 6.403 | 0.034 |
| AT1G19530.1 | Hypoxia unknown protein 36; N-terminal protein myristoylation, anaerobic respiration | 4.055 | 0.000 |
| AT2G07707.1 | Plant mitochondrial atpase, subunit 8 protein | 2.653 | 0.004 |
| AT1G21400.1 | Branched chain alpha-keto de-hydrogenase complex subunit e1-alpha | 2.175 | 0.000 |
| AT1G08880.1 | Histone superfamily protein | 2.063 | 0.028 |
| AT3G04500.1 | RNA-binding (RRM/RBD/RNP motifs) family protein | 2.036 | 0.005 |
| AT5G53330.1 | Ubiquitin-associated/translation elongation factor EF1B protein | 1.957 | 0.007 |
| AT2G41520.1 | Heat shock protein dnaj with tetratricopeptide repeat | 1.930 | 0.001 |
| AT1G77760.1 | Nitrate reductase 1 | 1.827 | 0.012 |
| AT1G09560.1 | Germin-like protein 5 | 1.823 | 0.019 |
| AT5G42180.1 | Peroxidase superfamily protein | 1.812 | 0.013 |
| AT1G10070.1 | Branched-chain amino acid transaminase 2 | 1.714 | 0.005 |
| AT1G23100.1 | Groes-like family protein | 1.657 | 0.011 |
| AT2G31490.1 | Subunit of mitochondrial respiratory chain complex I | 1.652 | 0.036 |
| AT2G48010.1 | Receptor-like kinase in in flowers 3 | 1.652 | 0.017 |
| AT2G27370.1 | Casparian strip membrane domain protein 3 | 1.618 | 0.000 |
| AT1G28330.5 | Dormancy-associated protein-like 1 | 1.617 | 0.003 |
| AT4G37260.1 | Myb domain protein 73 | 1.614 | 0.002 |
| AT3G12140.3 | Emsy N Terminus (ENT)/ plant Tudor-like domains-containing protein | 1.578 | 0.003 |
| AT5G45500.1 | RNI-like superfamily protein | 1.572 | 0.034 |
| AT4G13010.1 | Oxidoreductase, zinc-binding dehydrogenase family protein | 1.567 | 0.025 |
| AT5G60720.1 | Electron transporter, putative protein of unknown function, DUF547 | 1.559 | 0.010 |
| AT5G12220.1 | Las1-like family protein | 1.553 | 0.014 |
| AT4G29000.1 | Tesmin/TSO1-like CXC domain-containing protein | 1.543 | 0.013 |
| AT2G33830.2 | Dormancy/auxin associated family protein | 1.490 | 0.003 |
| AT5G02460.1 | Dof-type zinc finger DNA-binding family protein | 1.488 | 0.047 |
| AT1G11720.2 | Starch synthase 3 | 1.485 | 0.003 |
| AT3G20780.1 | Topoisomerase 6 subunit B | 1.479 | 0.034 |
| AT2G42210.2 | Arabidopsis OEP16 family; located in mitochondrial respiratory chain complex I | 1.477 | 0.007 |
| AT3G10020.1 | Hypoxia unknown protein 26; response to oxidative stress, anaerobic respiration | 1.469 | 0.013 |
| AT4G27450.1 | Hypoxia unknown protein 54, Aluminium induced protein with YGL and LRDR motifs | 1.209 | 0.033 |



**Table S5.2 Most down-regulated proteins by ethylene in Arabidopsis root tips.**

Table showing the normalized ratios of the 30 most reduced differentially regulated proteins in seedling root tips by ethylene, expressed as the protein fold change ratio of ethylene treated seedlings compared to air ($p<0.05$, Student's t-Test, n=5).

| Gene | Description | Ratio ethylene vs air | p value |
|---|---|---|---|
| AT5G02230.1 | Haloacid dehalogenase-like hydrolase (HAD) superfamily protein | 0.470 | 0.000 |
| AT1G73940.1 | Tumor necrosis factor receptor family protein | 0.485 | 0.010 |
| AT4G39800.1 | Myo-inositol-1-phosphate synthase 1 | 0.492 | 0.003 |
| AT2G16005.1 | MD-2-related lipid recognition domain-containing protein | 0.514 | 0.045 |
| AT1G21110.1 | O-methyltransferase family protein | 0.571 | 0.013 |
| AT2G47320.1 | Cyclophilin-like peptidyl-prolyl cis-trans isomerase family protein | 0.590 | 0.002 |
| AT4G21850.1 | Methionine sulfoxide reductase B9 | 0.607 | 0.000 |
| AT5G06760.1 | Late embryogenesis abundant 4-5 | 0.612 | 0.022 |
| AT3G22300.1 | Ribosomal protein S10 | 0.652 | 0.008 |
| AT2G05790.1 | O-Glycosyl hydrolases family 17 protein | 0.665 | 0.013 |
| AT4G19810.1 | Glycosyl hydrolase family protein with chitinase insertion domain | 0.672 | 0.030 |
| AT4G23560.1 | Glycosyl hydrolase 9B15 | 0.677 | 0.013 |
| AT5G59480.1 | Haloacid dehalogenase-like hydrolase (HAD) superfamily protein | 0.679 | 0.001 |
| AT1G23130.1 | Polyketide cyclase/dehydrase and lipid transport superfamily protein | 0.682 | 0.017 |
| AT4G39330.1 | Cinnamyl alcohol dehydrogenase 9 | 0.688 | 0.016 |

| | | | |
|---|---|---|---|
| AT4G02290.1 | Glycosyl hydrolase 9B13 | 0.690 | 0.000 |
| AT3G56350.1 | Iron/manganese superoxide dismutase family protein | 0.699 | 0.022 |
| AT3G62040.1 | Haloacid dehalogenase-like hydrolase (HAD) superfamily protein | 0.706 | 0.000 |
| AT3G03640.1 | Beta glucosidase 25 | 0.716 | 0.035 |
| AT2G21490.1 | Dehydrin LEA | 0.716 | 0.049 |
| AT3G30775.1 | Methylenetetrahydrofolate reductase family protein | 0.717 | 0.002 |
| AT4G01560.1 | Ribosomal RNA processing Brix domain protein | 0.717 | 0.004 |
| AT1G32940.1 | Subtilase family protein | 0.720 | 0.025 |
| AT2G23600.1 | Acetone-cyanohydrin lyase | 0.721 | 0.021 |
| AT5G43320.1 | Casein kinase I-like 8 | 0.731 | 0.010 |
| AT3G02570.1 | Mannose-6-phosphate isomerase, type I | 0.732 | 0.000 |
| AT1G73330.1 | Drought-repressed 4 | 0.735 | 0.040 |
| AT3G55750.1 | Ribosomal protein L35Ae family protein | 0.736 | 0.022 |
| AT5G55060.1 | Rab3 gtpase-activating protein catalytic subunit | 0.742 | 0.017 |
| AT3G02910.1 | AIG2-like (avirulence induced gene) family protein | 0.745 | 0.008 |

**Table S5.3 The effect of ethylene on MC-protein abundance.**
Table showing the normalized ratios of N-terminal MC-proteins detected in the dataset in seedling root tips by ethylene, expressed as the protein fold change ratio of ethylene treated seedlings compared to air (**Bold** indicates p<0.05, Student's t-Test, n=5).

| Gene | Description | Ratio ethylene vs air | p value |
|---|---|---|---|
| AT4G14430.1 | Indole-3-butyric acid response 10 | 1.107 | 0.060 |
| AT3G51640.1 | Stress response NST1-like protein | 1.107 | 0.730 |
| AT4G24020.1 | NIN like protein 7 | 1.088 | 0.329 |
| AT2G26110.1 | Protein of unknown function (DUF761) | 1.070 | 0.668 |
| AT5G54830.1 | DOMON domain-containing protein / dopamine beta-monooxygenase N-terminal domain | 1.065 | 0.274 |
| AT5G65010.2 | Asparagine synthetase 2 | 1.049 | 0.126 |
| AT3G24090.1 | Glutamine-fructose-6-phosphate transaminase; sugar binding; transaminases | 1.041 | 0.552 |
| AT2G33230.1 | Yucca 7 | 1.037 | 0.574 |
| AT4G28820.1 | HIT-type Zinc finger family protein | 1.030 | 0.459 |
| AT1G06570.1 | Phytoene desaturation 1 | 1.012 | 0.894 |



| | | | |
|---|---|---|---|
| AT3G47340.1 | Glutamine-dependent asparagine synthase 1 | 1.002 | 0.991 |
| AT4G16845.1 | VEFS-Box of polycomb protein | 0.999 | 0.995 |
| AT5G10240.1 | Asparagine synthetase 3 | 0.984 | 0.555 |
| AT1G65520.1 | Delta(3), delta(2)-enoyl coa isomerase 1 | 0.977 | 0.684 |
| AT1G22950.1 | 2-oxoglutarate (2OG) and Fe(II)-dependent oxygenase superfamily protein | 0.977 | 0.582 |
| AT2G41900.1 | CCCH-type zinc finger protein with ARM repeat domain | 0.973 | 0.561 |
| AT4G14440.1 | 3-hydroxyacyl-coa dehydratase 1 | 0.972 | 0.891 |
| AT3G03773.2 | HSP20-like chaperones superfamily protein | 0.959 | 0.524 |
| AT3G12600.1 | Nudix hydrolase homolog 16 | 0.957 | 0.419 |
| AT5G48180.1 | Nitrile specifier protein 5 | 0.946 | 0.383 |
| AT2G03667.1 | Asparagine synthase family protein | 0.946 | 0.276 |
| AT4G09320.1 | Nucleoside diphosphate kinase family protein | 0.925 | 0.219 |
| AT1G63610.2 | Unknown protein | 0.923 | 0.144 |
| AT3G63220.2 | Galactose oxidase/kelch repeat superfamily protein | 0.907 | 0.166 |
| AT4G02860.1 | Phenazine biosynthesis phzc/phzf protein | 0.880 | 0.160 |
| AT2G07640.1 | NAD(P)-binding Rossmann-fold superfamily protein | 0.836 | 0.134 |
| AT5G12850.1 | **CCCH-type zinc finger protein with ARM repeat domain** | 0.816 | 0.000 |
| AT2G10450.1 | **14-3-3 family protein** | 0.805 | 0.034 |
| AT2G26470.1 | **Embryonic stem cell-specific 5-hydroxymethylcytosine-binding protein** | 0.785 | 0.030 |

**Table S5.4 Comparison of identified proteins regulated by the PRT6 N-degron pathway and ethylene.**

The table shows the normalized ratios of protein abundance significantly enriched in both N-degron pathway mutants *prt6-1* and *ate1ate2* (adapted from (Zhang *et al.*, 2015)), compared to the protein fold change of those treated with ethylene compared to air (**Bold** indicates p<0.05, Student's t Test). *Indicates whether the genes encoding for these proteins are direct targets of ethylene transcriptional regulator EIN3 (Chang *et al.*, 2013).

| Gene | Description | Ratio *prt6*: Col-0 | Ratio *ate1/2*: Col-0 | Ratio ethylene : air (in Col-0) | EIN3 target |
|---|---|---|---|---|---|
| AT4G27450.1 | **HUP54, Aluminium induced protein with YGL and LRDR motifs** | 3.826 | 6.642 | **1.209** | Yes* |
| AT2G16060.1 | **PGB1, Phytoglobin 1** | 3.218 | 5.200 | **6.403** | No |
| AT3G03270.1 | HRU1, Hypoxia-Responsive Universal Stress Protein 1 | 2.143 | 3.373 | 1.004 | Yes* |
| AT5G19550.1 | ASP2, Aspartate aminotransferase 2 | 1.364 | 1.629 | 0.954 | No |
| AT5G26280.1 | TRAF-like family protein | 1.344 | 1.490 | 1.085 | No |
| AT1G52070.1 | Mannose-binding lectin superfamily protein | 1.314 | 1.201 | 0.891 | No |
| AT5G63550.2 | **DEK domain-containing chromatin associated protein** | 1.279 | 1.404 | **1.256** | No |
| AT3G12580.1 | HSP70, heat shock protein 70 | 1.198 | 1.319 | 1.001 | No |
| AT5G61210.1 | SNP33, soluble N-ethylmaleimide-sensitive factor adaptor protein 33 | 1.194 | 1.331 | 1.103 | No |
| AT5G12110.1 | Glutathione S-transferase, C-terminal-like; Translation elongation factor | 1.152 | 1.454 | 1.191 | No |
| AT4G08770.1 | PRX37, Peroxidase superfamily protein | 1.127 | 1.349 | 1.120 | No |
| AT3G07720.1 | Galactose oxidase/kelch repeat superfamily protein | 1.126 | 1.379 | 1.072 | No |



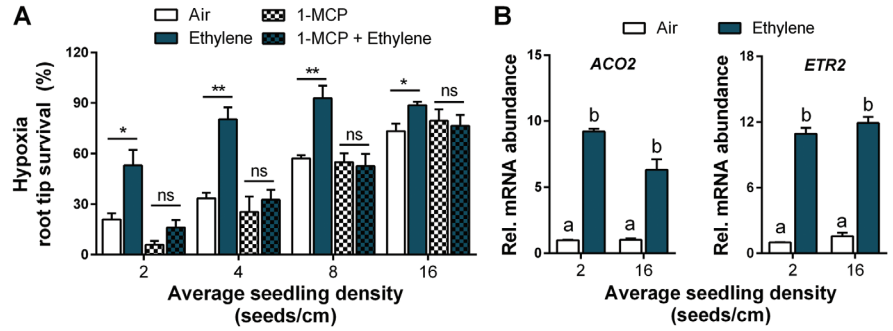


**Figure S5.1 The effects of seeding density on root tip survival and ethylene responses.**
**(A)** Seedling root tip survival of 5-day old Col-0 seedlings grown under 4 different seeding densities after 4 hours of pre-treatment with air (white) or ~5µll$^{-1}$ ethylene (blue) in combination with ethylene action antagonist 1-MCP, followed by 3.5 hours of hypoxia and 3 days of recovery. Asterisks indicate significant differences between air and ethylene treatments (Error bars are SEM, *p<0.05, **p<0.01, Student's t-Test, n=4 rows of seedlings). **(B)** Relative mRNA transcript abundance of the ethylene and EIN3-regulated genes *ACO2* and *ETR2* in root tips of 5-day old Col-0 seedlings grown under 2 different seeding densities after 4 hours of treatment with air (white) or ~5µll$^{-1}$ ethylene (blue). Values are relative to the mean of air treated seedlings of the lower density. Statistically similar groups are indicated using the same letter (Error bars are SEM, p<0.05, 1-way ANOVA, Tukey's HSD, n=3 rows of root tips).

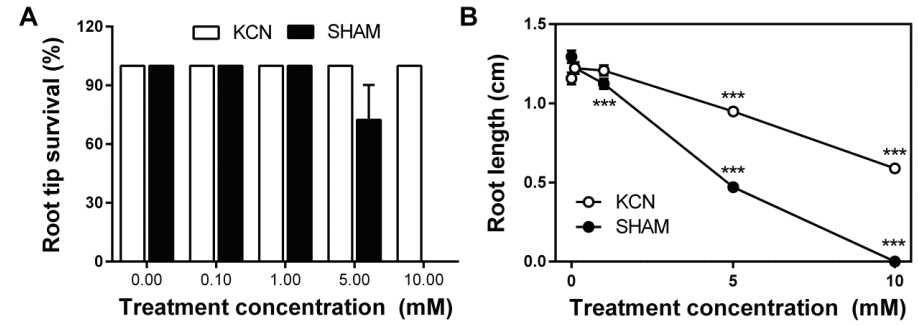


**Figure S5.2 The effects of KCN and SHAM application on root tip performance.**
**(A, B)** Seedling root tip survival (A) and growth (B) after treatment with different concentrations of cytochrome c oxidase (COX) inhibitor KCN and alternative oxidase (AOX) inhibitor SHAM. Measurements were taken 4 days after application of inhibitors. KCN was diluted in autoclaved water (mock), whereas SHAM was diluted in 10% EtOH (v/v, final concentration) and autoclaved water. Asterisks indicate significant differences between control (mock) and treatments at given concentrations (Error bars are SEM, ***p<0.001, 1-way ANOVA with planned comparisons, Tukey's HSD, n=60-81 root tips).

# CHAPTER 6

## EXPLORING ETHYLENE-MEDIATED HYPOXIA TOLERANCE IN WILD AND CULTIVATED SOLANUM SPECIES


Sjon Hartman
Nienke van Dongen
Rob A.M. Welschen-Evertman
Johanna Kociemba
Hans van Veen
Rashmi Sasidharan*
Laurentius A.C.J. Voesenek*



**MODIFIED EXCERPTS OF THIS CHAPTER ARE PUBLISHED IN:**

- Hartman, S., *et al.* (2019). Ethylene-mediated nitric oxide depletion pre-adapts plants to hypoxia stress, Nature Communications, 10 (1), 4020.



Plant Ecophysiology, Institute of Environmental Biology, Utrecht University, Utrecht, The Netherlands

*Shared senior authors

## ABSTRACT

Floods damage agricultural crop production and threaten global food security. Previous research has shown that the early flooding signal ethylene mediates responses to survive oxygen (O2) deprivation (hypoxia) in Arabidopsis thaliana. The majority of vegetable crops are highly sensitive to flooding and it is unclear how these crops coordinate early flooding signals and adapt to impending hypoxia. To unravel how cultivated and wild Solanum species integrate the early ethylene signal to control subsequent hypoxia acclimation, we studied the transcript levels of a selection of representative marker genes that were previously shown to control ethylene-mediated hypoxia tolerance in Arabidopsis. Our results suggest that ethylene-mediated hypoxia tolerance is conserved in both shoots and roots of the wild Solanum species bittersweet (Solanum dulcamara) and a waterlogging-tolerant potato (Solanum tuberosum) cultivar. However, early ethylene signaling did not enhance the transcriptional hypoxia response in the roots of a waterlogging-sensitive potato cultivar, suggesting that waterlogging tolerance in potato could depend on ethylene-controlled hypoxia responses in the roots. Finally, we show that ethylene does not enhance hypoxia-adaptive genes and subsequent survival in tomato (Solanum lycopersicum) plants. We conclude that analyzing genes indicative of ethylene-mediated hypoxia acclimation is a promising approach to uncover the conservation of this mechanism across species. In addition, this approach could contribute to revealing key signaling cascades that confer flooding tolerance in crops.




## INTRODUCTION

Global food demand is expected to double by 2050 as a result of the rising world population and shifting human diets (Myers *et al.*, 2017). However, future food security is highly challenged by a decline in arable land and an increase in crop losses due to the consequences of a changing climate (Lobell *et al.*, 2008; Myers *et al.*, 2017). Indeed, elevated temperatures and extreme precipitation patterns due to climate change have led to an increase in the frequency and severity of flooding events (Hirabayashi *et al.*, 2013). Floods strongly impair agricultural crop production and exacerbate the food security crisis (Hirabayashi *et al.*, 2013; Voesenek & Bailey-Serres, 2015a). In order to minimize crop losses and safeguard global food security, it is therefore paramount to develop flood-tolerant crops in the near future.

Flooding tolerance in plants is regulated by variety of signals that mediate responses to combat oxygen ($O_2$) deprivation (hypoxia) and ameliorate reactive oxygen species (ROS) (Voesenek & Bailey-Serres, 2015a; Sasidharan *et al.*, 2018). Indeed, as a result of impaired gas diffusion underwater, submerged terrestrial plants ultimately encounter hypoxia, and flooding survival therefore strongly depends on traits that enhance hypoxia tolerance (Shiono *et al.*, 2008; Voesenek and Bailey-Serres, 2015, Chapter 2). In addition, passive ethylene entrapment acts as a rapid signal for submergence and regulates a plethora of flood adaptive responses that include morphological and anatomical modifications that prevent hypoxia (Voesenek & Sasidharan, 2013). Ethylene also mediates metabolic hypoxia acclimation in the wetland species *Rumex palustris* and model species *Arabidopsis thaliana* (van Veen *et al.*, 2013; Chapter 2). In Arabidopsis, ethylene-mediated hypoxia tolerance is conserved in root and shoot meristems and is associated with an enhanced expression of core hypoxia genes when $O_2$ levels decline (Chapter 3, (Mustroph *et al.*, 2009)). These genes are predominantly controlled by the group VII Ethylene Response Factor (ERFVII) transcription factors RELATED TO APETALA2.2 (RAP2.2), RAP2.12 and RAP2.3 (Bui *et al.*, 2015; Gasch *et al.*, 2016). ERFVIIs possess a conserved N-terminal sequence that regulates their turnover through the PROTEOLYSIS6 (PRT6) N-degron pathway under $O_2$ and nitric oxide (NO) replete conditions (Gibbs *et al.*, 2011, 2014; Licausi *et al.*, 2011). When the cellular levels of either $O_2$ or NO decline, ERFVII proteolysis is restricted and these proteins stabilize ultimately resulting in target hypoxia adaptive gene expression (Gibbs *et al.*, 2011, 2014; Licausi *et al.*, 2011). We discovered that ethylene can already stabilize ERFVIIs prior to hypoxia through active NO reduction (Chapter 3). In addition, we showed in chapter 4 that ethylene-mediated NO depletion is

dependent on enhanced levels of the NO-scavenging protein PHYTOGLOBIN1 (PGB1). Moreover, we demonstrated that ethylene ameliorates oxidative stress tolerance in Arabidopsis root tips, which was partly regulated through the ERFVIIs RAP2.2 and RAP2.12 (Chapter 5). Taken together, we showed in Arabidopsis that early ethylene signaling upon submergence can prevent N-degron targeted ERFVII proteolysis by enhanced production of the NO-scavenger PGB1. This in turn augments the transcription of downstream target genes that improve energy homeostasis and oxidative stress tolerance during hypoxia and re-oxygenation (Fig. 4.5, Chapter 5).

Our results with *pgb1* mutants in Arabidopsis revealed that if ethylene was not able to induce PGB1 levels, the mechanism of ethylene-mediated hypoxia tolerance was not induced (Chapter 4). Similarly, the inability to enhance hypoxia tolerance after ethylene treatment correlated with the absence of ethylene-induced *PGB1*, *RAP2.12* and hypoxia adaptive gene induction in the terrestrial species *Rumex acetosa* (van Veen *et al.*, 2013). Contrastingly, but similar to Arabidopsis, *R. palustris* benefitted from an early ethylene signal and this correlated with *PGB1*, *RAP2.12* and hypoxia adaptive transcript induction (van Veen *et al.*, 2013). Finally, natural variation for flooding tolerance is correlated with enhanced ethylene signaling (Zhao *et al.*, 2018), PGB1 levels and NO removal (Li *et al.*, 2005; Rivera-Contreras *et al.*, 2016), ERFVII levels (Wei *et al.*, 2019; Yu *et al.*, 2019) and hypoxia adaptive gene transcripts (Zhang *et al.*, 2017; Zhao *et al.*, 2018; Pan *et al.*, 2019) in many crop and ornamental plant species. Taken together, the mechanism of ethylene-mediated hypoxia tolerance could be instrumental in restoring flooding tolerance of intolerant crops through manipulation of ethylene responsiveness of *PGB1* genes and its downstream signaling targets.

Potato (*Solanum tuberosum*) and tomato (*Solanum lycopersicum*) plants are the most economically important cultivated vegetable crops in the world, but are both considered to be highly intolerant to abiotic stresses, including flooding (Biemelt *et al.*, 1999; Vidoz *et al.*, 2010; Schwarz *et al.*, 2010). Conversely, the closely related wild plant species bittersweet (*Solanum dulcamara*) is highly tolerant to a variety of abiotic stresses (Zhang *et al.*, 2016). All three species display multiple ethylene-mediated flood-adaptive responses including adventitious root (AR) and aerenchyma formation (Vidoz *et al.*, 2010; Gururani *et al.*, 2013; Dawood *et al.*, 2014), but still show differences in flooding tolerance. However, whether ethylene also contributes to metabolic hypoxia acclimation and if this correlates with tolerance under submergence in these species is currently unknown. Several studies



showed that genes involved in ethylene signaling and ethanolic fermentation are induced in response to flooding and hypoxia, but not consistently across all plant tissues in these *Solanum* species (Biemelt *et al.*, 1999; Vidoz *et al.*, 2010; Dawood *et al.*, 2016). The previously described mechanism could be instrumental to unravel if flooding tolerance in these *Solanum* species is achieved through differences in ethylene-mediated hypoxia tolerance.

To unravel if and how these cultivated and wild *Solanum* species integrate the early flooding signal ethylene to control subsequent hypoxia acclimation, we studied the transcript levels of a selection of representative marker genes that were previously shown to control ethylene-mediated hypoxia tolerance in Arabidopsis. In addition, we tested whether early ethylene was able to enhance hypoxia survival in both bittersweet and tomato. Interestingly, our results suggest that ethylene contributes to hypoxia acclimation in bittersweet and a waterlogging-tolerant potato cultivar, but not in tomato and an intolerant potato cultivar. We propose that the mechanism of ethylene-mediated hypoxia acclimation could be instrumental to uncover signaling cascades that confer flooding tolerance in crops but that alternative pathways are likely also involved.

## RESULTS

### Potato cultivars show variation in waterlogging tolerance

To unravel whether ethylene-mediated hypoxia tolerance contributes to flooding tolerance in potato, we first explored whether variation in flooding tolerance exists across 6 elite potato cultivars. Plants grown from tubers were waterlogged for up to 12 days and shoot growth parameters were scored every 3 days. The cultivars Festien and Avarna retained the highest biomass and leaf area, whereas the cultivars Seresta and Ambition showed the highest loss in biomass and leaf area during waterlogging (Fig. 6.1A, B). The differences between the more tolerant cultivar Festien and lesser tolerant Seresta were significant and consistent for both biomass and leaf area during the full duration of the waterlogging experiment. Plants of the six cultivars were also scored for adventitious root formation (Fig. 6.1C). Interestingly, there was no clear correlation between the adventitious root number and shoot performance during waterlogging (Fig. 6.1C), suggesting that differences in waterlogging tolerance are caused by other factors. To explore whether ethylene-mediated hypoxia tolerance contributes to these differences in waterlogging tolerance, we selected Festien and Seresta for further analysis.

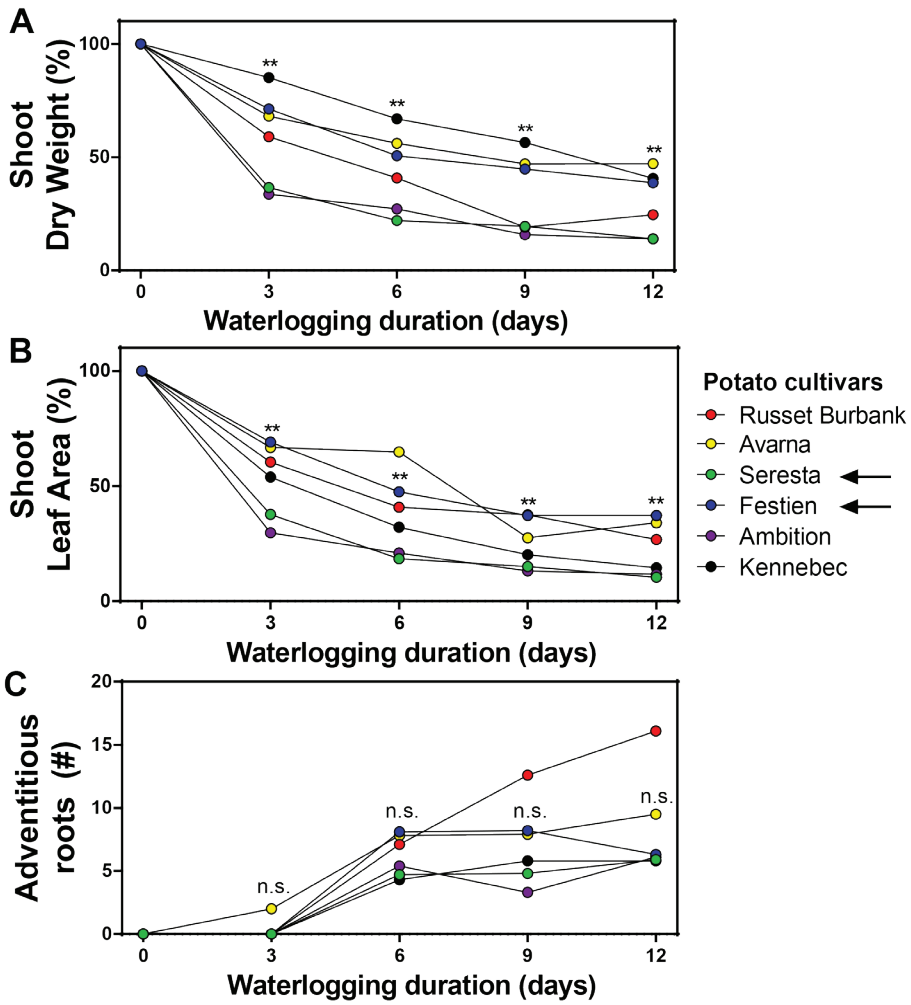


**Figure 6.1. Elite potato cultivars show variation in waterlogging tolerance.**
**(A-C)** Relative shoot dry weight **(A)**, relative leaf area **(B)** and the number of newly formed adventitious roots **(C)** of 6 potato (*S. tuberosum*) cultivars during 12 days of waterlogging. Values are relative to non-waterlogged plants per time-point (A, B). Asterisks indicate a significant differences between the Seresta (green) and Festien (blue) cultivars per time-point and these were the cultivars selected for further analysis (indicated by arrows,**p<0.01, Generalized linear model, negative binomial error structure, Tukey's HSD, n=10 plants).

## Ethylene differentially mediates the transcriptional hypoxia response between a tolerant and intolerant potato cultivar

We selected several potato orthologues of Arabidopsis genes associated with ethylene-mediated hypoxia tolerance as markers for this mechanism. These included: *ETHYLENE RESPONSE 2* (*ETR2*) (Chang *et al.*, 2013), to test whether ethylene led



to ethylene-dependent signaling; *PGB1* as a marker gene for enhanced NO-scavenging capacity (Hebelstrup *et al.*, 2006); *RAP2.12* to test whether ethylene induces potato ERFVIIs at the transcriptional level and *PYRUVATE DECARBOXYLASE* (*PDC1*), encoding the rate limiting protein for hypoxia-induced fermentation (Mithran *et al.*, 2014), as a representative marker gene for the transcriptional hypoxia response. *ETR2* and *PGB1* are also among the ERFVII-controlled core hypoxia genes in Arabidopsis (Gasch *et al.*, 2016), and therefore also interpreted as markers for the hypoxia response.

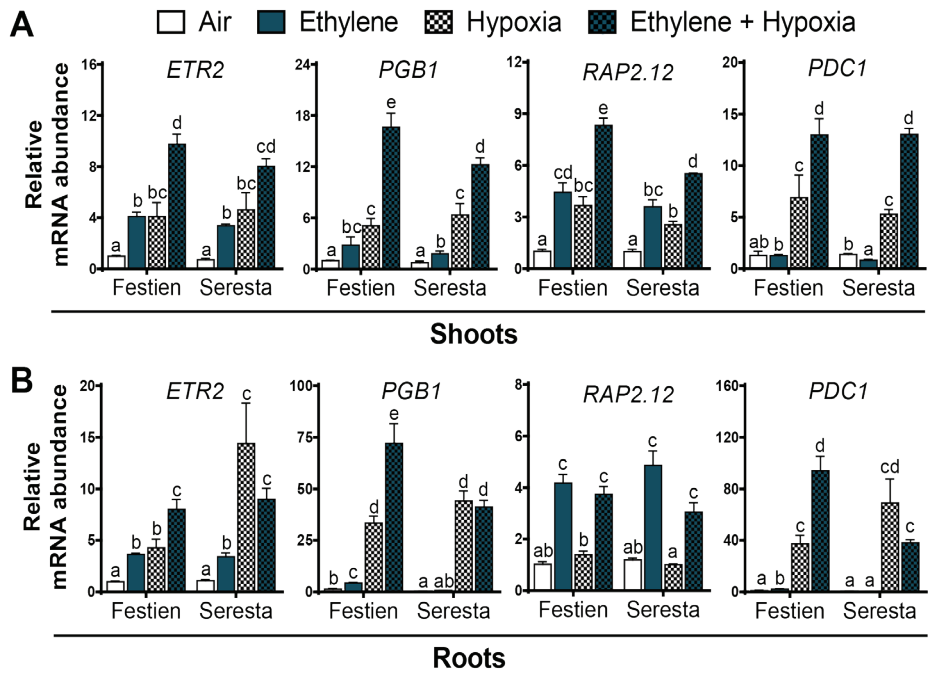


**Figure 6.2. Transcript levels of genes associated with ethylene-mediated hypoxia tolerance in potato shoots and roots.**
**(A, B)** Relative mRNA transcript abundance of 4 marker genes for ethylene-mediated hypoxia tolerance in both shoot (A) and root tissues (B) of the potato cultivars Festien and Seresta after 4 hours of pre-treatment with air (white) or ~5µll$^{-1}$ ethylene (blue), followed by (4h) hypoxia (blocks). Marker genes are orthologues of the Arabidopsis genes: ethylene signaling gene *ETR2*, NO-scavenging phytoglobin *PGB1*, ERFVII transcription factor *RAP2.12* and hypoxia adaptive gene *PDC1*. Values are relative to air treated samples of Festien. Different letters indicate significant differences (Error bars are SEM, p<0.05, 2-way ANOVA, Tukey's HSD, n=3 containing 2 shoot meristems (A) or ~10 root tips (B)).

To unravel whether ethylene-mediated hypoxia acclimation is conserved in potato and contributes to the observed differences in waterlogging tolerance of the cultivars Festien and Seresta, plants were pre-treated with air and ethylene followed by 4 hours of hypoxia. Ethylene enhanced the transcript abundance of *ETR2* and *RAP2.12* orthologues in shoot and root tissues of both potato cultivars (Fig. 6.2). Interestingly, *PGB1* transcripts were enhanced in response to ethylene in both tissues of the more tolerant cultivar Festien but were not significantly enriched in the roots of Seresta (Fig. 6.2). Moreover, ethylene pre-treatment strongly enhanced *ETR2*, *PGB1*, *RAP2.12* and *PDC1* transcripts upon hypoxia in the tolerant cultivar Festien (Fig. 6.2). Conversely, while ethylene pre-treatment did enhance the hypoxia response of *PGB1*, *RAP2.12* and *PDC1* in shoots of the sensitive cultivar Seresta this induction was less for *PGB1* and *RAP2.12* compared to the more tolerant Festien. Finally, ethylene had no beneficial effect on the hypoxia-responsive genes *ETR2*, *PGB1* and *PDC1* in root tissues of the intolerant cultivar Seresta (Fig. 6.2B). Together these data suggest that the capacity to enhance hypoxia-responsiveness of marker genes by ethylene in roots correlates with waterlogging tolerance in these potato cultivars.

### Ethylene differentially mediates the transcriptional hypoxia response in bittersweet and tomato plants

Next, we assessed whether the cultivated *Solanum* species tomato and related wild species bittersweet integrate the early flooding ethylene signal to enhance subsequent hypoxia acclimation. We quantified transcript levels of the representative marker genes stated earlier, but now also included the hypoxia marker *ALCOHOL DEHYDROGENESE1 (ADH1)* orthologue of both species. Our results reveal that ethylene alone already increased the mRNA abundance of *ETR2*, *PGB1*, *RAP2.12, PDC1* and *ADH1* orthologues in shoot and root tissues of both bittersweet and tomato (Fig. 6.3). Furthermore, ethylene pre-treatment strongly enhanced the hypoxia-responsiveness of *PGB1* transcripts in the tissues of both bittersweet and tomato (Fig. 6.3A, B). However, ethylene pre-treatment followed by subsequent hypoxia only augmented the transcripts of *ETR2*, *PDC1* and *ADH1* in bittersweet, but not in tomato tissues (Fig. 6.3). Surprisingly, compared to the pre-treatment under normoxia, hypoxia did not further enhance *PDC1* transcript levels in either bittersweet or tomato. Taken together, these data illustrate that ethylene strongly augments the hypoxia response in bittersweet, but not tomato. Next, we assessed whether this differential transcriptional hypoxia response in bittersweet and tomato plants is correlated with enhanced hypoxia survival.



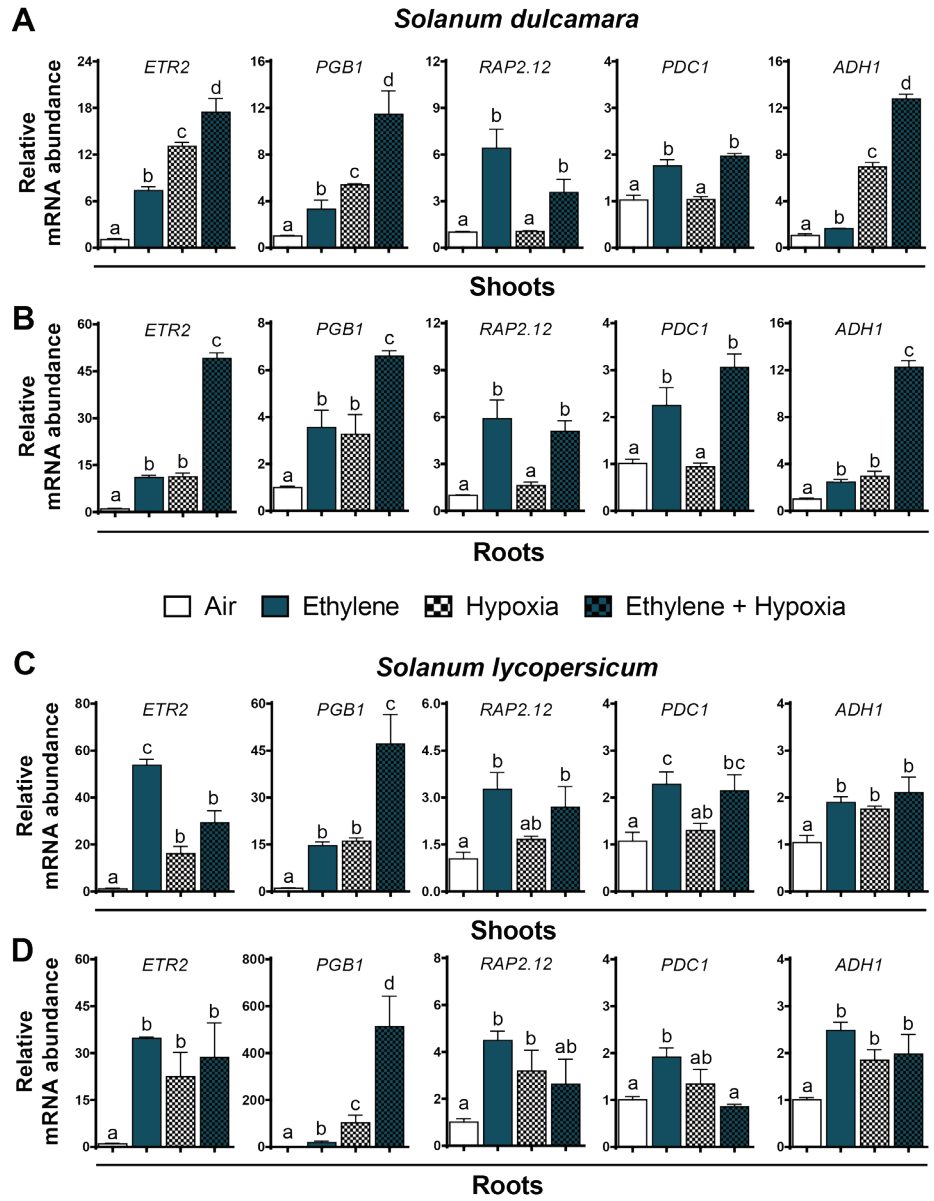


**Figure 6.3. Transcript levels of genes associated with ethylene-mediated hypoxia tolerance in *S. dulcamara* and *S. lycopersicum*.**
**(A-D)** Relative mRNA transcript abundance of 5 marker genes for ethylene-mediated hypoxia tolerance in both shoot and root tissues of *S. dulcamara* (A, B) and *S. lycopersicum* (C, D) after 4 hours of pre-treatment with air (white) or ~5µl$l^{-1}$ ethylene (blue), followed by (4h) hypoxia (blocks). Marker genes are orthologues of the Arabidopsis genes: ethylene signaling gene *ETR2*, NO-scavenging phytoglobin *PGB1*, ERFVII transcription factor *RAP2.12* and hypoxia adaptive genes *PDC1* and *ADH1*. Values are relative to air treated samples. Different letters indicate significant differences (Error bars are SEM, $p<0.05$, 1-way ANOVA, Tukey's HSD, n=3 containing 5-10 shoot meristems (A, C) or 5-10 root tips (B, D)).

### Ethylene pre-treatment increases hypoxia survival of bittersweet, but not tomato plants

To uncover whether ethylene pre-treatment confers increased hypoxia tolerance in tomato and bittersweet, we performed a root tip survival assay as previously described for Arabidopsis. Furthermore, we grew young plants of bittersweet and tomato in pots and tested these plants for their shoot survival after air and ethylene pre-treatments and subsequent hypoxia. Interestingly, ethylene pre-treatment strongly enhanced survival and biomass retention (fresh weight) of bittersweet shoot tissues after subsequent hypoxia treatments and recovery periods (Fig. 6.4A, B). However, ethylene had no effect on hypoxia tolerance of tomato shoots (Fig. 6.4C). Similar effects were observed for roots, where ethylene pre-treatment enhanced hypoxia survival of bittersweet, but not tomato root tip meristems (Fig. 6.4D). Together our results indicate that the mechanism of ethylene-mediated hypoxia tolerance is largely conserved in the shoots and roots of the flood tolerant plant bittersweet, but not of tomato (Overview in Fig. 6.5).

## DISCUSSION

In this chapter we made a first step in translating the mechanism of ethylene-mediated hypoxia tolerance to vegetable crops. Our results reveal that ethylene generally leads to rapid up-regulation of ethylene signaling, *PGB1* and *RAP2.12* transcripts in all three *Solanum* species, but that the more downstream hypoxia-responsive genes are not consistently enhanced by early ethylene signaling when $O_2$ levels decline (Overview in Fig. 6.5). When ethylene enhanced transcript levels of *PGB1* and *RAP2.12* orthologues, it is unclear whether this also enhanced corresponding protein levels and biological function. However, our results suggest that ethylene indeed stimulates RAP2.12 or other ERFVII orthologue protein levels in bittersweet and the more waterlogging tolerant potato cultivar Festien as the ERFVII-target hypoxia gene transcripts were strongly enhanced during subsequent hypoxia treatments (Fig. 6.2, 6.3). One explanation could be that ethylene impairs NO-dependent ERFVII proteolysis in these *Solanum* species through the up-regulation of PGB1 orthologues, causing enhanced ERFVII stability (Chapter 4). Alternatively, ethylene could enhance protein synthesis of one or more *Solanum* ERFVIIs that escape N-degron mediated proteolysis through structural differences, as was recently shown for the ethylene-mediated rice ERFVII SUB1A-1 (Lin *et al.*, 2019). Further research is required to determine if ethylene indeed leads to higher *Solanum* ERFVII levels under normoxia, and whether this is mediated through enhanced PGB1-dependent NO scavenging.



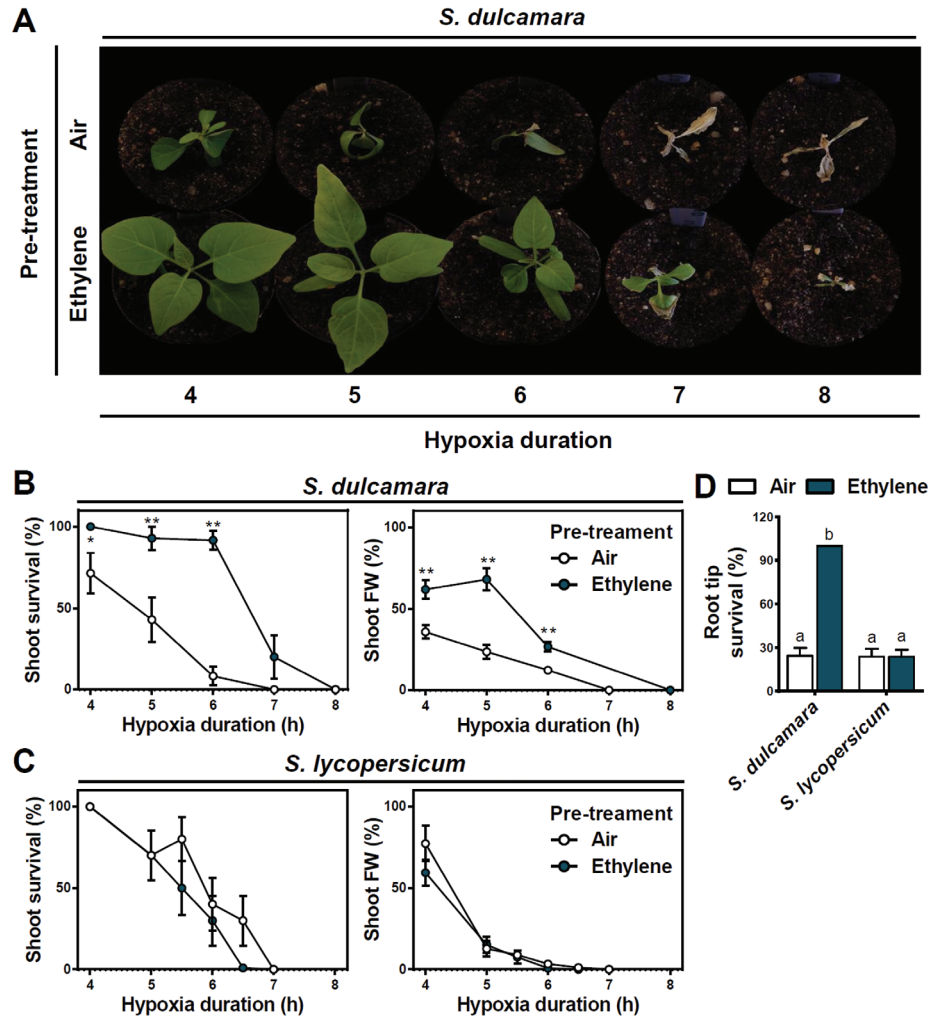


**Figure 6.4. Ethylene pre-treatment confers hypoxia tolerance in *S. dulcamara* but not *S. lycopersicum*.**

**(A)** *S. dulcamara* shoot phenotypes after 4 hours of pre-treatment (air/ ~5µll$^{-1}$ ethylene) followed by hypoxia and 7 days recovery. **(B, C)** *S. dulcamara* (B) and *S. lycopersicym* (C) shoot meristem survival and fresh weight (FW) of survived plants after 4 hours of air (white) or ~5µll$^{-1}$ ethylene (blue) followed by hypoxia and 7 days of recovery. Values are relative to control (normoxia) plants. Asterisks indicate significant differences between air and ethylene (Error bars are SEM, **p<0.01, Generalized linear model, negative binomial error structure, n=10-13 plants). **(D)** Root tip survival of *S. dulcamara* and *S. lycopersicum* seedlings after 4 hours of pre-treatment with air (white) or ~5µll$^{-1}$ ethylene (blue) followed by 4 hours of hypoxia and 2 days of recovery. Values are relative to control (normoxia) plants. Statistically similar groups are indicated using the same letter (Error bars are SEM, p<0.05, 2-way ANOVA, Tukey's HSD, n=5-12 rows containing ~10 seedlings).

Interestingly, in root tissues of the waterlogging-intolerant potato cultivar Seresta, ethylene treatments did not enhance *PGB1* mRNA levels and subsequent hypoxia-responsive gene transcripts (Fig. 6.2B). In the future it would be interesting to unravel whether the inability to enhance *PGB1* levels in Seresta roots indeed explains the subsequent limited hypoxia transcriptional response. Moreover, while ethylene did induce the upstream marker genes *ETR2*, *PGB1* and *RAP2.12* in tomato, ethylene pre-treatment did not enhance mRNA levels of most core hypoxia gene orthologues when $O_2$ levels declined (Fig. 6.3C, D). These results suggest that ethylene-mediated ERFVII stability could in some cases be uncoupled from enhanced target-gene expression upon hypoxia. Strikingly, ethylene did prime *PGB1* mRNA levels upon hypoxia in tomato tissues, suggesting that not all hypoxia-responsive genes are uncoupled from ERFVII stability in the same fashion. One explanation could be that ethylene regulates only a subset of ERFVII orthologues, and that specific ERFVIIs mediate different target genes. Alternatively, it is possible that ethylene does not lead to more PGB1 protein levels, that PGB1 does not effectively scavenge NO, or that ERFVII turnover is not NO-dependent in tomato plants and in the roots of the potato cultivar Seresta. It is important to note that we only studied a minor subset of core hypoxia gene orthologues and that the overall induction of *ADH1* and *PDC1* transcripts in tomato upon hypoxia was limited. Moreover, it is unknown whether these hypoxia-responsive genes are even similarly regulated in these *Solanum* species compared to Arabidopsis (Gasch *et al.*, 2016).

In addition, it is unclear which hypoxia genes actually confer hypoxia tolerance. For instance, several studies suggest transcriptional *ADH1* induction may not be required for anaerobic fermentation, maintenance of glycolysis and subsequent hypoxia tolerance in potato tubers and Arabidopsis (Biemelt *et al.*, 1999; Bui *et al.*, 2019). Previous research showed that protein levels of ADH1 in tomato roots increased only 1.7-fold after 24 hours of waterlogging, whereas PDC1 levels were even down-regulated (Ahsan *et al.*, 2007). It is possible that the functional implications of specific up-regulated hypoxia genes for hypoxia tolerance are dependent on the plant tissue and are determined by the severity of the stress. Therefore, other ERFVII-dependent hypoxia responsive genes could be tested to uncover their role in ethylene-mediated hypoxia acclimation. Especially oxidative stress amelioration is thought to be a major determinant of flooding and hypoxia tolerance (Chapter 5, Liu et al., 2019 (PhD thesis), Yeung *et al.*, 2018), and it would therefore be interesting to assess the effect of ethylene on ROS tolerance during hypoxia and re-oxygenation in *Solanum* species in the future.



**A**

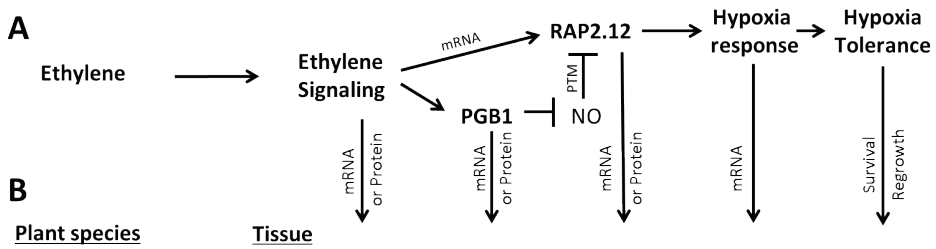


**B**

| Plant species | Tissue | | | | Hypoxia response | |
|---|---|---|---|---|---|---|
| ***A. thaliana*** | Shoot | ✓ | ✓ | ✓ | ✓ 12/12 | ✓ |
| | Root | ✓ | ✓ | ✓ | ✓ 13/15 | ✓ |
| ***S. dulcamara*** | Shoot | ✓ | ✓ | ✓ | ✓ 4/4 | ✓ |
| | Root | ✓ | ✓ | ✓ | ✓ 4/4 | ✓ |
| ***S. tuberosum*** Tolerant | Shoot | ✓ | ✓ | ✓ | ✓ 3/3 | ? |
| | Root | ✓ | ✓ | ✓ | ✓ 3/3 | ? |
| ***S. tuberosum*** Intolerant | Shoot | ✓ | ✓ | ✓ | ✓ 2/3 | ? |
| | Root | ✓ | ✗ | ✓ | ✗ 0/3 | ? |
| ***S. lycopersicum*** | Shoot | ✓ | ✓ | ✓ | ✗ 1/4 | ✗ |
| | Root | ✓ | ✓ | ✓ | ✗ 1/4 | ✗ |

**Figure 6.5. Conservation of ethylene-mediated hypoxia tolerance in *Solanum* species (A)**
Overview showing the proposed mechanism of ethylene-mediated hypoxia tolerance as discovered in Arabidopsis (Chapter 2 to 4). Arrows pointing downward indicate key players that were verified in Arabidopsis at the mRNA and protein level, or tested in the *Solanum* species at mRNA level in both roots and shoots. (B) Table showing whether marker genes or hypoxia tolerance were enhanced by ethylene treatment (green check mark = yes, red cross = no, question mark = not tested). The n/n in the hypoxia response column indicates the amount of hypoxia genes that are ethylene-enhanced compared to the total amount of hypoxia-responsive genes tested. Experimental data underlying this table is shown in chapters 2, 3 and 4 and the current chapter of this thesis.

Finally, it is uncertain whether the (re-)introduction of ethylene-mediated hypoxia genes would enhance flooding tolerance of tomato and sensitive potato cultivars. Moreover, it will be challenging to accomplish this technically, as it is currently unclear what processes are uncoupled from ethylene-regulation in between the signaling cascade from potential ERFVII stability to the regulation of its hypox-

ia-responsive target genes. For now, it appears it is more complex than simply introducing ethylene-regulated promoter elements into key genes involved in ethylene-mediated hypoxia tolerance. An alternative and promising approach could be to enhance waterlogging tolerance through interspecific grafting of high yield tomato cultivar shoots onto waterlogging tolerant root stocks of compatible *Solanum* species (Schwarz *et al.*, 2010; Bhatt *et al.*, 2015). Unfortunately, this seems unfeasible for potato, as the harvestable organs are the tubers underground.

Summarizing, we show that ethylene-mediated hypoxia tolerance is conserved in bittersweet shoot and root tissues and leads to enhanced hypoxia survival similar to Arabidopsis and *R. palustris* (Chapter 2-4, van Veen *et al.*, 2013). In potato cultivars, the induction of this mechanism was also conserved in shoots and roots of the waterlogging-tolerant cultivar Festien. Conversely, early ethylene signaling was uncoupled from *PGB1* induction and enhanced hypoxia response in the roots of waterlogging-intolerant cultivar Seresta, suggesting that waterlogging tolerance in potato could be dependent on ethylene-induced hypoxia responses in the roots. Similarly, ethylene signaling did not prime most of the transcriptional hypoxia response and subsequent survival in tomato roots and shoots, suggesting that this could potentially be (re-)introduced to enhance flooding tolerance in the future. However, more research is required to unravel why tomato plants and roots of the potato cultivar Seresta do not integrate ethylene signaling to enhance its transcriptional hypoxia response. We conclude that studying genes indicative of ethylene-mediated hypoxia acclimation is a useful approach to explore the universality of this mechanism across species and helps to identify key signaling cascades that confer flooding and hypoxia (in-)tolerance in vegetable crops.

## ACKNOWLEDGEMENTS

We thank Mariëlle Muskens of Agrico Research B.V. and Jan De Haas of HZPC Research B.V. for valuable feedback, growth protocols and providing tubers of the potato cultivars. In addition, we kindly acknowledge Eric Visser and Sarah Courbier for providing us with the seeds of bittersweet and tomato, respectively. Furthermore, we thank Emilie Reinen and Ankie Ammerlaan for technical assistance.

## MATERIALS AND METHODS

### Plant material and growth conditions

Plant material: Potato (*S. tuberosum L.*) tubers of the elite cultivars Russet Burbank, Kennebec, Festien, Seresta, Avarna and Ambition were obtained from Jan De Haas of HZPC Research B.V, Metslawier, The Netherlands and Mariëlle Muskens



of Agrico Research B.V., Bant, The Netherlands. Seeds of bittersweet (*S. dulcamara*) were obtained from Dr. Eric Visser, Radboud University, Nijmegen, The Netherlands. Tomato (*S. lycopersicum L.*) seeds of the variety Moneymaker were shared by Sarah Courbier, Utrecht University, The Netherlands and were obtained from a garden center (Intratuin).

Growth conditions potted plants: Potato tubers were kept in the dark at room temperature for 1 month until the eye buds were starting to sprout. Tubers were placed individually in 11cm x 11cm sized square pots filled with a sand soil mixture (1:2), were covered by ~5 cm of soil mixture and stratified at 4°C in the dark for 3 days. Seedlings of tomato and bittersweet were germinated on agar plates as described below and subsequently transplanted in small round pots (diameter = 5 cm) filled with a sand soil mixture (1:2). Pots were then transferred to a growth chamber for germination/growth under short day conditions (9:00 – 17:00, Temperature (T) = 20°C, Photosynthetic Photon Flux Density (PPFD) = ~130 µmol $m^{-2}s^{-1}$, Relative Humidity (RH) = 70%). Potato plants were used for waterlogging and ethylene/hypoxia gassing experiments after 3 weeks. Tomato and bittersweet plants were 2 weeks old for the shoot survival experiments described below. Per species, homogeneous groups of plants were selected and randomized over treatment groups for phenotypic and molecular analysis under various treatments. Tomato and bittersweet used for survival experiments were transferred back to the same growth room conditions after treatments to recover for 7 days before scoring survival and measuring fresh weight.

Growth conditions seedlings: Tomato and bittersweet seeds were vapor sterilized by incubation with a beaker containing a mixture of 50 ml bleach and 3 ml of 37% fuming HCl in a gas tight desiccator jar for 4 hours. Seeds were then individually transplanted in 2 rows of 10 seeds on sterile square petri dishes containing 25 ml autoclaved and solidified ¼ MS, 1% plant agar without additional sucrose. Petri dishes were sealed with gas-permeable tape (Leukopor, Duchefa) and stratified at 4°C in the dark for 3 to 4 days. Seedlings were grown vertically on the agar plates under short day conditions (9:00 – 17:00, T= 20°C, PPFD = ~120 µmol $m^{-2}s^{-1}$, RH= 70%) for 7 days before root tip survival experiments and harvests for RT-qPCR.

### Tolerance assays, treatments and sample harvests

Waterlogging tolerance potato cultivars: Plants were waterlogged by submerging the pots in large tubs under long day conditions (7:00 – 23:00, T= 20°C, PPFD = ~150 µmol $m^{-2}s^{-1}$) in water that was left stagnant for 1 day, with the water

level 1 cm above the soil. Control plants were placed in similar tubs without water. Of each cultivar, 10 pots were taken out of control and waterlogging treatments after 3, 6, 9 and 12 days. Shoot biomass, total leaf area and the amount of clearly emerged adventitious roots were measured at the start of the treatment (t=0) and at each subsequent harvest time-point. Root tip survival performance assays of tomato and bittersweet 7-day old seedlings grown vertically on agar plates were performed as described for Arabidopsis in Chapter 2. Shoot meristem survival was performed on 2-week-old plants grown in pots, as described for Arabidopsis rosettes in Chapter 2. Samples of potato, tomato and bittersweet were harvested after 4 hours of air and ethylene treatments and after 4 hours of subsequent hypoxia treatment. For shoot tissues, 1-2 primary shoot meristems were harvested including the first young leaf. For root tissues, multiple segments (5-10) of ~ 1 cm long root tips were harvested per sample.

**RNA extraction, cDNA synthesis, RT-qPCR and statistical analyses**

RNA extraction, cDNA synthesis, RT-qPCR were performed as described in chapter 2. Gene orthologue sequences were obtained by BLASTing the coding sequences of Arabidopsis genes against the bittersweet transcriptome (Dawood *et al.*, 2016), tomato genome (version SL3.0 and Annotation ITAG3.10) and potato genome (Potato Genome Sequencing Consortium *et al.*, 2011) using the tblastx tool on https://solgenomics.net/tools/blast/. Primers used in this chapter are listed in appendix II. For potato, the orthologue of *ACTIN11* (PGSC0003DMP400048248) was used as a reference gene, for tomato and bittersweet, the orthologue of *TUBULIN* (Solyc02g087880) was used a reference gene. Statistical analyses were performed as described in Chapter 2.

# CHAPTER 7

## GENERAL DISCUSSION

**MODIFIED EXCERPTS OF THIS CHAPTER ARE PUBLISHED IN:**

- Hartman, S., *et al.* (2019). The role of ethylene in metabolic acclimations to low oxygen. New Phytologist, Accepted.

## GENERAL DISCUSSION

In this thesis we reveal that the early gaseous flooding signal ethylene acclimates plants to impending hypoxia. We show that this mechanism is dependent on an ethylene-initiated cascade of reactions, starting with PGB1-controlled NO removal and enhanced ERFVII stability prior to hypoxia, in turn priming the transcriptional hypoxia response only when $O_2$ levels decline (Fig. 4.5, (Hartman *et al.*, 2019)). We uncovered this mechanism in root tips of the model plant species Arabidopsis, and show that all processes investigated in shoot meristems behave in a similar fashion as the roots (Chapter 2-4). Interestingly, while ethylene-mediated hypoxia tolerance is conserved in multiple Arabidopsis accessions (Chapter 2), it does not show a clear correlation with natural variation for flooding tolerance across natural Arabidopsis accessions (Vashisht *et al.*, 2011). However, we do provide evidence that the mechanism is also conserved across several *Solanum* species, in which an ethylene-enhanced transcriptional hypoxia response correlates with the capacity to confer hypoxia and flooding tolerance (Fig. 6.5). Here we discuss the potential and limitations of ethylene-mediated hypoxia tolerance under more realistic flooding conditions, and suggest that components of this mechanism could be involved in other plant developmental and stress responses.

### Ethylene-mediated hypoxia tolerance under natural flooding conditions

While our results indicate that Arabidopsis is a powerful tool to uncover molecular pathways driving hypoxia acclimation in plants, the question remains whether ethylene-mediated hypoxia tolerance is actually functional under real flooding conditions. The proposed mechanism is based on the premise that the ethylene signal precedes the severe decline of $O_2$ levels in plants cells. While ethylene quickly and invariably accumulates to high levels in several submerged plant species, the internal $O_2$ levels are strongly dependent on tissue type and the external environment (Voesenek & Sasidharan, 2013). Several studies show that the internal $O_2$ concentration of plants can decline from normoxic levels during the day, to severe hypoxia at night. However, cellular $O_2$ quantifications with a high spatial and temporal resolution are still lacking (Colmer & Pedersen, 2008; Vashisht *et al.*, 2011). For this reason, a grand challenge in flooding biology is to generate either chemically or genetically encoded fluorescent $O_2$ sensors to monitor cellular *in planta* $O_2$ dynamics (Ast *et al.*, 2012; Puerta *et al.*, 2019). We propose that ethylene entrapment during daytime (normoxic) can prime plant tissues for impending severe hypoxia during the subsequent night for as long as the flood lasts or sufficient carbohydrates are available to maintain fermentation pathways



(Zabalza *et al.*, 2008; Mithran *et al.*, 2014; Loreti *et al.*, 2018). The reduced light levels in turbid flood waters may augment this hypoxia acclimation during the day (Fig. 2.5B), possibly through enhanced ERFVII stability in the dark (Abbas *et al.*, 2015; Voesenek & Bailey-Serres, 2015b; Liu, 2019). Furthermore, we show that ethylene signaling also contributes to enhanced ROS amelioration during hypoxia and re-oxygenation (Tsai *et al.*, 2014; Liu, 2019; Yeung *et al.*, 2019), partially through an ERFVII-dependent mechanism (Chapter 5).

### Ethylene signal generation under submergence

Ethylene-mediated hypoxia tolerance does not only depend on the spatial and temporal dynamics of ethylene entrapment and the $O_2$ decline, but also on additional factors that can either enhance or impair key signaling hubs of the mechanism. Indeed, a complex web of interacting factors including the microbiome, light, carbohydrate and nutrient status can affect the signaling cascade from ethylene biosynthesis and signaling all the way down to hypoxia gene regulation. Generally, ethylene production by the plant is considered not to be a limiting factor for the generation of the signal, as ethylene is produced in the cells of almost all higher plants (Voesenek & Sasidharan, 2013; Ju *et al.*, 2015). However, several studies suggest that the presence of specific microbes in the rhizosphere can alter ethylene production of plants (Singh *et al.*, 2015). For instance, bacteria producing ACC deaminase can drastically modulate plant responses to flooding as they metabolize ACC, the pre-cursor of ethylene biosynthesis (Ravanbakhsh *et al.*, 2017). Moreover, ethylene sensitivity and signaling is tightly controlled by the stability of EIN3 (Alonso *et al.*, 2003; Pierik *et al.*, 2006). Interestingly, depending on the plant tissue, EIN3 stability is either enhanced or reduced by changes in the light availability and carbohydrate status of the plant (Yanagisawa *et al.*, 2003; Xie *et al.*, 2015; Shi *et al.*, 2016). Together these reports suggest that under real flooding conditions, the generation of the ethylene signal could either be enhanced or impaired depending on the plant's surroundings.

### NO dynamics in submerged plants

Downstream of ethylene signaling, PGB1-dependent NO removal is key for the progression of the response cascade of ethylene-mediated hypoxia tolerance (Chapter 3 & 4). However, while we uncovered that ethylene reduces NO levels in an experimental setup where gas diffusion is unchanged, it is currently unclear what happens to cellular NO dynamics when gas diffusion is restricted. Since NO is a highly reactive and short-lived gaseous molecule, accumulation as a result of impaired gas diffusion underwater is considered to be limited if NO

biosynthesis rates are unchanged (Sasidharan *et al.*, 2018). However, NO production is highly dependent on nitrate and nitrite levels in the plant, in addition to NR activity (Chamizo-Ampudia *et al.*, 2017). Especially in modern agricultural fields, nitrate levels are considerably high due to fertilizer application (Sebilo *et al.*, 2013), and ethylene-mediated NO removal could therefore be impaired in these plants. However, PGB1 levels are also strongly dependent on nitrate levels and could counter these effects (Ohwaki *et al.*, 2005; Sanz-Luque *et al.*, 2015). While several studies show that NR activity increased upon hypoxia (Fig. 4.1; Shi *et al.*, 2008; Gupta *et al.*, 2012), others show that NR activity is reduced when light is limited or under long-term waterlogging conditions (Nemie-Feyissa *et al.*, 2013; Rivera-Contreras *et al.*, 2016; Zhang *et al.*, 2017). Interestingly, the ERFVIIs quickly stabilize when NO is limited as a result of impaired NR activity (Gibbs *et al.*, 2014; Vicente *et al.*, 2017). Taken together, reduced NO levels either as a result of ethylene-enhanced PGB1 or reduced NR activity could maintain ERFVII stability in flooded but $O_2$ replete plant tissues, and subsequently facilitate hypoxia acclimation when $O_2$ levels decline.

### Underwater ERFVII stability and hypoxia sensing

The work in this thesis reveals that ethylene can stabilize constitutively expressed Arabidopsis ERFVIIs prior to the onset of hypoxia, in addition to the reported hypoxia-mediated ERFVII stability (Gibbs *et al.*, 2011; Licausi *et al.*, 2011). These results illustrate that Arabidopsis can use at least two signals to stabilize constitutively expressed ERFVIIs under submergence, making ERFVII stability alone an unspecific sensor for internal $O_2$ levels. Recent reports illustrate that other hypoxia-induced signals could contribute to $O_2$ sensing and acclimation in plants, including calcium ion waves and a decline in the (mitochondrial) energy charge (Holdsworth, 2017; Wang *et al.*, 2017; Schmidt *et al.*, 2018; Wagner *et al.*, 2019). This is in line with our observations that ethylene-enhanced ERFVII stability does not strongly enhance hypoxia gene transcripts until $O_2$ levels decline (Chapter 3 & 6). This uncoupling of ERFVII stability and activation could give submerged plants the flexibility to prepare for impending hypoxia without switching to valuable carbohydrate consuming processes until it is actually necessary to survive hypoxia. Interestingly, recent reports illustrate that this dual regulation is not conserved for all ERFVIIs across other plant species. In flood-tolerant lowland rice cultivars, the ethylene-regulated ERFVII SUB1A-1 is protected from N-degron mediated proteolysis through physical protection of the N-terminus, enhancing its stability (Lin *et al.*, 2019). However, among SUB1A-1's transcriptional targets are the two hypoxia-inducible ERFVIIs *ERF66* and *ERF67,* that are confirmed targets of the N-degron pathway



(Lin *et al.*, 2019). Here also ethylene could function as an initial signal to acclimate to submergence through enhanced SUB1A-1 production, in turn activating the hypoxia response through stabilizing ERF66 and ERF67 levels once $O_2$ levels decline. Together, these results suggest that plants have evolved slightly different mechanisms to integrate ethylene signals upon submergence and translate this into hypoxia acclimation. Future research is required to determine how conserved these pathways are among plants.

### Ethylene-mediated NO removal as a universal mechanism that controls plant stress and developmental responses

The discovery of ethylene-mediated hypoxia tolerance reveals an elegant mechanism that prepares plant cells for the impending hypoxia, but requires the specificity of the hypoxia signal to turn on the fully enhanced acclimation response (Chapter 3). This 'primed' state is controlled through ethylene-mediated NO removal that leads to enhanced ERFVII stability (Chapter 3 & 4). Interestingly, scattered evidence throughout the literature suggests that this pathway could also operate upstream in the signaling cascades of other plant stress and developmental responses that are ethylene-mediated but countered by NO. For example, ethylene pre-treatment conferred salt tolerance through enhanced ROS amelioration (Peng *et al.*, 2014), and salt stress tolerance was shown to be dependent on NO-mediated ERFVII stability (Vicente *et al.*, 2017). Similarly, flower senescence and vase life are accelerated by ethylene but countered by NO, potentially in a PGB1-dependent manner (Badiyan *et al.*, 2004; Hebelstrup *et al.*, 2006; Zeng *et al.*, 2011; Liao *et al.*, 2013). Moreover, climacteric fruit ripening is ethylene-controlled but inhibited as long as NO levels are replete (Singh *et al.*, 2009; Manjunatha *et al.*, 2012; Barman *et al.*, 2014; González-Gordo *et al.*, 2019). Interestingly, ethylene enhanced respiration rates in strawberry and tomato fruits in a dose responsive manner, reducing internal $O_2$ levels and stimulating ripening (Boe & Salunkhe, 1967; Tian, 1998). Knowing that $O_2$ consumption, mitochondrial respiration and COX activity are enhanced when NO levels decline (Millar *et al.*, 1997; Yamasaki *et al.*, 2001; Borisjuk & Rolletschek, 2008), it is interesting to speculate that ethylene controls respiration rates and internal $O_2$ levels in fruits through NO-removal. This hypothesis is in correspondence with the observations that *ERFVII* and hypoxia marker gene expression progressively increase in ripening fruits and that NO counters ethylene-mediated fruit ripening (Licausi *et al.*, 2010b; Manjunatha *et al.*, 2012; Min *et al.*, 2012; Cukrov, 2018). Finally, ethylene, PGB1, and the ERFVIIs RAP2.2 and RAP2.3 enhanced the resistance of Arabidopsis plants to the necrotrophic fungus *Botrytis cinerea* (Zhao *et al.*, 2012; Mur *et al.*, 2013; Kim *et al.*, 2018). Together

these reports illustrate that the upstream molecular mechanism of ethylene-mediated NO removal and ERFVII stability could control a plethora of additional biological processes related to plant stress and development responses.

### Concluding remarks and future perspectives

Flooding tolerance in plants can be achieved through a wide range of morphological, anatomical and metabolic adaptive responses that either assist to avoid and/or combat hypoxia. We show that ethylene-mediated hypoxia tolerance can enhance survival of plant species that have not evolved morphological adaptive traits to avoid hypoxia. In addition, this mechanism could contribute to survival of plant species exploiting the 'escape' strategy through enhanced hypoxia tolerance until they restore gas diffusion with the atmosphere (Chapter 6, van Veen *et al.*, 2013). The discovery of ethylene-mediated hypoxia tolerance in Arabidopsis allowed us to quickly uncover the presence of this mechanism in multiple *Solanum* species through a set of marker genes (Chapter 6). Moreover, our results in *Solanum* species reveal that the full induction of the ethylene-mediated hypoxia tolerance pathway correlates with flooding tolerance and hypoxia survival. In the future it would therefore be interesting to uncover whether components of this mechanism were lost in flooding-intolerant crop species through artificial selection. If so, the re-introduction of ethylene-responsiveness of key regulators could prove to be a powerful tool to enhance flooding tolerance in crops.



## REFERENCES


**Abbas M, Berckhan S, Rooney DJ, Gibbs DJ, Vicente Conde J, Sousa Correia C, Bassel GW, Marín-De La Rosa N, León J, Alabadí D, *et al.* 2015**. Oxygen sensing coordinates photomorphogenesis to facilitate seedling survival. *Current Biology* **25**: 1483–1488.

**Ahsan N, Lee DG, Lee SH, Lee KW, Bahk JD, Lee BH. 2007**. A proteomic screen and identification of waterlogging-regulated proteins in tomato roots. *Plant and Soil* **295**: 37–51.

**Akman M, Bhikharie A V., McLean EH, Boonman A, Visser EJW, Schranz ME, van Tienderen PH. 2012**. Wait or escape? Contrasting submergence tolerance strategies of Rorippa amphibia, Rorippa sylvestris and their hybrid. *Annals of Botany* **109**: 1263–1276.

**Alonso JM, Hirayama T, Roman G, Nourizadeh S, Ecker JR. 1999**. EIN2, a bifunctional transducer of ethylene and stress responses in Arabidopsis. *Science*.

**Alonso JM, Stepanova AN, Solano R, Wisman E, Ferrari S, Ausubel FM, Ecker JR. 2003**. Five components of the ethylene-response pathway identified in a screen for weak ethylene-insensitive mutants in Arabidopsis. *Proceedings of the National Academy of Sciences of the United States of America* **100**: 2992–7.

**An F, Zhao Q, Ji Y, Li W, Jiang Z, Yu X, Zhang C, Han Y, He W, Liu Y, *et al.* 2010**. Ethylene-Induced Stabilization of ETHYLENE INSENSITIVE3 and EIN3-LIKE1 Is Mediated by Proteasomal Degradation of EIN3 Binding F-Box 1 and 2 That Requires EIN2 in Arabidopsis. *the Plant Cell Online* **22**: 2384–2401.

**Armstrong W, Beckett PM, Colmer TD, Setter TL, Greenway H. 2019**. Tolerance of roots to low oxygen: 'anoxic' cores, the phytoglobin-nitric oxide cycle, and energy or oxygen sensing. *Journal of Plant Physiology* **239**: 92–108.

**Ast C, Schmälzlin E, Löhmannsröben HG, van Dongen JT. 2012**. Optical oxygen micro- and nanosensors for plant applications. *Sensors (Switzerland)* **12**: 7015–7032.

**Astier J, Rasul S, Koen E, Manzoor H, Besson-Bard A, Lamotte O, Jeandroz S, Durner J, Lindermayr C, Wendehenne D. 2011**. S-nitrosylation: An emerging post-translational protein modification in plants. *Plant Science* **181**: 527–533.

**Badiyan D, Wills RBH, Bowyer MC. 2004**. Use of a nitric oxide donor compound to extend the vase life of cut flowers. *HortScience* **39**: 1371–1372.

**Bailey-Serres J, Fukao T, Gibbs DJ, Holdsworth MJ, Lee SC, Licausi F, Perata P, Voesenek LACJ, Dongen JT Van. 2012**. Making sense of low oxygen sensing. *Trends in Plant Science* **17**: 129–138.

**Bailey-Serres J, Fukao T, Ronald P, Ismail A, Heuer S, Mackill D. 2010**. Submergence Tolerant Rice: SUB1's Journey from Landrace to Modern Cultivar. *Rice* **3**: 138–147.

**Banga M, Slaa EJ, Blom C, Voesenek L. 1996**. Ethylene Biosynthesis and Accumulation under Drained and Submerged Conditions (A Comparative Study of Two Rumex Species). *Plant physiology* **112**: 229–237.

**Barman K, Asrey R, Pal RK, Jha SK, Bhatia K. 2014**. Post-harvest nitric oxide treatment reduces chilling injury and enhances the shelf-life of mango ( *Mangifera indica* L.) fruit during low-temperature storage. *The Journal of Horticultural Science and Biotechnology* **89**: 253–260.

**Bhatt RM, Upreti KK, Divya MH, Bhat S, Pavithra CB, Sadashiva AT. 2015**. Interspecific grafting to enhance physiological resilience to flooding stress in tomato (Solanum lycopersicum L.). *Scientia Horticulturae* **182**: 8–17.

**Biemelt S, Hajirezaei MR, Melzer M, Albrecht G, Sonnewald U. 1999**. Sucrose synthase activity does not restrict glycolysis in roots of transgenic potato plants under hypoxic conditions. *Planta* **210**: 41–49.

**Bloom AJ, Sukrapanna SS, Warner RL. 1992**. Root respiration associated with ammonium and nitrate absorption and assimilation by barley. *Plant physiology* **99**: 1294–301.

**Boe AA, Salunkhe DK. 1967**. Ripening tomatoes: Ethylene, oxygen, and light treatments. *Economic Botany* **21**: 312–319.

**Borisjuk L, Rolletschek H. 2008**. Nitric oxide is a versatile sensor of low oxygen stress in plants. *Plant signaling & behavior* **3**: 391–3.

**Borsani O, Zhu J, Verslues PE, Sunkar R, Zhu J-K. 2005**. Endogenous siRNAs Derived from a Pair of Natural cis-Antisense Transcripts Regulate Salt Tolerance in Arabidopsis. *Cell* **123**: 1279–1291.

**Botrel A, Kaiser WM. 1997**. Nitrate reductase activation state in barley roots in relation to the energy and carbohydrate status. *Planta* **201**: 496–501.

**Bui LT, Giuntoli B, Kosmacz M, Parlanti S, Licausi F. 2015**. Constitutively expressed ERF-VII transcription factors redundantly activate the core anaerobic response in Arabidopsis thaliana. *Plant Science* **236**: 37–43.

**Bui LT, Novi G, Lombardi L, Iannuzzi C, Rossi J, Santaniello A, Mensuali A, Corbineau F, Giuntoli B, Perata P, *et al.* 2019**. Conservation of ethanol fermentation and its regulation in land plants. *Journal of Experimental Botany*.

**Bustos-Sanmamed P, Tovar-Méndez A, Crespi M, Sato S, Tabata S, Becana M. 2011**. Regulation of nonsymbiotic and truncated hemoglobin genes of Lotus japonicus in plant organs and in response to nitric oxide and hormones. *New Phytologist* **189**: 765–776.

**Chamizo-Ampudia A, Sanz-Luque E, Llamas A, Galvan A, Fernandez E. 2017**. Nitrate Reductase Regulates Plant Nitric Oxide Homeostasis. *Trends in Plant Science* **22**: 163–174.

**Chang KN, Zhong S, Weirauch MT, Hon G, Pelizzola M, Li H, Huang SC, Schmitz RJ, Urich MA, Kuo D, *et al.* 2013**. Temporal transcriptional response to ethylene gas drives growth hormone cross-regulation in Arabidopsis. *eLife* **2**: e00675.

**Cheng C-Y, Krishnakumar V, Chan AP, Thibaud-Nissen F, Schobel S, Town CD. 2017**. Araport11: a complete reannotation of the *Arabidopsis thaliana* reference genome. *The Plant Journal* **89**: 789–804.

**De Col V, Fuchs P, Nietzel T, Elsässer M, Voon CP, Candeo A, Seeliger I, Fricker MD, Grefen C, Møller IM, *et al.* 2017**. ATP sensing in living plant cells reveals tissue gradients and stress dynamics of energy physiology. *eLife* **6**.

**Colmer TD. 2003**. Aerenchyma and an Inducible Barrier to Radial Oxygen Loss Facilitate Root Aeration in Upland, Paddy and Deep-water Rice (Oryza sativa L.). *Annals of Botany* **91**: 301–309.

**Colmer TD, Pedersen O. 2008**. Oxygen dynamics in submerged rice (Oryza sativa). *New Phytologist* **178**: 326–334.

**Cukrov D. 2018**. Progress toward Understanding the Molecular Basis of Fruit Response to Hypoxia. *Plants* **7**: 78.

**Dahan J, Tcherkez G, Macherel D, Benamar A, Belcram K, Quadrado M, Arnal N, Mireau H. 2014**. Disruption of the CYTOCHROME C OXIDASE DEFICIENT1 Gene Leads to Cytochrome c Oxidase Depletion and Reorchestrated Respiratory Metabolism in Arabidopsis. *Plant Physiology* **166**: 1788–1802.

**Dawood T, Rieu I, Wolters-Arts M, Derksen EB, Mariani C, Visser EJW. 2014**. Rapid flooding-induced adventitious root development from preformed primordia in Solanum dulcamara. *AoB PLANTS* **6**.

**Dawood T, Yang X, Visser EJW, Te Beek TAH, Kensche PR, Cristescu SM, Lee S, Floková K, Nguyen D, Mariani C, *et al.* 2016**. A Co-Opted Hormonal Cascade Activates Dormant Adventitious Root Primordia upon Flooding in Solanum dulcamara. *Plant physiology* **170**: 2351–64.

**van Dongen JT, Licausi F. 2015**. Oxygen Sensing and Signaling. *Annual Review of Plant Biology* **66**: 345–367.

**van Dongen JT, Licausi F, Nick P. 2014**. Low-Oxygen Stress in Plants: Oxygen Sensing and Adaptive Responses to Hypoxia. *Plant Cell Monographs* **21**.

**Dordas C, Hasinoff BB, Igamberdiev AU, Manac'h N, Rivoal J, Hill RD. 2003**. Expression of a stress-induced hemoglobin affects NO levels produced by alfalfa root cultures under hypoxic stress. *The Plant Journal* **35**: 763–770.

**Eden E, Navon R, Steinfeld I, Lipson D, Yakhini Z. 2009**. GOrilla: a tool for discovery and visualization of enriched GO terms in ranked gene lists. *BMC Bioinformatics* **10**: 48.

**Fick A. 1855**. Ueber Diffusion. *Annalen der Physik und Chemie* **170**: 59–86.



**Frungillo L, Skelly MJ, Loake GJ, Spoel SH, Salgado I. 2014**. S-nitrosothiols regulate nitric oxide production and storage in plants through the nitrogen assimilation pathway. *Nature Communications* **5**: 5401.

**Fukao T, Bailey-Serres J. 2004**. Plant responses to hypoxia – is survival a balancing act? *Trends in Plant Science* **9**: 449–456.

**Fukao T, Yeung E, Bailey-Serres J. 2011**. The submergence tolerance regulator SUB1A mediates crosstalk between submergence and drought tolerance in rice. *Plant Cell* **23**: 412–427.

**Gagne JM, Smalle J, Gingerich DJ, Walker JM, Yoo S-D, Yanagisawa S, Vierstra RD. 2004**. Arabidopsis EIN3-binding F-box 1 and 2 form ubiquitin-protein ligases that repress ethylene action and promote growth by directing EIN3 degradation. *Proceedings of the National Academy of Sciences of the United States of America* **101**: 6803–8.

**García I, Arenas-Alfonseca L, Moreno I, Gotor C, Romero LC. 2019**. HCN Regulates Cellular Processes through Posttranslational Modification of Proteins by S-cyanylation. *Plant physiology* **179**: 107–123.

**Garzón M, Eifler K, Faust A, Scheel H, Hofmann K, Koncz C, Yephremov A, Bachmair A. 2007**. *PRT6* /At5g02310 encodes an *Arabidopsis* ubiquitin ligase of the N-end rule pathway with arginine specificity and is not the *CER3* locus. *FEBS Letters* **581**: 3189–3196.

**Gasch P, Fundinger M, Müller JT, Lee T, Bailey-Serres J, Mustroph A. 2016**. Redundant ERF-VII Transcription Factors Bind to an Evolutionarily Conserved cis-Motif to Regulate Hypoxia-Responsive Gene Expression in Arabidopsis. *The Plant Cell* **28**: 160–180.

**Geiger DR, Servaites JC. 2003**. Diurnal Regulation of Photosynthetic Carbon Metabolism in C3 Plants. *Annual Review of Plant Physiology and Plant Molecular Biology* **45**: 235–256.

**Gibbs DJ, Conde JV, Berckhan S, Prasad G, Mendiondo GM, Holdsworth MJ. 2015**. Group VII Ethylene Response Factors Coordinate Oxygen and Nitric Oxide Signal Transduction and Stress Responses in Plants. *Plant Physiology* **169**: 23–31.

**Gibbs DJ, Lee SC, Md Isa N, Gramuglia S, Fukao T, Bassel GW, Correia CS, Corbineau F, Theodoulou FL, Bailey-Serres J, *et al.* 2011**. Homeostatic response to hypoxia is regulated by the N-end rule pathway in plants. *Nature* **479**: 415–418.

**Gibbs DJ, Md Isa N, Movahedi M, Lozano-Juste J, Mendiondo GM, Berckhan S, Marín-de la Rosa N, Vicente Conde J, Sousa Correia C, Pearce SP, *et al.* 2014**. Nitric Oxide Sensing in Plants Is Mediated by Proteolytic Control of Group VII ERF Transcription Factors. *Molecular Cell* **53**: 369–379.

**Gibbs DJ, Tedds HM, Labandera A-M, Bailey M, White MD, Hartman S, Sprigg C, Mogg SL, Osborne R, Dambire C, *et al.* 2018**. Oxygen-dependent proteolysis regulates the stability of angiosperm polycomb repressive complex 2 subunit VERNALIZATION 2. *Nature Communications* **9**: 5438.

**González-Gordo S, Bautista R, Claros MG, Cañas A, Palma JM, Corpas FJ. 2019**. Nitric oxide-dependent regulation of sweet pepper fruit ripening. *Journal of Experimental Botany*.

**Gonzali S, Loreti E, Cardarelli F, Novi G, Parlanti S, Pucciariello C, Bassolino L, Banti V, Licausi F, Perata P. 2015**. Universal stress protein HRU1 mediates ROS homeostasis under anoxia. *Nature Plants* **1**: 1–9.

**Graciet E, Mesiti F, Wellmer F. 2010**. Structure and evolutionary conservation of the plant N-end rule pathway. *The Plant Journal* **61**: 741–751.

**Guo H, Ecker JR. 2004**. The ethylene signaling pathway: new insights. *Current Opinion in Plant Biology* **7**: 40–49.

**Gupta KJ, Hebelstrup KH, Mur LAJ, Igamberdiev AU. 2011**. Plant hemoglobins: Important players at the crossroads between oxygen and nitric oxide. *FEBS Letters* **585**: 3843–3849.

**Gupta KJ, Igamberdiev AU. 2016**. Reactive Nitrogen Species in Mitochondria and Their Implications in Plant Energy Status and Hypoxic Stress Tolerance. *Frontiers in Plant Science* **7**: 1–6.

R

**Gupta KJ, Shah JK, Brotman Y, Jahnke K, Willmitzer L, Kaiser WM, Bauwe H, Igamberdiev AU. 2012**. Inhibition of aconitase by nitric oxide leads to induction of the alternative oxidase and to a shift of metabolism towards biosynthesis of amino acids. *Journal of Experimental Botany* **63**: 1773–1784.

**Gururani MA, Upadhyaya CP, Baskar V, Venkatesh J, Nookaraju A, Park SW. 2013**. Plant Growth-Promoting Rhizobacteria Enhance Abiotic Stress Tolerance in Solanum tuberosum Through Inducing Changes in the Expression of ROS-Scavenging Enzymes and Improved Photosynthetic Performance. *Journal of Plant Growth Regulation* **32**: 245–258.

**Hartman S, Liu Z, Veen H van, Vicente J, Reinen E, Martopawiro S, Zhang H, Dongen N van, Bosman F, Bassel GW, *et al.* 2019**. Ethylene-mediated nitric oxide depletion pre-adapts plants to hypoxia stress. *Nature Communications 2019 10:1* **10**: 1–9.

**Hattori Y, Nagai K, Furukawa S, Song X-J, Kawano R, Sakakibara H, Wu J, Matsumoto T, Yoshimura A, Kitano H, *et al.* 2009**. The ethylene response factors SNORKEL1 and SNORKEL2 allow rice to adapt to deep water. *Nature* **460**: 1026–1030.

**He X, Jiang J, Wang C-Q, Dehesh K. 2017**. ORA59 and EIN3 interaction couples jasmonate-ethylene synergistic action to antagonistic salicylic acid regulation of PDF expression. *Journal of Integrative Plant Biology* **59**: 275–287.

**Hebelstrup KH, Hunt P, Dennis E, Jensen SB, Jensen EØ. 2006**. Hemoglobin is essential for normal growth of Arabidopsis organs. *Physiologia Plantarum* **127**: 157–166.

**Hebelstrup KH, van Zanten M, Mandon J, Voesenek LACJ, Harren FJM, Cristescu SM, Møller IM, Mur LAJ. 2012**. Haemoglobin modulates NO emission and hyponasty under hypoxia-related stress in Arabidopsis thaliana. *Journal of Experimental Botany* **63**: 5581–5591.

**Hess N, Klode M, Anders M, Sauter M. 2011**. The hypoxia responsive transcription factor genes ERF71 / HRE2 and ERF73 / HRE1 of Arabidopsis are differentially regulated by ethylene. : 41–49.

**Hinz M, Wilson IW, Yang J, Buerstenbinder K, Llewellyn D, Dennis ES, Sauter M, Dolferus R. 2010**. Arabidopsis RAP2.2: An Ethylene Response Transcription Factor That Is Important for Hypoxia Survival. *Plant Physiology* **153**: 757–772.

**Hirabayashi Y, Mahendran R, Koirala S, Konoshima L, Yamazaki D, Watanabe S, Kim H, Kanae S. 2013**. Global flood risk under climate change. *Nature Climate Change* **3**: 816–821.

**Holdsworth MJ. 2017**. First hints of new sensors. *Nature Plants*: 1–2.

**Horchani F, Prévot M, Boscari A, Evangelisti E, Meilhoc E, Bruand C, Raymond P, Boncompagni E, Aschi-Smiti S, Puppo A, *et al.* 2011**. Both plant and bacterial nitrate reductases contribute to nitric oxide production in Medicago truncatula nitrogen-fixing nodules. *Plant physiology* **155**: 1023–36.

**Hunt PW, Klok EJ, Trevaskis B, Watts RA, Ellis MH, Peacock WJ, Dennis ES. 2002**. Increased level of hemoglobin 1 enhances survival of hypoxic stress and promotes early growth in Arabidopsis thaliana. *Proceedings of the National Academy of Sciences of the United States of America* **99**: 17197–202.

**Igamberdiev AU, Baron K, Manac'h-Little N, Stoimenova M, Hill RD. 2005**. The haemoglobin/nitric oxide cycle: Involvement in flooding stress and effects on hormone signalling. *Annals of Botany* **96**: 557–564.

**Igamberdiev AU, Hill RD. 2018**. Elevation of cytosolic Ca2+ in response to energy deficiency in plants: the general mechanism of adaptation to low oxygen stress. *The Biochemical journal* **475**: 1411–1425.

**Ikuma H, Bonner WD. 1967**. Properties of Higher Plant Mitochondria. III. Effects of Respiratory Inhibitors. *Plant physiology* **42**: 1535–44.

**Ju C, Van de Poel B, Cooper ED, Thierer JH, Gibbons TR, Delwiche CF, Chang C. 2015**. Conservation of ethylene as a plant hormone over 450 million years of evolution. *Nature Plants* **1**: 14004.

**Juntawong P, Bailey-Serres J. 2012**. Dynamic Light Regulation of Translation Status in Arabidopsis thaliana. *Frontiers in Plant Science* **3**: 66.



**Juntawong P, Girke T, Bazin J, Bailey-Serres J. 2014**. Translational dynamics revealed by genome-wide profiling of ribosome footprints in Arabidopsis. *Proceedings of the National Academy of Sciences of the United States of America* **111**: E203-12.

**Kaiser WM, Spill D, Glaab J. 1993**. Rapid modulation of nitrate reductase in leaves and roots: Indirect evidence for the involvement of protein phosphorylation/dephosphorylation. *Physiologia Plantarum* **89**: 557–562.

**Kim NY, Jang YJ, Park OK. 2018**. AP2/ERF Family Transcription Factors ORA59 and RAP2.3 Interact in the Nucleus and Function Together in Ethylene Responses. *Frontiers in Plant Science* **9**: 1675.

**Konert G, Trotta A, Kouvonen P, Rahikainen M, Durian G, Blokhina O, Fagerstedt K, Muth D, Corthals GL, Kangasjärvi S. 2015**. Protein phosphatase 2A (PP2A) regulatory subunit B'y interacts with cytoplasmic ACONITASE 3 and modulates the abundance of AOX1A and AOX1D in *Arabidopsis thaliana*. *New Phytologist* **205**: 1250–1263.

**Koornneef M, Meinke D. 2010**. The development of Arabidopsis as a model plant. *The Plant Journal* **61**: 909–921.

**Ku HS, Suge H, Rappaport L, Pratt HK. 1970**. Stimulation of rice coleoptile growth by ethylene. *Planta* **90**: 333–339.

**Lee SC, Mustroph A, Sasidharan R, Vashisht D, Pedersen O, Oosumi T, Voesenek LACJ, Bailey-Serres J. 2011**. Molecular characterization of the submergence response of the Arabidopsis thaliana ecotype Columbia. *New Phytologist* **190**: 457–471.

**León J, Costa-Broseta Á. 2019**. Present knowledge and controversies, deficiencies and misconceptions on nitric oxide synthesis, sensing and signaling in plants. *Plant, Cell & Environment*: pce.13617.

**León J, Costa Á, Castillo MC. 2016**. Nitric oxide triggers a transient metabolic reprogramming in Arabidopsis. *Scientific Reports* **6**: 1–14.

**Li X, Peng R-H, Fan H-Q, Xiong A-S, Yao Q-H, Cheng Z-M, Li Y. 2005**. Vitreoscilla hemoglobin overexpression increases submergence tolerance in cabbage. *Plant Cell Reports* **23**: 710–715.

**Liao W-B, Zhang M-L, Yu J-H. 2013**. Role of nitric oxide in delaying senescence of cut rose flowers and its interaction with ethylene. *Scientia Horticulturae* **155**: 30–38.

**Libourel IGL, Bethke PC, De Michele R, Jones RL. 2006**. Nitric oxide gas stimulates germination of dormant Arabidopsis seeds: Use of a flow-through apparatus for delivery of nitric oxide. *Planta* **223**: 813–820.

**Licausi F, Van Dongen JT, Giuntoli B, Novi G, Santaniello A, Geigenberger P, Perata P. 2010a**. HRE1 and HRE2, two hypoxia-inducible ethylene response factors, affect anaerobic responses in Arabidopsis thaliana. *The Plant Journal* **62**: 302–315.

**Licausi F, Giorgi FM, Zenoni S, Osti F, Pezzotti M, Perata P. 2010b**. Genomic and transcriptomic analysis of the AP2/ERF superfamily in Vitis vinifera. *BMC Genomics* **11**: 719.

**Licausi F, Kosmacz M, Weits DA, Giuntoli B, Giorgi FM, Voesenek LACJ, Perata P, van Dongen JT. 2011**. Oxygen sensing in plants is mediated by an N-end rule pathway for protein destabilization. *Nature* **479**: 419–422.

**Lin C-C, Chao Y-T, Chen W-C, Ho H-Y, Chou M-Y, Li Y-R, Wu Y-L, Yang H-A, Hsieh H, Lin C-S, *et al.* 2019**. Regulatory cascade involving transcriptional and N-end rule pathways in rice under submergence. *Proceedings of the National Academy of Sciences of the United States of America* **116**: 3300–3309.

**Liu Z. 2019**. Ethylene-mediated hypoxia tolerance in Arabidopsis thaliana. *PhD Thesis*.

**Liu K, Li Y, Chen X, Li L, Liu K, Zhao H, Wang Y, Han S. 2018**. ERF72 interacts with ARF6 and BZR1 to regulate hypocotyl elongation in Arabidopsis. *Journal of Experimental Botany* **69**: 3933–3947.

**Livak KJ, Schmittgen TD. 2001**. Analysis of Relative Gene Expression Data Using Real-Time Quantitative PCR and the 2−ΔΔCT Method. *Methods* **25**: 402–408.

**Lobell DB, Burke MB, Tebaldi C, Mastrandrea MD, Falcon WP, Naylor RL. 2008**. Prioritizing climate change adaptation needs for food security in 2030. *Science (New York, N.Y.)* **319**: 607–10.

**Loreti E, Valeri MC, Novi G, Perata P. 2018**. Gene Regulation and Survival under Hypoxia Requires Starch Availability and Metabolism. *Plant physiology* **176**: 1286–1298.

**Magalhaes JR, Monte DC, Durzan D. 2000**. Nitric oxide and ethylene emission in Arabidopsis thaliana. : 6 117-127.

**Manjunatha G, Gupta KJ, Lokesh V, Mur LA, Neelwarne B. 2012**. Nitric oxide counters ethylene effects on ripening fruits. *Plant Signaling & Behavior* **7**: 476–483.

**Métraux JP, Kende H. 1983**. The role of ethylene in the growth response of submerged deep water rice. *Plant physiology* **72**: 441–6.

**Millar AH, Day DA, Millar AH, Day DA. 1997**. Nitric oxide inhibits the cytochrome oxidase but not the alternative oxidase of plant mitochondria Nitric oxide inhibits the cytochrome oxidase but not the alternative oxidase of plant mitochondria. *FEBS Journal* **398**: 155–158.

**Min T, Yin X, Shi Y, Luo Z, Yao Y, Grierson D, Ferguson IB, Chen K. 2012**. Ethylene-responsive transcription factors interact with promoters of ADH and PDC involved in persimmon (Diospyros kaki) fruit de-astringency. *Journal of Experimental Botany* **63**: 6393–6405.

**Mira MM, Hill RD, Stasolla C. 2016**. Phytoglobins Improve Hypoxic Root Growth by Alleviating Apical Meristem Cell Death. *Plant Physiology* **172**: 2044–2056.

**Mithran M, Paparelli E, Novi G, Perata P, Loreti E. 2014**. Analysis of the role of the pyruvate decarboxylase gene family in *Arabidopsis thaliana* under low-oxygen conditions (J Whelan, Ed.). *Plant Biology* **16**: 28–34.

**Mittler R. 2017**. ROS Are Good. *Trends in Plant Science* **22**: 11–19.

**Mot AC, Puscas C, Miclea P, Naumova-Letia G, Dorneanu S, Podar D, Dissmeyer N, Silaghi-Dumitrescu R. 2018**. Redox control and autoxidation of class 1, 2 and 3 phytoglobins from Arabidopsis thaliana. *Scientific Reports* **8**: 1–13.

**Mugnai S, Azzarello E, Baluka F, Mancuso S. 2012**. Local root apex hypoxia induces no-mediated hypoxic acclimation of the entire root. *Plant and Cell Physiology* **53**: 912–920.

**Müller M, Munné-Bosch S. 2015**. Ethylene Response Factors: A Key Regulatory Hub in Hormone and Stress Signaling. *Plant physiology* **169**: 32–41.

**Mur LAJ, Prats E, Pierre S, Hall MA, Hebelstrup KH. 2013**. Integrating nitric oxide into salicylic acid and jasmonic acid/ ethylene plant defense pathways. *Frontiers in Plant Science* **4**: 215.

**Mustroph A. 2018**. Improving Flooding Tolerance of Crop Plants. *Agronomy* **8**: 160.

**Mustroph A, Lee SC, Oosumi T, Zanetti ME, Yang H, Ma K, Yaghoubi-Masihi A, Fukao T, Bailey-Serres J. 2010**. Cross-Kingdom Comparison of Transcriptomic Adjustments to Low-Oxygen Stress Highlights Conserved and Plant-Specific Responses. *Plant Physiology* **152**: 1484–1500.

**Mustroph A, Zanetti ME, Jang CJH, Holtan HE, Repetti PP, Galbraith DW, Girke T, Bailey-Serres J. 2009**. Profiling translatomes of discrete cell populations resolves altered cellular priorities during hypoxia in Arabidopsis. *Proceedings of the National Academy of Sciences of the United States of America* **106**: 18843–8.

**Myers SS, Smith MR, Guth S, Golden CD, Vaitla B, Mueller ND, Dangour AD, Huybers P. 2017**. Climate Change and Global Food Systems: Potential Impacts on Food Security and Undernutrition. *Annual Review of Public Health* **38**: 259–277.

**Nakagawa T, Suzuki T, Murata S, NAKAMURA S, HINO T, MAEO K, TABATA R, KAWAI T, TANAKA K, NIWA Y, *et al.* 2007**. Improved Gateway Binary Vectors: High-Performance Vectors for Creation of Fusion Constructs in Transgenic Analysis of Plants. *Bioscience, Biotechnology, and Biochemistry* **71**: 2095–2100.

**Nemie-Feyissa D, Królicka A, Førland N, Hansen M, Heidari B, Lillo C. 2013**. Post-translational control of nitrate reductase activity responding to light and photosynthesis evolved already in the early vascular plants. *Journal of Plant Physiology* **170**: 662–667.



**Nietzel T, Elsässer M, Ruberti C, Steinbeck J, Ugalde JM, Fuchs P, Wagner S, Ostermann L, Moseler A, Lemke P, *et al.* 2018**. The fluorescent protein sensor ro GFP 2-Orp1 monitors *in vivo* $H_2O_2$ and thiol redox integration and elucidates intracellular $H_2O_2$ dynamics during elicitor-induced oxidative burst in Arabidopsis. *New Phytologist* **221**: nph.15550.

**Ohwaki Y, Kawagishi-Kobayashi M, Wakasa K, Fujihara S, Yoneyama T. 2005**. Induction of Class-1 Non-symbiotic Hemoglobin Genes by Nitrate, Nitrite and Nitric Oxide in Cultured Rice Cells. *Plant and Cell Physiology* **46**: 324–331.

**Pan R, He D, Xu L, Zhou M, Li C, Wu C, Xu Y, Zhang W. 2019**. Proteomic analysis reveals response of differential wheat (Triticum aestivum L.) genotypes to oxygen deficiency stress. *BMC Genomics* **20**: 60.

**Papdi C, Pérez-Salamõ I, Joseph MP, Giuntoli B, Bögre L, Koncz C, Szabados L. 2015**. The low oxygen, oxidative and osmotic stress responses synergistically act through the ethylene response factor VII genes RAP2.12, RAP2.2 and RAP2.3. *Plant Journal* **82**: 772–784.

**Pedersen O, Colmer TD, Garcia-Robledo E, Revsbech NP. 2018**. CO2 and O2 dynamics in leaves of aquatic plants with C3 or CAM photosynthesis – application of a novel CO2 microsensor. *Annals of Botany* **122**: 605–615.

**Pedersen O, Rich SM, Colmer TD. 2009**. Surviving floods: leaf gas films improve O2 and CO2 exchange, root aeration, and growth of completely submerged rice. *The Plant Journal* **58**: 147–156.

**Peng H-P. 2001**. Signaling Events in the Hypoxic Induction of Alcohol Dehydrogenase Gene in Arabidopsis. *Plant Physiology* **126**: 742–749.

**Peng J, Li Z, Wen X, Li W, Shi H, Yang L, Zhu H, Guo H. 2014**. Salt-Induced Stabilization of EIN3/EIL1 Confers Salinity Tolerance by Deterring ROS Accumulation in Arabidopsis (H Yu, Ed.). *PLoS Genetics* **10**: e1004664.

**Peng C, Uygun S, Shiu S-H, Last RL. 2015**. The Impact of the Branched-Chain Ketoacid Dehydrogenase Complex on Amino Acid Homeostasis in Arabidopsis. *Plant physiology* **169**: 1807–20.

**Pierik R, van Aken JM, Voesenek LACJ. 2009**. Is elongation-induced leaf emergence beneficial for submerged Rumex species? *Annals of Botany* **103**: 353–357.

**Pierik R, Tholen D, Poorter H, Visser EJW, Voesenek LACJ. 2006**. The Janus face of ethylene: growth inhibition and stimulation. *Trends in Plant Science* **11**: 176–183.

**Planchet E, Kaiser WM. 2006**. Nitric oxide (NO) detection by DAF fluorescence and chemiluminescence: A comparison using abiotic and biotic NO sources. *Journal of Experimental Botany* **57**: 3043–3055.

**Potato Genome Sequencing Consortium, Xu X, Pan S, Cheng S, Zhang B, Mu D, Ni P, Zhang G, Yang S, Li R, *et al.* 2011**. Genome sequence and analysis of the tuber crop potato. *Nature* **475**: 189–195.

**Pré M, Atallah M, Champion A, De Vos M, Pieterse CMJ, Memelink J. 2008**. The AP2/ERF Domain Transcription Factor ORA59 Integrates Jasmonic Acid and Ethylene Signals in Plant Defense. *Plant Physiology* **147**: 1347–1357.

**Pucciariello C, Perata P. 2017**. New insights into reactive oxygen species and nitric oxide signalling under low oxygen in plants. *Plant Cell and Environment* **40**: 473–482.

**Puerta ML, Shukla V, Carbonare LD, Weits DA, Perata P, Licausi F, Giuntoli B. 2019**. A Ratiometric Sensor Based on Plant N-Terminal Degrons Able to Report Oxygen Dynamics in Saccharomyces cerevisiae. *Journal of Molecular Biology*.

**Qu Z-L, Wang H-Y, Xia G-X. 2005**. GhHb1: A nonsymbiotic hemoglobin gene of cotton responsive to infection by Verticillium dahliae. *Biochimica et Biophysica Acta (BBA) - Gene Structure and Expression* **1730**: 103–113.

**Rauniyar N, Yates JR. 2014**. Isobaric Labeling-Based Relative Quantification in Shotgun Proteomics. *Journal of Proteome Research* **13**: 5293–5309.

**Ravanbakhsh M, Sasidharan R, Voesenek LACJ, Kowalchuk GA, Jousset A. 2017**. ACC deaminase-producing rhizosphere bacteria modulate plant responses to flooding (D Cameron, Ed.). *Journal of Ecology* **105**: 979–986.

**Rivera-Contreras IK, Zamora-Hernández T, Huerta-Heredia AA, Capataz-Tafur J, Barrera-Figueroa BE, Juntawong P, Peña-Castro JM. 2016**. Transcriptomic analysis of submergence-tolerant and sensitive Brachypodium distachyon ecotypes reveals oxidative stress as a major tolerance factor. *Scientific Reports* **6**: 1–15.

**Roberts EH. 1986**. SEEDS. PHYSIOLOGY OF DEVELOPMENT AND GERMINATION (Book). *Plant, Cell and Environment* **9**: 356–356.

**Rocklin AM, Kato K, Liu H, Que L, Lipscomb JD. 2004**. Mechanistic studies of 1-aminocyclopropane-1-carboxylic acid oxidase: single turnover reaction. *JBIC Journal of Biological Inorganic Chemistry* **9**: 171–182.

**Sanz-Luque E, Ocaña-Calahorro F, de Montaigu A, Chamizo-Ampudia A, Llamas Á, Galván A, Fernández E. 2015**. THB1, a truncated hemoglobin, modulates nitric oxide levels and nitrate reductase activity. *The Plant Journal* **81**: 467–479.

**Sanz L, Fernandez-Marcos M, Modrego A, Lewis DR, Muday GK, Pollmann S, Duenas M, Santos-Buelga C, Lorenzo O. 2014**. Nitric Oxide Plays a Role in Stem Cell Niche Homeostasis through Its Interaction with Auxin. *Plant Physiology* **166**: 1972–1984.

**Sasidharan R, Hartman S, Liu Z, Martopawiro S, Sajeev N, van Veen H, Yeung E, Voesenek LACJ. 2018**. Signal Dynamics and Interactions during Flooding Stress. *Plant physiology* **176**: 1106–1117.

**Schertl P, Braun H-P. 2014**. Respiratory electron transfer pathways in plant mitochondria. *Frontiers in Plant Science* **5**: 163.

**Schmidt RR, van Dongen JT. 2019**. The ACBP1-RAP2.12 signalling hub: A new perspective on integrative signalling during hypoxia in plants. *Plant Signaling & Behavior* **0**: 1–4.

**Schmidt RR, Fulda M, Paul M V, Anders M, Plum F, Weits DA, Kosmacz M, Larson TR, Graham IA, Beemster GTS, *et al.* 2018**. Low-oxygen response is triggered by an ATP-dependent shift in oleoyl-CoA in Arabidopsis. *Proceedings of the National Academy of Sciences of the United States of America* **115**: E12101–E12110.

**Schwarz D, Rouphael Y, Venema JH. 2010**. Grafting as a tool to improve tolerance of vegetables to abiotic stresses: Thermal stress, water stress and organic pollutants. *Scientia Horticulturae* **127**: 162–171.

**Sebilo M, Mayer B, Nicolardot B, Pinay G, Mariotti A. 2013**. Long-term fate of nitrate fertilizer in agricultural soils. *Proceedings of the National Academy of Sciences of the United States of America* **110**: 18185–9.

**Shi K, Ding X-T, Dong D-K, Zhou Y-H, Yu JQ. 2008**. Putrescine enhancement of tolerance to root-zone hypoxia in Cucumis sativus: a role for increased nitrate reduction. *Functional Plant Biology* **35**: 337.

**Shi H, Liu R, Xue C, Shen X, Wei N, Deng XW, Zhong S. 2016**. Seedlings Transduce the Depth and Mechanical Pressure of Covering Soil Using COP1 and Ethylene to Regulate EBF1/EBF2 for Soil Emergence. *Current Biology* **26**: 139–149.

**Shingaki-Wells R, Millar AH, Whelan J, Narsai R. 2014**. What happens to plant mitochondria under low oxygen? An omics review of the responses to low oxygen and reoxygenation. *Plant, Cell & Environment* **37**: n/a-n/a.

**Shiono K, Takahashi H, Colmer TD, Nakazono M. 2008**. Role of ethylene in acclimations to promote oxygen transport in roots of plants in waterlogged soils. *Plant Science* **175**: 52–58.

**Shukla V, Lombardi L, Iacopino S, Pencik A, Novak O, Perata P, Giuntoli B, Licausi F. 2019**. Endogenous Hypoxia in Lateral Root Primordia Controls Root Architecture by Antagonizing Auxin Signaling in Arabidopsis. *Molecular Plant* **12**: 538–551.

**Singh RP, Shelke GM, Kumar A, Jha PN. 2015**. Biochemistry and genetics of ACC deaminase: a weapon to "stress ethylene" produced in plants. *Frontiers in Microbiology* **6**: 937.

**Singh SP, Singh Z, Swinny EE. 2009**. Postharvest nitric oxide fumigation delays fruit ripening and alleviates chilling injury during cold storage of Japanese plums (Prunus salicina Lindell). *Postharvest Biology and Technology* **53**: 101–108.



**Solano R, Stepanova A, Chao Q, Ecker JR. 1998**. Nuclear events in ethylene signaling: a transcriptional cascade mediated by ETHYLENE-INSENSITIVE3 and ETHYLENE-RESPONSE-FACTOR1. *Genes & Development* **12**: 3703–3714.

**Somerville C, Koornneef M. 2002**. A fortunate choice: the history of Arabidopsis as a model plant. *Nature Reviews Genetics* **3**: 883–889.

**Stasolla C, Hill RD. 2017**. Determining Cellular Responses: Phytoglobins May Direct the Traffic. *Trends in Plant Science* **22**: 820–822.

**Stasolla C, Huang S, Hill RD, Igamberdiev AU. 2019**. Spatio-temporal expression of phytoglobin – a determining factor in the NO specification of cell fate. *Journal of Experimental Botany*.

**Sunil B, Raghavendra AS. 2017**. Measurement of Mitochondrial Respiration in Isolated Protoplasts: Cytochrome and Alternative Pathways. In: Humana Press, New York, NY, 253–265.

**Tasaki T, Sriram SM, Park KS, Kwon YT. 2012**. The N-End Rule Pathway. *Annual Review of Biochemistry* **81**: 261–289.

**Tesniere C, Pradal M, El-Kereamy A, Torregrosa L, Chatelet P, Roustan J-P, Chervin C. 2004**. Involvement of ethylene signalling in a non-climacteric fruit: new elements regarding the regulation of ADH expression in grapevine. *Journal of Experimental Botany* **55**: 2235–2240.

**Tian MS. 1998**. Responses of strawberry fruit to 1-MCP and ethylene. *Scientific programme & book of abstracts / Biology and biotechnology of the plant hormone ethylene* **2nd**: 89.

**Tsai K-J, Chou S-J, Shih M-C. 2014**. Ethylene plays an essential role in the recovery of Arabidopsis during post-anaerobiosis reoxygenation. *Plant, Cell & Environment* **37**: 2391–2405.

**Ursache R, Andersen TG, Marhavý P, Geldner N. 2018**. A protocol for combining fluorescent proteins with histological stains for diverse cell wall components. *The Plant Journal* **93**: 399–412.

**Vanlerberghe G, Vanlerberghe, C. G. 2013**. Alternative Oxidase: A Mitochondrial Respiratory Pathway to Maintain Metabolic and Signaling Homeostasis during Abiotic and Biotic Stress in Plants. *International Journal of Molecular Sciences* **14**: 6805–6847.

**Varshavsky A. 2019**. N-degron and C-degron pathways of protein degradation. *Proceedings of the National Academy of Sciences of the United States of America* **116**: 358–366.

**Vashisht D, Hesselink A, Pierik R, Ammerlaan JMH, Bailey-Serres J, Visser EJW, Pedersen O, van Zanten M, Vreugdenhil D, Jamar DCL, *et al.* 2011**. Natural variation of submergence tolerance among Arabidopsis thaliana accessions. *New Phytologist* **190**: 299–310.

**van Veen H, Mustroph A, Barding GA, Eijk MV, Welschen-Evertman RAM, Pedersen O, Visser EJW, Larive CK, Pierik R, Bailey-Serres J, *et al.* 2013**. Two Rumex Species from Contrasting Hydrological Niches Regulate Flooding Tolerance through Distinct Mechanisms. *The Plant Cell* **25**: 4691–4707.

**Vicente J, Mendiondo GM, Movahedi M, Peirats-Llobet M, Juan Y ting, Shen Y yen, Dambire C, Smart K, Rodriguez PL, Charng Y yung, *et al.* 2017**. The Cys-Arg/N-End Rule Pathway Is a General Sensor of Abiotic Stress in Flowering Plants. *Current Biology* **27**: 3183-3190.e4.

**Vicente J, Mendiondo GM, Pauwels J, Pastor V, Izquierdo Y, Naumann C, Movahedi M, Rooney D, Gibbs DJ, Smart K, *et al.* 2019**. Distinct branches of the N-end rule pathway modulate the plant immune response. *New Phytologist* **221**: 988–1000.

**Vidoz ML, Loreti E, Mensuali A, Alpi A, Perata P. 2010**. Hormonal interplay during adventitious root formation in flooded tomato plants. *The Plant Journal* **63**: 551–562.

**Vishwakarma A, Kumari A, Mur LAJ, Gupta KJ. 2018**. A discrete role for alternative oxidase under hypoxia to increase nitric oxide and drive energy production. *Free Radical Biology and Medicine* **122**: 40–51.

**Voesenek LACJ, Bailey-Serres J. 2015a**. Flood adaptive traits and processes: an overview. *New Phytologist* **206**: 57–73.

**Voesenek LAC, Bailey-Serres J. 2015b**. Hypoxia and development: Air conditional. *Nature Plants* **1**: 15095.

R

**Voesenek LACJ, Pierik R, Sasidharan R. 2015**. Plant Life without Ethylene. *Trends in plant science* **20**: 783–786.
**Voesenek LACJ, Sasidharan R. 2013**. Ethylene - and oxygen signalling - drive plant survival during flooding. *Plant Biology* **15**: 426–435.
**Voesenek LACJ, Sasidharan R, Visser EJW, Bailey-Serres J. 2016**. Flooding stress signaling through perturbations in oxygen, ethylene, nitric oxide and light. *New Phytologist* **209**: 39–43.
**Wagner S, Steinbeck J, Fuchs P, Lichtenauer S, Elsässer M, Schippers JHM, Nietzel T, Ruberti C, Van Aken O, Meyer AJ, *et al.* 2019**. Multiparametric real-time sensing of cytosolic physiology links hypoxia responses to mitochondrial electron transport. *New Phytologist*: nph.16093.
**Wang F, Chen ZH, Shabala S. 2017**. Hypoxia Sensing in Plants: On a Quest for Ion Channels as Putative Oxygen Sensors. *Plant and Cell Physiology* **58**: 1126–1142.
**Wei X, Xu H, Rong W, Ye X, Zhang Z. 2019**. Constitutive expression of a stabilized transcription factor group VII ethylene response factor enhances waterlogging tolerance in wheat without penalizing grain yield. *Plant, Cell & Environment*.
**Weits DA, Giuntoli B, Kosmacz M, Parlanti S, Hubberten H-M, Riegler H, Hoefgen R, Perata P, van Dongen JT, Licausi F. 2014**. Plant cysteine oxidases control the oxygen-dependent branch of the N-end-rule pathway. *Nature Communications* **5**: 3425.
**Weits DA, Kunkowska AB, Kamps NCW, Portz KMS, Packbier NK, Nemec Venza Z, Gaillochet C, Lohmann JU, Pedersen O, van Dongen JT, *et al.* 2019**. An apical hypoxic niche sets the pace of shoot meristem activity. *Nature* **569**: 714–717.
**Wen X, Zhang C, Ji Y, Zhao Q, He W, An F, Jiang L, Guo H. 2012**. Activation of ethylene signaling is mediated by nuclear translocation of the cleaved EIN2 carboxyl terminus. *Cell Research* **22**: 1613–1616.
**White MD, Klecker M, Hopkinson RJ, Weits DA, Mueller C, Naumann C, O'Neill R, Wickens J, Yang J, Brooks-Bartlett JC, *et al.* 2017**. Plant cysteine oxidases are dioxygenases that directly enable arginyl transferase-catalysed arginylation of N-end rule targets. *Nature Communications* **8**: 14690.
**Wu K. 2002**. Transcription Factor RAP2.2 and Its Interacting Partner SINAT2: Stable Elements in the Carotenogenesis of Arabidopsis Leaves. *PLANT PHYSIOLOGY* **128**: 30–37.
**Wu L, Zhang Z, Zhang H, Wang X-C, Huang R. 2008**. Transcriptional modulation of ethylene response factor protein JERF3 in the oxidative stress response enhances tolerance of tobacco seedlings to salt, drought, and freezing. *Plant physiology* **148**: 1953–63.
**Xie LJ, Chen QF, Chen MX, Yu LJ, Huang L, Chen L, Wang FZ, Xia FN, Zhu TR, Wu JX, *et al.* 2015**. Unsaturation of Very-Long-Chain Ceramides Protects Plant from Hypoxia-Induced Damages by Modulating Ethylene Signaling in Arabidopsis. *PLoS Genetics* **11**: 1–33.
**Xu K, Xu X, Fukao T, Canlas P, Maghirang-Rodriguez R, Heuer S, Ismail AM, Bailey-Serres J, Ronald PC, Mackill DJ. 2006**. Sub1A is an ethylene-response-factor-like gene that confers submergence tolerance to rice. *Nature* **442**: 705–708.
**Yamasaki H, Shimoji H, Ohshiro Y, Sakihama Y. 2001**. Inhibitory Effects of Nitric Oxide on Oxidative Phosphorylation in Plant Mitochondria. *Nitric Oxide* **5**: 261–270.
**Yamauchi T, Watanabe K, Fukazawa A, Mori H, Abe F, Kawaguchi K, Oyanagi A, Nakazono M. 2014**. Ethylene and reactive oxygen species are involved in root aerenchyma formation and adaptation of wheat seedlings to oxygen-deficient conditions. *Journal of Experimental Botany* **65**: 261–273.
**Yanagisawa S, Yoo S-D, Sheen J. 2003**. Differential regulation of EIN3 stability by glucose and ethylene signalling in plants. *Nature* **425**: 521–525.
**Yeung E, Bailey-Serres J, Sasidharan R. 2019**. After The Deluge: Plant Revival Post-Flooding. *Trends in Plant Science* **24**: 443–454.



**Yeung E, van Veen H, Vashisht D, Sobral Paiva AL, Hummel M, Rankenberg T, Steffens B, Steffen-Heins A, Sauter M, de Vries M, *et al.* 2018**. A stress recovery signaling network for enhanced flooding tolerance in Arabidopsis thaliana. *Proceedings of the National Academy of Sciences of the United States of America* **115**: E6085–E6094.
**Youssef MS, Mira MM, Millar JL, Becker MG, Belmonte MF, Hill RD, Stasolla C. 2019**. Spatial identification of transcripts and biological processes in laser micro-dissected sub-regions of waterlogged corn roots with altered expression of phytoglobin. *Plant Physiology and Biochemistry* **139**: 350–365.
**Yu F, Liang K, Fang T, Zhao H, Han X, Cai M, Qiu F. 2019**. A group VII ethylene response factor gene, *ZmEREB180* , coordinates waterlogging tolerance in maize seedlings. *Plant Biotechnology Journal*: pbi.13140.
**Zabalza A, van Dongen JT, Froehlich A, Oliver SN, Faix B, Gupta KJ, Schmalzlin E, Igal M, Orcaray L, Royuela M, *et al.* 2008**. Regulation of Respiration and Fermentation to Control the Plant Internal Oxygen Concentration. *Plant Physiology* **149**: 1087–1098.
**Zarban R, Vogler M, Wong A, Eppinger J, Al-Babili S, Gehring C, Zarban R, Vogler M, Wong A, Eppinger J, *et al.* 2019**. Discovery of a Nitric Oxide-Responsive Protein in Arabidopsis thaliana. *Molecules* **24**: 2691.
**Zeng C, Liu L, Xu G. 2011**. The physiological responses of carnation cut flowers to exogenous nitric oxide. *Scientia Horticulturae* **127**: 424–430.
**Zhang H, Deery MJ, Gannon L, Powers SJ, Lilley KS, Theodoulou FL. 2015**. Quantitative proteomics analysis of the Arg/N-end rule pathway of targeted degradation in Arabidopsis roots. *Proteomics* **15**: 2447–2457.
**Zhang H, Gannon L, Hassall KL, Deery MJ, Gibbs DJ, Holdsworth MJ, van der Hoorn RAL, Lilley KS, Theodoulou FL. 2018a**. N-terminomics reveals control of Arabidopsis seed storage proteins and proteases by the Arg/N-end rule pathway. *New Phytologist* **218**: 1106–1126.
**Zhang Y, Kong X, Dai J, Luo Z, Li Z, Lu H, Xu S, Tang W, Zhang D, Li W, *et al.* 2017**. Global gene expression in cotton (Gossypium hirsutum L.) leaves to waterlogging stress. *PLoS ONE* **12**: 1–24.
**Zhang L, Li G, Wang M, Di D, Sun L, Kronzucker HJ, Shi W. 2018b**. Excess iron stress reduces root tip zone growth through nitric oxide-mediated repression of potassium homeostasis in Arabidopsis. *New Phytologist* **219**: 259–274.
**Zhang Q, Peters JL, Visser EJW, de Kroon H, Huber H. 2016**. Hydrologically contrasting environments induce genetic but not phenotypic differentiation in *Solanum dulcamara* (M Semchenko, Ed.). *Journal of Ecology* **104**: 1649–1661.
**Zhang L-T, Zhang Z-S, Gao H-Y, Meng X-L, Yang C, Liu J-G, Meng Q-W. 2012**. The mitochondrial alternative oxidase pathway protects the photosynthetic apparatus against photodamage in Rumex K-1 leaves. *BMC Plant Biology* **12**: 40.
**Zhao N, Li C, Yan Y, Cao W, Song A, Wang H, Chen S, Jiang J, Chen F. 2018**. Comparative transcriptome analysis of waterlogging-sensitive and waterlogging-tolerant Chrysanthemum morifolium cultivars under waterlogging stress and reoxygenation conditions. *International Journal of Molecular Sciences* **19**.
**Zhao Y, Wei T, Yin K-Q, Chen Z, Gu H, Qu L-J, Qin G. 2012**. Arabidopsis RAP2.2 plays an important role in plant resistance to Botrytis cinerea and ethylene responses. *New Phytologist* **195**: 450–460.
**Zottini M, Formentin E, Scattolin M, Carimi F, Lo Schiavo F, Terzi M. 2002**. Nitric oxide affects plant mitochondrial functionality in vivo. *FEBS Letters* **515**: 75–78.
**Zubo YO, Potapova T V., Yamburenko M V., Tarasenko VI, Konstantinov YM, Börner T. 2014**. Inhibition of the electron transport strongly affects transcription and transcript levels in Arabidopsis mitochondria. *Mitochondrion* **19**: 222–230.

# APPENDIX I.

## List of genotyping primers used in this thesis

| T-DNA lines | Primer info | Oligo sequence 5′ → 3′ | Additional info |
|---|---|---|---|
| *rap2.2-5 (AY201781)* | WT FW | ccgcgtcactaacgagtttat | *Gasch et al., 2015* |
| | WT REV | ctccactgggttttcctcttc | |
| | T-DNA REV | cgattaccgtatttatcccgt | |
| *rap2.12-2 (SAIL_1215_H10)* | WT FW | tcttcgattttgacgctgagt | *Gasch et al., 2015* |
| | WT REV | agggtttgcaccattgtcctgag | |
| | T-DNA REV | gaatttcataaccaatctcgatacac | |
| *rap2.3-1 (SAIL_1031_D10)* | WT FW | atgtgtggcggtgctattatt | *Gibbs et al., 2014* |
| | WT REV | ttactcatacgacgcaatgac | |
| | T-DNA REV | gaatttcataaccaatctcgatacac | |
| *hre1 (SALK_039484)* | WT FW | ttacagacagtggcgaaatca | *Gibbs et al., 2014* |
| | WT REV | tcaggaccatagacccatgt | |
| | T-DNA REV | attttgccgatttcggaac | |
| *hre2 (SALK_052858)* | WT FW | tgcaaaaggttatagagcacac | *Gibbs et al., 2014* |
| | WT REV | ggcaaccggaatctgataga | |
| | T-DNA REV | attttgccgatttcggaac | |
| *prt6-1 (SAIL_1278_H11)* | WT FW | ggcagaaacatccctgaaag | *Gibbs et al., 2011* |
| | WT REV | gcagcacaacactggagaag | |
| | T-DNA REV | gaatttcataaccaatctcgatacac | |
| *pgb1-1 (SALK_058388)* | WT FW | aagtgttacgtgagactacgact | This thesis |
| | WT REV | cttcgttgttggtgcaatctca | |
| | T-DNA REV | attttgccgatttcggaac | |
| *eil1-1* | WT FW | tttgatcgtaatggtccagc | *Alonso et al., 2003* |
| | WT REV | attttgctgtgaggacactg | |
| | Transp.REV | gtcggtccccacacttctata | |
| **Transgenic lines** | **Primer info** | **Oligo sequence 5′ → 3′** | **Additional info** |
| *35S:PGB1* | 35S:FW | ggaagttcatttcatttggagagg | Kanamycin Resistance *Hebelstrup et al., 2006* |
| | PGB1 REV | tgacactccaagacttcactaca | |
| *35S:RAP2.3-HA* | 35S:FW | ggaagttcatttcatttggagagg | Basta Resistance *Gibbs et al., 2014* |
| | RAP2.3 REV | taatcggaaataatagcaccgcc | |
| *35S:EIN3-GFP* | 35S:FW | ggaagttcatttcatttggagagg | in *ein3eil1-1* background *Xie et al., 2015* |
| | EIN3 REV | atgcttgataaccgcagtca | |
| *35S:RAP2.12-GFP* | 35S:FW | ggaagttcatttcatttggagagg | Kanamycin Resistance *Licausi et al., 2011* |
| | RAP2.12 REV | agggtttgcaccattgtcctgag | |
| *35S:δ13-RAP2.12-GFP* | 35S:FW | ggaagttcatttcatttggagagg | Kanamycin Resistance *Licausi et al., 2011* |
| | RAP2.12 REV | agggtttgcaccattgtcctgag | |
| *promRAP2.12:RAP2.12-GUS* | RAP2.12 FW | actgaatgggacgcttcactgg | Hygromycin Resistance Hartman et al., 2019 |
| | GUS REV | ccatcagcacgttatcgaat | |



| Other | Primer info | Oligo sequence 5′ → 3′ | Additional info |
|---|---|---|---|
| *ein2-5* | WT FW | cgctcattccagtggtcttt | 7bp deletion *Alonso et al., 1999* |
| | WT REV | tggtatattccgtctgcacca | |
| *ein3* | WT FW | aggaggatgtggagagacaa | G to A substitution at nt1598 *Alonso et al., 2003* |
| | WT REV | atgcttgataaccgcagtca | |

# APPENDIX II.

## List of RT-qPCR primers used in this thesis

**Species: *Arabidopsis thaliana***

| Target gene | AT code | Primer name | Oligo sequence 5′ → 3′ |
|---|---|---|---|
| *ACBP1* | *AT5G53470* | ACBP1_FW | TGGAGATGCGTTATTGTGA |
| | | ACBP1_R | GCGAGAAGGTAAGCGAAG |
| *ACBP2* | *AT4G27780* | ACBP2_FW | GTGAGGCGGATTCGCTTGT |
| | | ACBP2_R | TGCGGCGGCGGTAGTC |
| *ACO1* | *AT2G19590* | ACO1_FW | CCTCAGATGCAGATTGGGAAAGC |
| | | ACO1_R | TCATCCATCGTCTTGCTGAGTTCC |
| *ADH1* | *AT1G77120* | ADH1_FW | GGTCTTGGTGCTGTTGGTTT |
| | | ADH1_R | CTCAGCGATCACCTGTTGAA |
| *APT1* | *AT1G27450* | APT1_FW | AATGGCGACTGAAGATGTGC |
| | | APT1_R | TCAGTGTCGAGAAGAAGCGT |
| *ATE1* | *AT5G05700* | ATE1_FW | TCCTCTCCGTTTCCAGTGGG |
| | | ATE1_R | CCACGAGAGTTTCAGAAGCACCAG |
| *ATE2* | *AT3G11240* | ATE2_FW | AGCAGTAGCAGAAACCGGAGTG |
| | | ATE2_R | TTCTTGAACCGCGGTATATCCTTG |
| *ETR2* | *AT3G23150* | ETR2_FW | TGTTAGATTCTCCGGCGGCTATG |
| | | ETR2_R | TTCCCATGAATCAACTGCACCAC |
| *HRA* | *AT3G10040* | HRA_FW | CATGACCAACAACCACCGCAAC |
| | | HRA_R | TTCTGCTGCTGACTCGGAATCG |
| *HRE1* | *AT1G72360* | HRE1_FW | TCCGATGAGCCATTTGTCTTCTCC |
| | | HRE1_R | CCATCTTCCCCAAGGCCTTC |
| *HRE2* | *AT2G47520* | HRE2_FW | TTGCTGCCATCAAAATCCGT |
| | | HRE2_R | CCCCTGGTTTAGTATCGGCT |
| *NR1* | *AT1G77760* | NIA1_FW | CTGAGCTGGCAAATTCCGAAGC |
| | | NIA1_R | TGCGTGACCAGGTGTTGTAATC |
| *NR2* | *AT1G37130* | NIA2_FW | AACTCGCCGACGAAGAAGGTTG |
| | | NIA2_R | GGGTTGTGAAAGCGTTGATGGG |
| *PCO1* | *AT5G1512* | PCO1_FW | ATTGGGTGGTTGATGCTCCAATG |
| | | PCO1_R | ATGCATGTTCCCGCCATCTTCC |
| *PCO2* | *AT5G39890* | PCO2_FW | TCCCCAGCCGAGTTCAGATA |
| | | PCO2_R | TCCATCAGCCGGGTACAGTA |
| *PDC1* | *AT4G33070* | PDC1_FW | TCGATTGGGTGGTCTGTTGG |
| | | PDC1_R | TGTCCTGAACCGTGACTTGG |
| *PDC2* | *AT5G54960* | PDC2_FW | TGAAAGCAATCAACACGGCA |
| | | PDC2_R | CAGCAGAGACTCTAGAGCCC |

| | | | |
|---|---|---|---|
| *PRT6* | *AT5G02310* | PRT6_FW | CATATGGAGCCCTTGTTGCAGAG |
| | | PRT6_R | TACACCAGTACCAGCACCACAG |
| *RAP2.2* | *AT3G14230* | RAP2.2_FW | CCTAGCGTCGTATCCCAGAA |
| | | RAP2.2_R | CTCAGATGTGTTGGCTGCTG |
| *RAP2.3* | *AT3G16770* | RAP2.3_FW | AACTCACGGCTGAGGAACTCTG |
| | | RAP2.3_R | ACGTTAACTTGGTTGGTGGGATGG |
| *RAP2.12* | *AT1G53910* | RAP2.12_FW | ACTGAATGGGACGCTTCACTGG |
| | | RAP2.12_R | AGGGTTTGCACCATTGTCCTGAG |
| *SRO5* | *AT5G62520* | SRO5_FW | AAGAGGCGGTGCAGATGAAACAC |
| | | SRO5_R | TTTCGAAACAGAGCACCAACCG |
| *ALAAT1* | *AT1G17290* | ALAAT1_FW | ATTCATGACAGATGGTGCAA |
| | | ALAAT1_R | TATTTCAAGACCCCATCCTG |
| *SUS4* | *AT3G43190* | SUS4_FW | TTCACCATGGCTAGGCTTGA |
| | | SUS4_R | CCACCAAGTTCACCAGTTCG |
| *PGB1* | *AT2G16060* | HB1_FW | GGCTCTTGTAGTGAAGTCTTGGA |
| | | HB1_R | CTTCGTTGTTGGTGCAATCTCA |
| *PGB2* | *AT3G10520* | HB2_FW | TGAAGTCCCTCACAACAATCCTA |
| | | HB2_R | AACGCCGCTTTTGAGATGAA |
| *PGB3* | *AT4G32690* | HB3_FW | TGGACGATTCGGTTGACATT |
| | | HB3_R | TGGTTTATTGGCTGCGTGTT |
| *HUP40* | *AT4G24110* | HUP40 _FW | GAAACTTGAGTGCGAGTGTG |
| | | HUP40 _R | CTCAAACCCAATCTTTTGCT |
| *RBOHD* | *AT5G47910* | RBOHD _FW | CTTCTGCAAACAAGCTCTCA |
| | | RBOHD _R | GTATCCTGCTGTCTCCCATC |

**Species: *Solanum tuberosum***

| Target gene | Identifier | Primer name | Oligo sequence 5′ → 3′ |
|---|---|---|---|
| *ETR2* | *PGSC0003DMP400028451* | ETR2_FW | CCTCATTCCAAATCGTCCTT |
| | | ETR2_R | CTGCAGGCATCTTCCAGTAA |
| *PGB1* | *PGSC0003DMP400053876* | PGB1_FW | CAGACAAGGATGCTGCTGAT |
| | | PGB1_R | TCCTTGGGTCACGTATTTCA |
| *RAP2.12* | *PGSC0003DMP400016096* | RAP2.12_FW | CAGACAAGGATGCTGCTGAT |
| | | RAP2.12_R | TCCTTGGGTCACGTATTTCA |
| *PDC1* | *PGSC0003DMP400011112* | PDC1_FW | ACGGAGAAGGAAAATGTTGG |
| | | PDC1_R | GCTGCTGAGACCCTAGAACC |
| *ACT11* | *PGSC0003DMP400048248* | ACT_FW | TCTTCGTTTGGATCTTGCTG |
| | | ACT_R | AGCCACATAGGCAAGCTTTT |

**Species: *Solanum lycopersicum***

| Target gene | Identifier | Primer name | Oligo sequence 5′ → 3′ |
|---|---|---|---|
| *ETR2* | *SOLYC06G053710.2.1* | ETR2_FW | CCTCATTCCAAATCGTCCTT |
| | | ETR2_R | TGAAGCTCATCAGCGATACC |
| *PGB1* | *SOLYC07G008240.2.1* | PGB1_FW | CAGACAAGGATGCTGCTGAT |
| | | PGB1_R | TCCTTGGGTCACGTATTTCA |
| *RAP2.12* | *SOLYC03G123500.2.1* | RAP2.12_FW | TTCCTGATGAAGCTCCAGTG |
| | | RAP2.12_R | ACTGAGCCCAGTCCCATATC |



| | | | |
|---|---|---|---|
| *PDC1* | *SOLYC10G076510.1.1* | PDC1_FW | AGGCTTTGAATATGGCTGCT |
| | | PDC1_R | ACCGTCCACCTTTAAACCAG |
| *ADH1* | *SOLYC04G064710.2.1* | ADH1_FW | TGAAGGATCAAAGGTGGTCA |
| | | ADH1_R | CGCATTTCTCTTGCCTCATA |
| *TUB6* | *SOLYC02G087880.2.1* | TUB_FW | AAAGCATGTACCTCGTGCTG |
| | | TUB_R | ACAGCATGGAACACCAAAAA |

**Species: *Solanum dulcamara***

| Target gene | Identifier | Primer name | Oligo sequence 5′ → 3′ |
|---|---|---|---|
| *ETR2* | *N.A.* | ETR2_FW | GGGCTTCCAAATAGCACAAT |
| | | ETR2_R | GCTGCTCAAAATCAAGGTGA |
| *PGB1* | *N.A.* | PGB1_FW | CCACAACCTTTCCAGCTTTT |
| | | PGB1_R | ATGGGAGTCCATGAAGAAGG |
| *RAP2.12* | *N.A.* | RAP2.12_FW | ATACGTGACCCAAGGAAAGG |
| | | RAP2.12_R | TTCTTGCCTCTGATCCTCCT |
| *PDC1* | *N.A.* | PDC1_FW | ATTGAGCTGGCTCCTCAGTT |
| | | PDC1_R | CACGGATATTCCTGTTGCAC |
| *ADH1* | *N.A.* | ADH1_FW | AATGTGTCCATGATGGTTGG |
| | | ADH1_R | GGCCACTACAGATGGAAGGT |
| *TUB6* | *N.A.* | TUB_FW | AATTCTCGGCCTCTTTACGA |
| | | TUB_R | CCAGGGCTGTTCTTATGGAT |

## APPENDIX III.

### Oxygen dynamics during ethylene priming experiments

Levels of molecular oxygen measured over time at the outflow of a desiccator during a typical ethylene pre-treatment and subsequent hypoxia in this thesis. Oxygen levels generally reached <0.00% between 40 and 50 minutes of flushing the desiccators with humidified 99.996% $N_2$ at a rate of 2l $min^{-1}$.

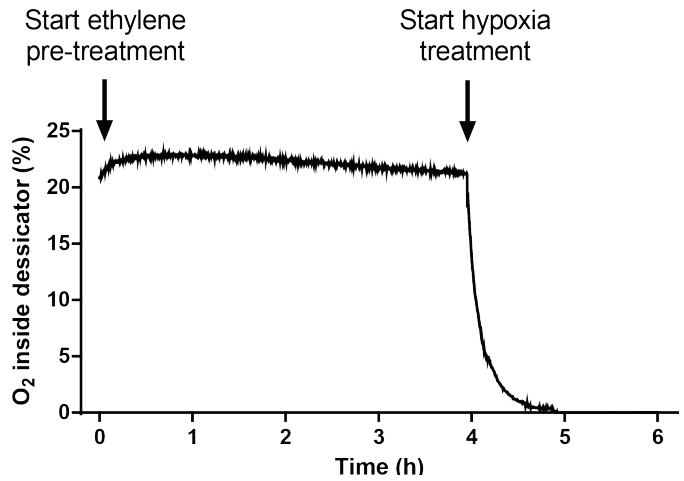


A

## SAMENVATTING

Een van de grootste maatschappelijke uitdagingen van deze eeuw is het garanderen van de wereldwijde voedselzekerheid. De sterk toenemende wereldbevolking staat haaks op het feit dat er steeds minder bruikbare landbouwgrond beschikbaar is. Daar komt bij, dat door klimaatverandering steeds meer oogsten verloren gaan door een toename in weers-extremen, zoals droogte en overstromingen. Om in de toekomst overstromingstolerante gewassen te ontwikkelen is het noodzakelijk om te begrijpen waarom planten onder water sterven en hoe planten processen in gang zetten om een verdrinkingsdood te voorkomen.

De meeste landplanten en ook nagenoeg alle landbouwgewassen zijn zeer intolerant tegen overstromingen, omdat planten net als wij zuurstof nodig hebben om te overleven. Door een sterk verlaagde snelheid in gasdiffusie onder water verspreiden gassen zoals zuurstof en koolstofdioxide zich ~10.000 keer trager door een vloeistof dan door lucht. Dit heeft tot gevolg dat overstroomde planten uiteindelijk te maken krijgen met een tekort aan zuurstof en/of koolstofdioxide. Omdat deze gassen belangrijk zijn voor respectievelijk ademhaling en fotosynthese, zullen de meeste overstroomde plantensoorten uiteindelijk sterven door een gebrek aan beschikbare energie en koolhydraten.

Ethyleen is een gasvorming plantenhormoon dat snel ophoopt in de cellen van overstroomde planten als gevolg van verlaagde gasdiffusie onder water. Hierdoor kan ethyleen dienen als een overstromingssignaal voor de plant en kan het processen aan zetten die hun overlevingskansen verbeteren. In het plantenrijk zijn er verschillende strategieën geëvolueerd om overstromingen te overleven. Eén strategie, die een aantal moerasplanten aanzetten wanneer zij overstromen, is de zogenaamde 'snorkelrespons'. Hierbij groeien de bladeren en stengels van planten versneld omhoog, om zo het contact met de lucht te herstellen. Door speciale holle structuren in de bladeren en stengels van deze planten kan zuurstof zich vervolgens door de planten verspreiden om zuurstofgebrek te voorkomen. Eerder onderzoek heeft aangetoond dat ethyleen dit soort snorkelresponsen reguleert. Daarnaast gebruiken veel plantensoorten de strategie om hun groei en metabolisme onder water actief te onderdrukken. Hierdoor gaan planten zuinig om met de aanwezige zuurstof, koolhydraten en energie voorraden tot de overstroming voorbij is. Recentelijk onderzoek heeft aangetoond dat ethyleen ook hier mogelijk een rol bij speelt. Hierbij liet men zien dat de plantensoort moeraszuring het vroege ethyleensignaal gebruikt om vervolgens langer zuurstofgebrek te overleven. Echter, het moleculaire mechanisme dat dit proces reguleert, is nog onbekend. Het doel



van het onderzoek dat beschreven staat in dit proefschrift is om te ontrafelen hoe ethyleen de overleving onder laag-zuurstof bevordert in de modelplant *Arabidopsis thaliana* (zandraket).

In **Hoofdstuk 2** laten wij zien dat het gevangen ethyleengas in overstroomde zandraket-zaailingen leidt tot zeer snelle ethyleen-afhankelijke signalering in wortelcellen. Daarnaast laten de resultaten zien dat ethyleen als vroeg signaal de laag-zuurstof overleving van zowel scheuten als wortelpunten sterk bevordert. Tenslotte laten wij zien dat dit proces stabiel is onder veranderende temperatuur- of licht-omstandigheden en daarnaast geconserveerd is in meerdere ecotypes van de zandraket.

Het doel van **Hoofdstuk 3** is om te achterhalen hoe ethyleen de laag-zuurstoftolerantie bevordert. In zandraket wordt de laag-zuurstoftolerantie gereguleerd door een cluster van genen die worden aangezet wanneer zuurstofgebrek optreedt. Ons onderzoek laat zien dat ethyleen de inductie van deze genen sterk bevordert wanneer de planten werden behandeld met lage zuurstofgehaltes. Laag-zuurstof genen worden normaliter gereguleerd door zogenaamde stabiele ERFVII eiwitten, die ophopen wanneer de zuurstof concentratie daalt en vervolgens deze laag-zuurstof respons aanzetten. Wij laten zien dat ethyleen al tot ophoping van stabiele ERFVII eiwitten leidt vóórdat de zuurstof concentratie daalt. Daarnaast laten de resultaten zien dat als ethyleen deze ERFVII eiwitten niet kan aanzetten, de planten ook geen verhoogde laag-zuurstoftolerantie meer hebben. Tenslotte laten onze resultaten zien dat ethyleen alleen ERFVII eiwitten stabiliseert als het eerst de concentratie van stikstofoxide (NO) in plantencellen laat dalen.

In **Hoofstuk 4** zoeken wij uit hoe ethyleen leidt tot verlaagde NO-niveaus in plantencellen. Eerder onderzoek heeft aangetoond dat plant-hemoglobine (PGB) in plantencellen NO kan verwijderen. Onze data laten zien dat ethyleen de concentraties van PGB-eiwitten sterk laat stijgen en hierdoor het cellulaire NO niveau laat dalen. Daarnaast laten wij zien dat ethyleen-toegift aan zandraket mutanten zonder PGB niet langer leidt tot verhoogde ERFVII eiwitten of laag-zuurstof tolerantie. We concluderen dat de regulatie van PGB door ethyleen essentieel is om de kettingreactie in werking te zetten die leidt tot verbeterde laag-zuurstoftolerantie. Een gesimplificeerd overzicht van dit mechanisme is weergegeven in Figuur 4.5.

Onderzoek in eerdere hoofdstukken heeft aangetoond dat ethyleen een vroeg overstromingssignaal is voor planten en belangrijke eiwitten aanzet om de over-

levingskansen tijdens zuurstofgebrek te verhogen. In **Hoofdstuk 5** gebruiken wij een speciale techniek om een groot aantal eiwitten op te sporen die door ethyleen worden gereguleerd. De techniek detecteerde meer dan 6500 verschillende eiwitten, waarvan er ongeveer 730 meer of minder aanwezig waren na een ethyleenbehandeling. Onder de ethyleen-gereguleerde eiwitten waren veel eiwitten die zich bevinden in het mitochondrium. In het mitochondrium vindt de ademhaling van de cel plaats, en wij denken dat ethyleen hier mogelijk effect op heeft. Daarnaast vonden we dat ethyleen verschillende andere eiwitten aanzet die laag-zuurstoftolerantie verbeteren maar waarvan de exacte functie nog onbekend is. Tenslotte verhoogde ethyleen ook de gehaltes van eiwitten (antioxidanten) die belangrijk zijn voor het opruimen van vrije zuurstofradicalen (oxidatieve stress). Eerder onderzoek heeft laten zien dat, wanneer een overstroming voorbij is, dit zorgt voor een hoge productie van schadelijke zuurstofradicalen in plantencellen. Onze resultaten laten zien dat een ethyleenbehandeling ook de tolerantie van planten verbetert wanneer deze vervolgens werden behandeld met een hoge concentratie zuurstofradicalen (waterstofperoxide). Wij concluderen daarom dat ethyleen niet alleen laag-zuurstoftolerantie tijdens overstromingen, maar ook oxidatieve stresstolerantie na overstromingen verbetert.

In de vorige hoofstukken hebben wij het mechanisme van ethyleen-gereguleerde laag-zuurstof tolerantie blootgelegd in de modelplant zandraket. Aardappel en tomaat zijn de twee belangrijkste groentewassen op aarde en zijn betrekkelijk intolerant voor overstromingen. De wilde plantensoort bitterzoet is nauw verwant aan aardappel en tomaat maar is wel is zeer tolerant voor overstromingen. In **Hoofdstuk 6** testen wij een aantal marker-genen om te achterhalen of ethyleen ook het mechanisme aanzet dat leidt tot verhoogde laag-zuurstof overleving in deze plantensoorten. Onze resultaten laten zien dat ethyleen dit mechanisme ook aanzet in bitterzoet en in een overstromings-tolerant aardappelras, maar niet in tomaat en in de wortels van een overstromings-gevoelig aardappelras. We concluderen dat de ontdekking van dit mechanisme een krachtig middel is om moleculaire schakels te vinden die leiden tot de aan- of afwezigheid van tolerantieprocessen in planten. Een overzicht van ethyleen-gereguleerde schakels die mogelijk leiden tot tolerantie in verschillende plantensoorten is weergegeven in Figuur 6.5. Samenvattend laten wij in dit proefschrift zien dat ethyleen een vroeg en essentieel overstromingssignaal is dat overstromingstolerantie in planten reguleert.



## RÉSUMÉ

Le changement climatique augmente fortement la fréquence et la gravité des inondations dans le monde. Ces inondations peuvent détruire bon nombre de nos cultures et réduire énormément les rendements agricole à l'échelle mondiale. Afin de rendre les cultures plus tolérantes aux inondations, il est important de comprendre pourquoi les plantes ne survivent pas sous l'eau et comment celles-ci déclenchent des processus qui les empêchent de se noyer. Comme les humains, les plantes manquent d'oxygène sous l'eau car la diffusion des gaz est ralenti (10 000 fois) dans les liquides, ce qui empêche l'apport en oxygène dans les cellules de la plante. Il est intéressant de noter que les plantes produisent des gaz qui se diffusent naturellement dans l'atmosphère. Sous, l`eau, ces gaz sont piégés et par conséquent, s'accumulent. L'un de ces gaz est connu sous le nom d'éthylène, une hormone végétale, qui s'accumule à l'intérieur des cellules végétales lorsque les plantes sont submergées. Des recherches antérieures ont montré que cette accumulation d'éthylène contrôle plusieurs réponses qui aident les plantes vivant en zones humides à survivre sous l'eau. Dans cette thèse, nous avons démontré que l'éthylène peut également aider des espèces végétales terrestres, y compris des espèces agricoles comme la pomme de terre, à augmenter leur taux de survie en l'absence quasi-totale d'oxygène. De plus, nous avons découvert le phénomène associé à cela. Nous savons maintenant que les plantes utilisent l'éthylène pour déclencher une cascade complexe d'événements augmentant la quantité de protéines détectant l'oxygène, ce qui les pousse à réagir plus rapidement et plus efficacement sous l'eau. Toute cette cascade d'événements est résumée dans les figures 4.5 et 6.5. Nous pensons que ces résultats aideront à mieux comprendre pourquoi certaines espèces de plantes cultivées meurent rapidement sous l'eau comme la tomate chez laquelle la cascade est interrompue. À l'avenir, les agriculteurs pourront utiliser ces informations pour rétablir la cascade d'événements, de sorte que même les plantes comme la tomate soit capable d'utiliser l'éthylène comme signal pour mieux survivre sous l'eau.

## ACKNOWLEDGEMENTS

There it is, the end of my PhD time. It has been a rollercoaster with some lows but fortunately many more highs. Overall it has been an amazing journey and here I would like to take the opportunity to express my gratitude to everyone who contributed to making it possible, exciting and fun.

First of all, I want to thank my promoter and mentor, **Rens**. It all started more than 6 years ago at one of the famous EvP barbecues at your house, where I asked you if it was possible to further study this interesting phenomenon we then called 'ethylene priming' in Arabidopsis. Your enthusiasm for flooding biology, experience, eye for detail and continuous support were highly contagious and motivated me to go the extra mile during my MSc and PhD. I am very grateful for everything you have taught me, it has been a privilege and I believe all your valuable lessons will benefit me strongly for the rest of my career. Then my co-promoter and co-citizen of Zeist, **Rashmi**. I am happy I could always just walk into your office for any question or second opinion. Thank you for all the great scientific discussions we have had and all your positive feedback throughout the years. I also really appreciated the flooding team dinners at your house. **Ronald**, thank you for already bringing me on the right path that is plant science during my BSc courses. Your insightful feedback and advice has been highly appreciated. **Eric**, I still can't believe you decided to do your sabbatical with me but I have enjoyed it so much. It was a beautiful sight to see you sow all those tiny seeds on agar plates. I am also really happy your experience and hard work helped us to quickly optimize (and survive) our NO experiments. Your support and our conversations really helped me through what I would consider my toughest 'PhD dip', thank you for that.

Support, inspiration and new friendship came from all around the world. **Mike**, thank you so much for hosting me in your lab in Nottingham, your involvement in the project and teaching me to *always think mechanistically*. I also really enjoyed our scientific sparring and discussions. **Jorge**, I couldn't be more lucky with you as my daily supervisor there. You taught me so much at the bench, thanks for all the fun both inside and outside of the lab. **Julia**, thank you for flying over frequently from sunny California to share and discuss science with us. Your feedback and support means a lot to me. I am also happy to have met **Kaisa**, who has strengthened our EvP staff team with new insights. I also really enjoyed your vodka party, thanks! **Dan**, I can't believe how helpful you have been over the years. If I asked you for your opinion, you always instantly gave a very insightful, elaborate and supportive response. I am really looking forward to working with you in the future. **Freddie** and **Hongtao**, I am really happy you got involved in the project when we met in Halle. I learned a lot from your expertise and high-quality way of work. Thank you for all your support in our ongoing project and for hosting me in Rothamsted, I had a fantastic time. **Kim,** thank you for your visit to Utrecht and our deep discussions on both phytoglobins and beer. **Angelika**, thank for all the friendly chats, advice and positive feedback over the years. **Nico,** your passion for the proteostasis field is glorious and contagious. Thank you for your support and inviting me to both Halle and Seoul, I really appreciate it.

My PhD would have been considerably harder and less enjoyable without the wonderful support staff of EvP. **Ankie**, **Rob**, **Diederik, Liao, Judith, Marleen** and **Yorrit**, thank you for all your help in the lab and the phytotron. I wish you all the best. **Emilie**, you are the true master of the molecular lab. While I will forever envy your organizational skills and know-how of both molecular and baking techniques, I am mostly grateful for your friendship and our frequent chats over coffee. Thank you for your advice and support and I really hope you find happiness at your new job.

Next the all-star EvP flooding team. First and foremost, my priming buddies **Zeguang** and **Shanice**. Zeguang, you are an amazing person and it was a privilege working with you for all these years. I also enjoyed your lessons on Chinese culture and cuisine. You're an incredible friend and hard-working colleague and I hope you find a job and life that makes you happy, you really deserve it. Shanice, you're such a fun, kind and positive-minded friend. I feel lucky I got to know you already as a student and later as colleagues, I wish you all the happiness in the world. **Hans**, I started my career in plant science as a BSc student under your supervision and it has been a blast to be your colleague and friend. I really enjoyed both our social and scientific discussions in addition to all the beers we shared during bowling(!) and burger nights. **Elaine**, thank you for all your help over the years, I enjoyed your company in the office and at all the parties we attended. You're probably the kindest person I know and I wish you all the best. **Tom**, you're a really smart and friendly guy and the team is lucky to have you. I enjoyed our days walking the streets of Taipei and sharing street food and beers. **Angelica**, you're a great addition to the flooding team and I think you're amazing for joining me and Sarah to the Muse concert already on one of your first days in Netherlands. Also, thank you for hosting the amazing thanksgiving dinner! **Jana** and **Putri**, your temporary stays in our team were great and I really enjoyed your presence, also at the parties. Thank you for housesitting and taking care of Yolo

and Twiggy. I also want to thank **Nikita**, **Maarten**, **Ana**, **Justine** and **JZ** for all their feedback and discussions throughout the years.

Then the more shady part of the team. **Lot** and **Scott**, you're both amazingly talented scientists and I feel honored to have been your colleague and learn from you. I want to thank you for all your advice and input over the years in addition to making every bar and party night more fun. **Kasper**, thank you for all your input on the confocal and lab borrels, I will really miss being confused for you. **Debatosh**, I had a lot of fun with you in the lab, thanks for all your help and trusting me as your paranymph. **Chrysa**, I am happy we have been office mates ever since we both joined the group, thank you for your company and always making liters of tzatziki for the barbecues. I also really appreciate all the conversations and help of **Sara, Chiakai, Franca, Paulien, Linge, Martina, Valérie, Mariana, Nicole** and **Lisa** over the years, thank you.

I had the privilege of supervising many students during my PhD. From the bottom of my heart I want to thank **Johanna, Max, Tamara, Joris, Femke, Nienke, Florian** and **Dominique** for placing your trust in me over the course of your projects. You have all contributed to the development of this thesis and for that I am really grateful. I was also happy to learn that several of you are now also pursuing a PhD and I am confident you will do great. Any employer is lucky to have either one of you in their team and I could even see some of you as leaders in the future.

Then I want to thank **Jan, Mariëlle, Sjoukje, Stefan** and **Arwa** and your companies for first believing in me and ultimately supporting this project. Your input has been very valuable and it was interesting to translate our work to various crop and ornamental plant species. I also want to thank the people from NWO, EPS and Plantum for their financial support. **René** and **Suzanne**, thank you for believing in me and letting me perform in your amazing theatre show ScienceBattle. I really had so much fun. It strongly increased my confidence in front of any audience and I am also grateful for all the media attention it created for our work and plant science in general.

Next I want to thank my friends. **Jason**, you're an amazing friend and I had a great time living and studying with you over the years. **Rutger**, you're a great guy and I always love talking to you about anything over a few beers and dinner. The Lullo's friend group: **Jesse, Thijs, Daniël** and **Lennart**, thank you for all great moments we shared. Your friendship and support means a lot to me. Jesse, thank you for being my paranymph, I admire you as both a friend and scientist and I am sure that you can achieve anything you want. The Homeboys friend group: **Bas, Eric** and **Job**, I am happy we are still friends after all these years and I always enjoy our time together, making new memories and sharing old ones. **Hao**, I am happy we became friends over the years and I really enjoyed our well-needed and deserved work distractions of playing WoW together. **Stephanie**, even though we hardly see each other anymore, your friendship means a lot to me. We became friends when life was not as easy and your unconditional support really helped my through these times. It is truly an honor you are standing next to me as my paranymph while I defend this thesis.

I want to thank a few more people who made it possible for me to even make it to University and start a PhD. **Yvonne, Willie, Wim, Paul** and **Lobke,** you all helped me in one way or another and I will never forget your help and support.

Finally, I couldn't have done this without the help of my supportive and loving family. **Mama, Maijkel, Jessica** & **Thomas, Iris** & **Patrick**, thank you for your unconditional love and understanding. Iris, thank you so much for taking these incredibly beautiful photos that are shown throughout this thesis. Ma famille française: **Thierry** et **Christine**, merci pour votre soutien et votre hospitalité. J'ai toujours hâte de venir vous voir et de passer du temps avec vous. Finally, **Sarah** I couldn't be more happy that we found each other and that we are in this rollercoaster together. You make the lows in life not as bad, and the highs so much better. I can't imagine my life without you and look forward to the future with you by my side.

## ABOUT THE AUTHOR

Sjon Johannes Gerardus Wilhelmus Hartman was born on the 28th of December 1987 in Woerden, the Netherlands. He obtained his Atheneum higher education diploma in June 2010 from the De Driemark in Winterswijk. Afterwards Sjon studied Biology at Utrecht University and did short-term internships at the research groups of Plant Microbe Interactions and Plant Ecophysiology. Sjon got his BSc in 2013 and subsequently started his MSc in Environmental Biology with a focus on plant science at Utrecht University. During his MSc studies he performed a 10-month internship at the Plant Ecophysiology group under the supervision of Prof. Rens Voesenek. Here he studied the effect of ethylene on hypoxia acclimation in Arabidopsis plants. Subsequently he went to do a six-month internship at the University of Nottingham under the supervision of Prof. Michael Holdsworth to study the effects of ethylene on protein stability. At the start of 2015, Sjon enrolled in the 'Experimental Plant Sciences (EPS) MSc talent program', where he wrote a research proposal on uncovering the mechanism of ethylene-mediated hypoxia tolerance under the supervision of Prof. Rens Voesenek. This proposal was awarded with a personal PhD grant from EPS and the Dutch Organization for Scientific Research (NWO) in the summer of 2015. Sjon received his MSc with honors (cum laude) and started his PhD research at the Plant Ecophysiology group at Utrecht University in September 2015. During his PhD research Sjon was actively engaged in science communication and outreach and he frequently presented his research in Dutch theaters for several years in a show called "ScienceBattle". This thesis is the result of his PhD research.



## PUBLICATIONS

**Hartman, S.**, Sasidharan, R. & Voesenek, L.A.C.J. (2019). The role of ethylene in metabolic acclimations to low oxygen. *New Phytologist*, Accepted.

**Hartman, S.**, Liu, Z., van Veen, H., Vicente, J., Reinen, E., Martopawiro, S., Zhang, H., van Dongen, N., Bosman, F., Bassel, G.W., Visser, E.J., Bailey-Serres, J., Theodoulou, F.L., Hebelstrup, K.H., Gibbs, D.J., Holdsworth, M.J., Sasidharan, R. & Voesenek, L.A.C.J. (2019). Ethylene-mediated nitric oxide depletion pre-adapts plants to hypoxia stress. *Nature Communications*, 10 (1), 4020.

Gibbs, D.J., Tedds, H.M., Labandera, A.M., Bailey, M., White, M.D., **Hartman, S.**, Sprigg, C., Mogg, S.L., Osborne, R., Dambire, C., Boeckx, T., Paling, Z., Voesenek, L.A.C.J., Flashman, E. & Holdsworth, M.J. (2018). Oxygen-dependent proteolysis regulates the stability of angiosperm polycomb repressive complex 2 subunit VERNALIZATION 2. *Nature Communications*, 9 (1), 5438.

Sasidharan, R., **Hartman, S.**, Liu, Z., Martopawiro, S., Sajeev, N., van Veen, H., Yeung, E. and Voesenek, L.A.C.J. (2018). Signal dynamics and interactions during flooding stress. *Plant Physiology*, 176 (2), 1106-1117.

Van Veen, H., Vashisht, D., Akman, M., Girke, T., Mustroph, A., Reinen, E., **Hartman, S.**, Kooiker, M., van Tienderen, P., Schranz, M.E., Bailey-Serres, J., Voesenek, L.A.C.J. & Sasidharan, R. (2016). Transcriptomes of eight Arabidopsis thaliana accessions reveal core conserved, genotype-and organ-specific responses to flooding stress. *Plant Physiology*, 172 (2), 668-689.